

**RELATIVE GROWTH AND MORPHOLOGICAL VARIATION IN THE
SKULL OF *AELUROGNATHUS* (THERAPSIDA: GORGONOPSIA)**

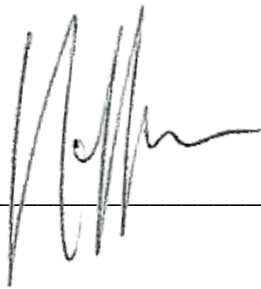
Luke Allan Norton

A Dissertation submitted to the Faculty of Science, University of the
Witwatersrand, Johannesburg, in fulfilment of the requirements for the degree of
Master of Science.

Johannesburg, 2012

DECLARATION

I declare that this Dissertation is my own, unaided work. It is being submitted for the Degree of Master of Science at the University of the Witwatersrand, Johannesburg. It has not been submitted before for any other degree or examination at any other University.



Luke Allan Norton

14 June 2012

ABSTRACT

Gorgonopsia represent a group of specialised carnivorous therapsids that filled the role of apex predator during the Late Permian of Gondwana. Skull size in the Gorgonopsia ranges from that of a cat, to larger than any extant, terrestrial predator. Despite this degree of size variation, the observed morphological variation in the skull is relatively conservative. This study set out to better understand the extent of size and morphological variation among species attributed to the South African genus, *Aelurognathus*, with the aim of possibly refining the taxonomy of the genus. *Aelurognathus* was chosen, as it contains the largest number of described specimens (16) of any of the Rubidgeinid genera. Previous work has led to numerous revisions to the taxonomic assignment of each specimen, at both the generic and specific levels. All available specimens were studied and morphological differences at both the intraspecific and interspecific levels noted. Morphological variations allowed for the division of the six previously recognised species into three morphotaxa based on the character state of the preparietal and the extent of contact by the frontal on the supraorbital margin. Both characters have been shown to vary among individuals of extant taxa. Taking this into account, a hypothesis that all 16 specimens represent a single taxon, exhibiting a high degree of morphological variation, was tested using allometric techniques. Linear measurements of the skull were selected, such that variation in skull size and shape was accounted for in all dimensions. Results of the bivariate analyses showed a high level of correlation with the bivariate fitted lines plotted, supporting the single taxon hypothesis. While *Aelurognathus* has previously been divided into six species, using morphological characters, this study has shown that the characters used in the past have been unreliable. As such it is proposed that all species attributed to *Aelurognathus* be synonymised with the type, *Aelurognathus tigriceps*.

In memory of my Grandmother,

Thelma Thomson

18 July 1921 - 2 September 2011

ACKNOWLEDGMENTS

I am indebted to my supervisors, Prof. Bruce Rubidge and Dr Fernando Abdala, for their advice, guidance and patience through the duration of this dissertation.

Thank you to Richard, Marion and Robert Rubidge (Rubidge Collection), Dr Bernhard Zipfel (Bernard Price Institute), Sheena Kaal and Dr Roger Smith (Iziko: South African Museum) & Stephaney Potze and Dr Heidi Fourie (Ditsong: National Museum of Natural History), for allowing access to their collections, and the loan of holotype material for preparation.

Additional preparation of material was undertaken by Sifelani Jirah (Bernard Price Institute). Michael Day (Bernard Price Institute) aided with the plotting of specimen localities on the 'Biozone Map' (Figure 5.1).

Financial support was received from the National Research Foundation (N.R.F.), Palaeontological Scientific Trust (PAST) & University of the Witwatersrand, via a Postgraduate Merit Award.

The following have taken the time to share their knowledge with me on a multitude of topics; Dr Adam Yates, Dr Denise Sigogneau-Russell, Dr Eva Gebauer, Dr Thomas Kemp, and Dr Sandra Jasinowski.

Finally, to my parents, Anthony and Shirley, thank you for your continual words of encouragement and support throughout this project, as well as for the keen interest you have shown towards my studies.

TABLE OF CONTENTS

DECLARATION	ii
ABSTRACT	iii
DEDICATION	iv
ACKNOWLEDGMENTS	v
TABLE OF CONTENTS	vi
LIST OF FIGURES	x
LIST OF TABLES	xvi
INSTITUTIONAL ABBREVIATIONS	xix
STATISTICAL SYMBOLS & ABBREVIATIONS	xx

CHAPTER ONE - INTRODUCTION

1.1	General Introduction	1
1.2	Early Taxonomy of the Gorgonopsia	3
1.3	Genera of the Rubidgeinae	8
1.4	The Genus <i>Aelurognathus</i>	13
1.4.1	<i>Aelurognathus tigriceps</i>	14
1.4.2	<i>Aelurognathus maccabei</i>	16
1.4.3	<i>Aelurognathus brodiei</i>	17
1.4.4	<i>Aelurognathus kingwilli</i>	19
1.4.5	<i>Aelurognathus ferox</i>	20
1.4.6	<i>Aelurognathus alticeps</i>	21
1.5	Summary	23

CHAPTER TWO - MATERIAL & METHODOLOGY

2.1	Specimens Examined	25
2.2	Methods	25
2.2.1	Morphology	27
2.2.2	Measurements	27
2.2.3	Univariate analysis	28
2.2.4	Allometry	28
2.2.5	Biostratigraphy	34

CHAPTER THREE - MORPHOLOGICAL DESCRIPTIONS

3.1	<i>Aelurognathus tigriceps</i>	35
3.2	<i>Aelurognathus maccabei</i>	41
3.3	<i>Aelurognathus brodiei</i>	44
3.4	<i>Aelurognathus kingwilli</i>	48
3.5	<i>Aelurognathus ferox</i>	51
3.6	<i>Aelurognathus alticeps</i>	54
3.7	Summary	57

CHAPTER FOUR - STATISTICAL & ALLOMETRIC ANALYSES

4.1	Introduction	61
4.2	Results of Univariate Analyses	61
4.2.1	Measurements with continuous range	62
4.2.2	Measurements without continuous range	64
4.2.2.1	Antorbital skull length (Variable 3)	65

4.2.2.2 Postorbital skull length (Variable 4)	67
4.2.2.3 Total postorbital length (Variable 5)	69
4.2.2.4 Interorbital width (Variable 12)	70
4.2.2.5 Lateral skull height (Variable 24)	72
4.2.2.6 Orbital length (Variable 26)	73
4.2.2.7 Snout-maxillary canine length (Variable 37)	75
4.2.2.8 Minimum height of the zygomatic arch (Variable 42)	77
4.2.2.9 Diastema between last incisor and canine (Variable 55)	78
4.2.2.10 Diastema between canine and first postcanine (Variable 57)	80
4.2.2.11 Maxillary postcanine series length (Variable 59)	81
4.3 Results of Allometric Analyses	83

CHAPTER FIVE - SPECIMEN LOCALITIES & BIOSTRATIGRAPHY

5.1 Specimens from the <i>Cistecephalus</i> Assemblage Zone	89
5.2 Specimens from the <i>Dicynodon</i> Assemblage Zone	91
5.3 Summary	92

CHAPTER SIX – DISCUSSION

6.1 Morphology	94
6.1.1 Introduction	94
6.1.2 Size of individuals	95

6.1.3	Characters of the skull roof	96
6.1.4	Dentition	97
6.2	Statistical Analyses	100
6.2.1	Univariate analyses	100
6.2.2	Allometry	100
6.3	Systematic Palaeontology	101
6.3.1	Holotype	103
6.3.2	Referred material	103
6.3.3	Revised diagnosis	105
CHAPTER SEVEN – CONCLUSION		106
8	REFERENCES	108
9	APPENDIX A	122
10	APPENDIX B	125
11	APPENDIX C	130
12	APPENDIX D	132
13	APPENDIX E	CD

LIST OF FIGURES

- Figure 1.1 Simplified cladogram of the Therapsida. Modified from Rubidge & Sidor (2001). An alternative cladogram of the interrelationships of the Therapsida is presented in Kemp (2011). 2
- Figure 1.2 Cladogram of the Gorgonopsia. *Biarmosuchus* represents an outgroup. Modified from Gebauer (2007). 10
- Figure 2.1 Illustration of the skull of *Aelurognathus* showing measurements used in the allometric analysis. Redrawn after Gebauer (2007). 31
- Figure 3.1 SAM-PK-2342, *Aelurognathus tigriceps* (Broom & Haughton 1913). Lateral view (top), dorsal view (bottom left), ventral view (bottom right). Scale bars equal 5 cm. 36
- Figure 3.2 SAM-PK-7847, *Aelurognathus tigriceps* (= *A. nyasaensis* Haughton 1926). Lateral view. Scale bar equals 5 cm. 39
- Figure 3.3 SAM-PK-2672, *Aelurognathus tigriceps* (= *A. serratidens* Haughton 1915). Lateral view. Scale bar equals 5 cm. 40
- Figure 3.4 RC 34, *Aelurognathus maccabei* (= *Prorubidgea maccabei* Broom 1940). Lateral view (top), dorsal view (bottom left), ventral view (bottom right). Scale bars equal 5 cm. 42
- Figure 3.5 TMP 1493, *Aelurognathus brodiei* (= *Sycosaurus brodiei* Broom 1941). Lateral view (top), dorsal view (bottom). Scale bars equal 5 cm. 45
- Figure 3.6 RC 60, *Aelurognathus kingwilli* (= *Tigricephalus kingwilli* Broom 1948). Lateral view (top), dorsal view (bottom left), ventral view (bottom right). Scale bars equal 5 cm. 49
- Figure 3.7 RC 62, *Aelurognathus ferox* (= *Smilesaurus ferox* Broom 1948). Lateral view (top), dorsal view (bottom). Scale bars equal 5 cm. 52
- Figure 3.8 RC 81, *Aelurognathus ferox* (= *Smilesaurus maccabei* Broom 1948). Lateral view (top). Scale bar equals 5 cm. 53
- Figure 3.9 RC 82, *Aelurognathus ferox* (= *Pardocephalus wallacei* Broom 1948). Lateral view (top). Scale bar equals 5 cm. 54

Figure 3.10 BP/1/813, <i>Aelurognathus alticeps</i> (=Prorubidgea alticeps Brink & Kitching 1952). Lateral view (top), dorsal view (bottom left), ventral view (bottom right). Scale bars equal 5 cm.	56
Figure 3.11 BP/1/1566, <i>Aelurognathus alticeps</i> (=Prorubidgea alticeps Manten 1958). Undistorted lateral view (top), dorsal view (bottom left), ventral view (bottom right). Scale bars equal 5 cm.	58
Figure 4.1 Average cell plot of the Total skull length (Appendix B, Variable 1). Error bars represent \pm one standard error (Table 4.1).	63
Figure 4.2 Average cell plot of the Antorbital Skull length (Appendix B, Variable 3) Error bars represent \pm one standard error (Table 4.2)	67
Figure 4.3 Average cell plot for postorbital skull length (Appendix B, Variable 4) Error bars represent \pm one standard error (Table 4.3).	68
Figure 4.4 Average cell plot of the total postorbital skull length (Appendix B, Variable 5) Error bars represent \pm one standard error (Table 4.4).	70
Figure 4.5 Average cell plot of the Interorbital width (Appendix B, Variable 12) Error bars represent \pm one standard error (Table 4.5).	71
Figure 4.6 Average cell plot of the Lateral skull height (Appendix B, Variable 24) Error bars represent \pm one standard error (Table 4.6).	73
Figure 4.7 Average cell plot of the Orbital length (Appendix B, Variable 26) Error bars represent \pm one standard error (Table 4.7).	75
Figure 4.8 Average cell plot of the Snout-maxillary canine length (Appendix B, Variable 37) Error bars represent \pm one standard error (Table 4.8).	76
Figure 4.9 Average cell plot of the Minimum height of the zygomatic arch (Appendix B, Variable 42) Error bars represent \pm one standard error (Table 4.9).	78
Figure 4.10 Average cell plot of the Diastema between last incisor and canine (Appendix B, Variable 55) Error bars represent \pm one standard error (Table 4.10).	79

Figure 4.11 Average cell plot of the Diastema between canine and first postcanine (Appendix B, Variable 57) Error bars represent \pm one standard error (Table 4.11).	81
Figure 4.12 Average cell plot of the Maxillary postcanine series length (Appendix B, Variable 59) Error bars represent \pm one standard error (Table 4.12).	82
Figure 5.1 Biozonation map of the southern Karoo Basin showing the localities of the South African specimens of <i>Aelurognathus</i> .	88
Figure D1 Average cell plot of the skull length (Appendix B, Variable 2) Error bars represent \pm one standard error (Table D1).	132
Figure D2 Average cell plot for prepineal skull length (Appendix B, Variable 6) Error bars represent \pm one standard error (Table D2).	133
Figure D3 Average cell plot of the postpineal skull length (Appendix B, Variable 7) Error bars represent \pm one standard error (Table D3).	134
Figure D4 Average cell plot of the intertemporal width (Appendix B, Variable 14) Error bars represent \pm one standard error (Table D4).	135
Figure D5 Average cell plot of the temporal opening length (Appendix B, Variable 18) Error bars represent \pm one standard error (Table D5).	136
Figure D6 Average cell plot of the temporal opening height (Appendix B, Variable 19) Error bars represent \pm one standard error (Table D6).	137
Figure D7 Average cell plot of the maxilla height (Appendix B, Variable 25) Error bars represent \pm one standard error (Table D7).	138
Figure D8 Average cell plot of the orbit length (Appendix B, Variable 27) Error bars represent \pm one standard error (Table D8).	139
Figure D9 Average cell plot of the minimum postorbital bar width (Appendix B, Variable 40) Error bars represent \pm one standard error (Table D9).	140
Figure D10 Average cell plot of minimum suborbital bar height (Appendix B, Variable 41) Error bars represent \pm one standard error (Table D10).	141

Figure D11 Average cell plot of the mandible length (Appendix B, Variable 45) Error bars represent \pm one standard error (Table D11).	142
Figure D12 Average cell plot of the dentary corpus height (Appendix B, Variable 49) Error bars represent \pm one standard error (Table D12).	143
Figure D13 Average cell plot of the dentary thickness (Appendix B, Variable 51) Error bars represent \pm one standard error (Table D13).	144
Figure D14 Average cell plot of the maxillary bicanine breadth (Appendix B, Variable 65) Error bars represent \pm one standard error (Table D14).	145
Figure D15 Average cell plot of the mesiodistal diameter of maxillary canine (Appendix B, Variable 67) Error bars represent \pm one standard error (Table D15).	146
Figure D16 Bivariate plot of the antorbital skull length (Variable 3) against the skull length (Variable 2).	147
Figure D17 Bivariate plot of the postorbital skull length (Variable 4) against the skull length (Variable 2).	148
Figure D18 Bivariate plot of the total postorbital length (Variable 5) against the skull length (Variable 2).	148
Figure D19 Bivariate plot of the prepineal skull length (Variable 6) against the skull length (Variable 2).	149
Figure D20 Bivariate plot of the interorbital width (Variable 12) against the skull length (Variable 2).	149
Figure D21 Bivariate plot of the intertemporal width (Variable 14) against the skull length (Variable 2).	150
Figure D22 Bivariate plot of the temporal opening length (Variable 18) against the skull length (Variable 2).	150
Figure D23 Bivariate plot of the lateral skull height (Variable 24) against the skull length (Variable 2).	151

Figure D24 Bivariate plot of the orbit length (Variable 26) against the skull length (Variable 2).	151
Figure D25 Bivariate plot of the orbit length (Variable 27) against the skull length (Variable 2).	152
Figure D26 Bivariate plot of the snout-maxillary canine length (Variable 37) against the skull length (Variable 2).	152
Figure D27 Bivariate plot of the minimum suborbital bar height (Variable 41) against the skull length (Variable 2).	153
Figure D28 Bivariate plot of the dentary corpus height (Variable 49) against the skull length (Variable 2).	153
Figure D29 Bivariate plot of the dentary thickness (Variable 51) against the skull length (Variable 2).	154
Figure D30 Bivariate plot of the minimum intercorporal breadth (Variable 52) against the skull length (Variable 2).	154
Figure D31 Bivariate plot of the mesiodistal diameter of maxillary canine (Variable 67) against the skull length (Variable 2).	155
Figure D32 Bivariate plot of the skull length (Variable 2) against the prepineal skull length (Variable 6).	156
Figure D33 Bivariate plot of the antorbital skull length (Variable 3) against the prepineal skull length (Variable 6).	157
Figure D34 Bivariate plot of the postorbital skull length (Variable 4) against the prepineal skull length (Variable 6).	157
Figure D35 Bivariate plot of the total postorbital length (Variable 5) against the prepineal skull length (Variable 6).	158
Figure D36 Bivariate plot of the interorbital width (Variable 12) against the prepineal skull length (Variable 6).	158
Figure D37 Bivariate plot of the intertemporal width (Variable 14) against the prepineal skull length (Variable 6).	159
Figure D38 Bivariate plot of the lateral skull height (Variable 24) against the prepineal skull length (Variable 6).	159
Figure D39 Bivariate plot of the Maxilla height (Variable 25) against the prepineal skull length (Variable 6).	160

Figure D40 Bivariate plot of the orbit length (Variable 26) against the prepineal skull length (Variable 6).	160
Figure D41 Bivariate plot of the orbit length (Variable 27) against the prepineal skull length (Variable 6).	161
Figure D42 Bivariate plot of the snout-maxillary canine length (Variable 37) against the prepineal skull length (Variable 6).	161
Figure D43 Bivariate plot of the minimum suborbital bar height (Variable 41) against the prepineal skull length (Variable 6).	162
Figure D44 Bivariate plot of the minimum height of the zygomatic arch (Variable 42) against the prepineal skull length (Variable 6).	162
Figure D45 Bivariate plot of the dentary corpus height (Variable 49) against the prepineal skull length (Variable 6).	163
Figure D46 Bivariate plot of the dentary thickness (Variable 51) against the prepineal skull length (Variable 6).	163
Figure D47 Bivariate plot of the minimum intercorporal breadth (Variable 52) against the prepineal skull length (Variable 6).	164
Figure D48 Bivariate plot of the Diastema between last incisor and canine (Variable 55) against the prepineal skull length (Variable 6).	164
Figure D49 Bivariate plot of the maxillary bicanine breadth (Variable 65) against the prepineal skull length (Variable 6).	165
Figure D50 Bivariate plot of the maxillary canine (Variable 67) against the prepineal skull length (Variable 6).	165

LIST OF TABLES

Table 2.1 List of specimens assigned to <i>Aelurognathus</i> by Gebauer (2007).	26
Table 2.2 List of specimens included in the allometric analyses. TL: total skull length (Variable 2), PL: prepineal skull length (Variable 6), PC: number of maxillary postcanines.	30
Table 3.1 Summary of observed morphological characters in <i>Aelurognathus</i> that have previously been used to diagnose taxa.	60
Table 4.1 Summary statistics for Total skull length (Appendix B, Variable 1).	64
Table 4.2 Summary statistics for Antorbital skull length (Appendix B, Variable 3).	66
Table 4.3 Summary statistics for postorbital skull length (Appendix B, Variable 4).	68
Table 4.4 Summary statistics for total postorbital skull length (Appendix B, Variable 5).	69
Table 4.5 Summary statistics for Interorbital width (Appendix B, Variable 12).	71
Table 4.6 Summary statistics for lateral skull height (Appendix B, Variable 24).	72
Table 4.7 Summary statistics for Orbital length (Appendix B, Variable 26).	74
Table 4.8 Summary statistics for Snout-maxillary canine length (Variable 37).	76
Table 4.9 Summary statistics for Minimum height of the zygomatic arch (Variable 42).	77
Table 4.10 Summary statistics for Diastema between last incisor and canine (Variable 55).	79
Table 4.11 Summary statistics for Diastema between canine and first postcanine (Variable 57).	80

Table 4.12 Summary statistics for Maxillary postcanine series length (Variable 59).	82
Table 4.13 Results of regressions on the skull length (Variable 2.) Expected coefficient of allometry under isometry is 1.0 for all variables.	84
Table 4.14 Results of regressions on the prepineal skull length (Variable 6.) Expected coefficient of allometry under isometry is 1.0 for all variables.	86
Table 5.1 Localities and Assemblage Zones for specimens belonging to <i>Aelurognathus</i> .	87
Table A1 List of African taxa recognised in previous taxonomic revisions of the Gorgonopsia. (For detailed information of the synonimisations that have occurred, refer to original texts).	122
Table C1 List of measurements used in the univariate and bivariate allometric analyses described in Chapter 2 and reported in Chapter 4. Variables that could not be measured are denoted by a dash (-).A table of the raw data is included as a spreadsheet on the accompanying CD (Appendix E).	130
Table D1 Summary statistics for skull length (Appendix B, Variable 2).	132
Table D2 Summary statistics for prepineal skull length (Appendix B, Variable 6).	133
Table D3 Summary statistics for postpineal skull length (Appendix B, Variable 7).	134
Table D4 Summary statistics for intertemporal width (Appendix B, Variable 14).	135
Table D5 Summary statistics for temporal opening length (Appendix B, Variable 18).	136
Table D6 Summary statistics for temporal opening height (Appendix B, Variable 19).	137
Table D7 Summary statistics for maxilla height (Appendix B, Variable 25).	138
Table D8 Summary statistics for orbit length (Appendix B, Variable 27).	139

Table D9 Summary statistics for minimum postorbital bar width (Appendix B, Variable 40).	140
Table D10 Summary statistics for minimum suborbital bar height (Appendix B, Variable 41).	141
Table D11 Summary statistics for mandible length (Appendix B, Variable 45).	142
Table D12 Summary statistics for dentary corpus height (Appendix B, Variable 49).	143
Table D13 Summary statistics for dentary thickness (Appendix B, Variable 51).	144
Table D14 Summary statistics for maxillary bicanine breadth (Appendix B, Variable 65).	145
Table D15 Summary statistics for mesiodistal diameter of maxillary canine (Appendix B, Variable 67).	146

INSTITUTIONAL ABBREVIATIONS

BP Bernard Price Institute for Palaeontological Research, Johannesburg.

RC Rubidge Collection, Wellwood, Graaff-Reinet.

SAM Iziko: South African Museum, Cape Town.

TMP Ditsong: National Museum of Natural History, Pretoria. (Formerly the Transvaal Museum, Pretoria)

STATISTICAL SYMBOLS & ABBREVIATIONS

b_0	slope
b_1	y-intercept
LS	least squares regression
MA	major axis regression
n	sample size
$p(b_0 = 1)$	probability of b_0 deviating from isometry
t	Student's t -test
r	Pearson's product-moment correlation coefficient
RMA	reduced major axis regression
Var.	variance

CHAPTER ONE - INTRODUCTION

1.1 General Introduction

The Gorgonopsia were the dominant carnivorous tetrapod group during the Late Permian (Broom 1932; Kemp 1982, 2005; Gebauer 2007). Different genera showed considerable variation in body size, ranging from about the size of a small dog, to larger than any living mammalian predator (Kemp 2005). Remains attributed to Gorgonopsia have been found mainly in Permian deposits of southern Africa and Russia (Sigogneau 1970; Sigogneau-Russell 1989; Kemp 1982, 2005; Gebauer 2007), as well as similarly aged deposits of Malawi, Niger, Tanzania and Zambia (Sigogneau 1970; Sigogneau-Russell 1989; Gebauer 2007, Smiley *et al.* 2008). Considered as primitive theriodont therapsids (Figure 1.1) (Rubidge & Sidor 2001), the Gorgonopsia possess a number of unique specialisations interpreted as adaptations to preying upon animals of large size (Kemp 1969, 2005). The most noticeable of these specialisations is the exaggerated size of the canines, and the associated jaw mechanism that would have allowed the animal to open its jaws to an angle of nearly 90 degrees (Kemp 1969, 1982). The gorgonopsian dentition also shows modification for a highly predatory lifestyle, with the incisors, canines and postcanines of some individuals bearing serrated edges.

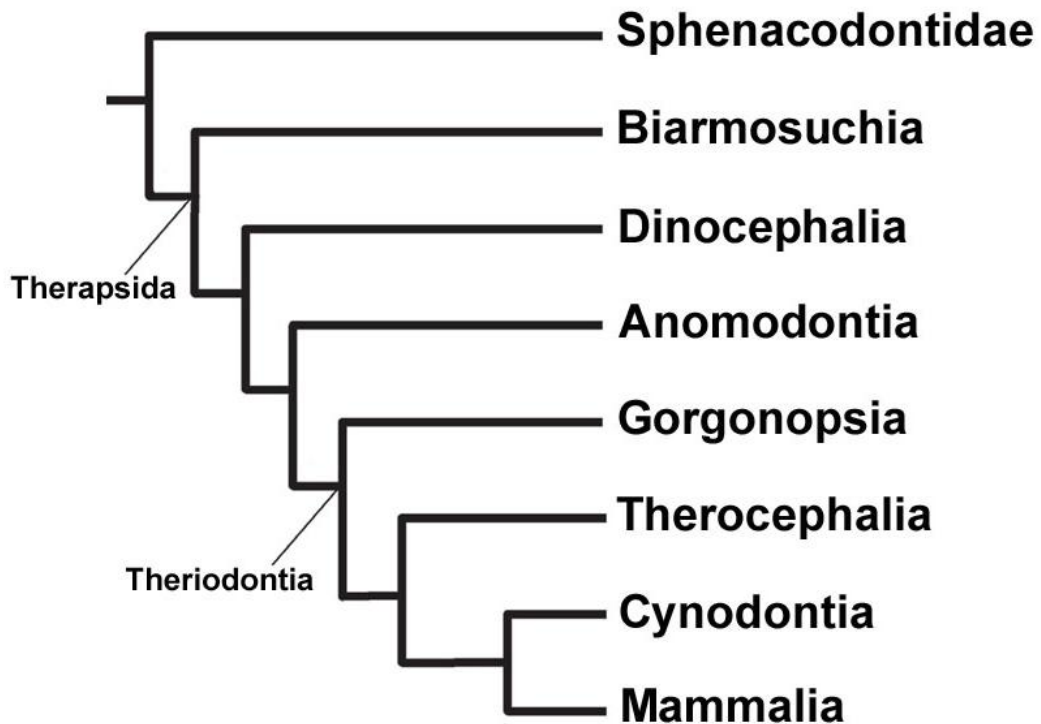


Figure 1.1 Simplified cladogram of the Therapsida. Modified from Rubidge & Sidor (2001). An alternative cladogram of the interrelationships of the Therapsida is presented in Kemp (2011).

The oldest gorgonopsian remains are known from rocks of the *Eodicynodon* Assemblage Zone (AZ) of South Africa, but these are poorly preserved and fragmentary (Rubidge 1988, 1993, 1995). In the overlying *Tapinocephalus* AZ, relatively complete skulls of several genera have been found (Smith & Keyser 1995a; Kemp 2005). These genera are small and are considered to be more primitive than later gorgonopsians, despite displaying the full complement of gorgonopsian features (Kemp 1982, 2005). By the later *Cistecephalus* and *Dicynodon* AZ's, members of the Gorgonopsia had filled the role as the dominant

terrestrial carnivore (Kemp 1982) and showed a high taxonomic diversity, particularly in South Africa (Sigogneau 1970; Sigogneau-Russell 1989; Smith & Keyser 1995b; Kitching 1995; Kemp 2005). By the end of the Permian Period, approximately 251 MYA (Bowring *et al.* 1998) all representatives of the Gorgonopsia had become extinct, leaving no known descendent lineages (Kemp 1982, 2005).

1.2 Early Taxonomy of the Gorgonopsia

When Owen first described *Gorgonops torvus* in 1876, he made it the holotype of a new group, the Tectinaria, based primarily on the shape of the nares which differed from that of the other known Theriodontia at the time. Owen also considered the skull of *G. torvus* to not have any temporal openings. Lydekker (1890) agreed with Owen's (1876) observation of *Gorgonops* lacking temporal openings and considered the specimen to be representative of a transitional group between pareiasaurs and theriodonts.

The group Gorgonopsia was created as a 'suborder' of the Therosuchia by Seeley (1894) in order to separate *Gorgonops* from other 'Therosuchia', on the basis that the, '*temporal vacuities* [of the skull were] *roofed over*,' (p.1014). Broom (1910a) recognised that this specimen of *Gorgonops* was damaged and in fact would have possessed temporal openings if the specimen were complete. Broom also commented on the specimen's affinity to *Titanosuchus* and interpreted the two

taxa as close relatives. As a result, Broom (1910b) placed *Gorgonops* in the suborder Dinocephalia, along with several other genera including *Delphinognathus*, *Tapinocephalus*, *Scapanodon*, *Pelosuchus*, *Archaeosuchus* and *Titanosuchus*. Broom (1913a) reduced the Gorgonopsia to the rank of family, but later (1913b, 1932) re-established Seeley's Gorgonopsia as a valid and distinct suborder of the Therapsida after the discovery of several, more complete specimens.

Broom (1913b) also provided a summary of the differences he observed between the Gorgonopsia and Therocephalia. Later, Broom (1915), provided a formal diagnosis of the Gorgonopsia, which included the following diagnostic characters: frontal excluded from orbital margin by the prefrontal and postfrontal; presence of a distinct preparietal; parietal excluded from the border of the temporal fenestra by the postorbital; no suborbital, nor inter-ptyergoid vacuities; the division of the internal nares by a median bone (Watson 1914, considered the bone to comprise of fused prevomers, while Broom thought that it was a true, unfused vomer); and finally a small pineal foramen. Gorgonopsia were recognised as being morphologically intermediate between the pelycosaur *Dimetrodon* and the cynodont *Diademodon* by Watson (1914).

After the discovery of several additional specimens belonging to the Gorgonopsia, including the near complete skeletons of *Lycaenops ornatus* and *Inostrancevia alexandri*, Broom (1932) was able to provide the first detailed diagnosis of the group.

Between 1913 and the late 1950s a large number of new gorgonopsian taxa were described, often from poorly preserved and fragmentary material. Many of these taxa were established on characters that are now considered trivial, such as skull size and differing numbers of postcanine teeth.

In 1970 Sigogneau published an extensive taxonomic revision of the Gorgonopsia. This revision saw the reduction of genera from 55, with over 100 recognised species, to 69 species placed in 23 genera (Sigogneau 1970). These genera were divided into two newly established subfamilies, the Gorgonopsinae and Rubidgeinae (Sigogneau 1970):

The Gorgonopsinae were characterised by the posterior edge of the cranial roof exceeding beyond the level of the postorbital bar; the ratio of the skull length to interorbital breadth varying from 3.2 to 7; ratio of the skull length to intertemporal breadth varying from 3.1 to 5.1; a poorly developed lateral expansion of the squamosal; cranial arcades that may show thickening; absence of any supraorbital thickening and the ventral projection of the zygomatic arch; as well as the presence of a preparietal, except in *Arctops? ferox*.

Members of the Rubidgeinae were categorised as having a cranial roof that does not exceed the posterior level of the postorbital bar; lateral expansion of the squamosals; a ratio of skull length to interorbital varying from 2.8 to 4.4; the ratio of the skull length to intertemporal breadth varying from 1.8 to 3.8; thick cranial arcades; a deep ventral projection of the posterior of the zygomatic arch; the

development of supraorbital protuberances; if present the preparietal is small; the sphenethmoid extends further posteriorly than in the Gorgonopsinae.

Sigogneau-Russell published a second revision of the Gorgonopsia in 1989, which included some east African and Russian taxa for the first time. The Gorgonopsinae as defined by Sigogneau-Russell (1989) contained 53 species and 18 genera. These genera were grouped together on the basis of having a narrow interorbital and intertemporal width, relative to the total length of the skull. The postorbital, suborbital and zygomatic arches are all slender, with the latter not possessing a ventral expansion of the squamosal. The Inostranceviinae according to Sigogneau-Russell (1989) is comprised of two Russian genera, *Inostrancevia* and *Pravoslavlevia*. Genera of the subfamily have an interorbital width to skull length ratio, and intertemporal width to skull length ratio intermediate to that seen in the Gorgonopsinae and Rubidgeinae. The preorbital length of the skull is much longer than the postorbital length of the skull, whereas in the other subfamilies these lengths are approximately the same (Sigogneau-Russell 1989).

In contrast, the Rubidgeinae, comprising six genera and 18 species, were characterised as having a wide interorbital and intertemporal width relative to the total skull length (Sigogneau-Russell 1989). Some genera have the unusual characteristic of the posterior portion of the skull being almost as wide as the skull is long. It is not known if this was the usual morphology of the skull or if it is due to taphonomic distortion. All the cranial arches are also far more robust than seen

in the Gorgonopsinae, with the zygomatic arch having a large ventral extension towards the posterior end.

In addition to these refinements to her work in 1970, Sigogneau-Russell (1989) excluded the Burnetiidae, Ictidorhinidae, Hipposauridae and Biarmosuchidae from the 'Infraorder' Gorgonopsia, placing them instead in the newly created Biarmosuchia, a taxonomic regrouping informally suggested by Hopson & Barghusen (1986).

The most recent taxonomic revision of Gebauer (2007) entailed the detailed re-description of a gorgonopsian from Tanzania, followed by a morphological comparison of specimens, as well as one of the first comprehensive phylogenetic analyses of the Gorgonopsia, using *PAUP** 4.0b10 (Swofford 1998). For this analysis each genus was represented by the type species, with other specimens assigned to the genus excluded from the analysis. From the analysis, Gebauer (2007) concluded that the genera *Aloposaurus*, *Cyonosaurus* and *Aelurosaurus* did not fall within the crown clade Gorgonopsidae, and were rather to be considered as stem groups of the Gorgonopsidae.

Gebauer's (2007) analysis provided support for only two of the three subfamilies suggested by Sigogneau (1970) and Sigogneau-Russell (1989), the Rubidgeinae and Inostranceviinae. Genera included in Rubidgeinae by Gebauer (2007) were *Sycosaurus*, *Rubidgea*, *Clelandina* and *Aelurognathus*. With the exception of *Aelurognathus*, which was previously considered as a taxon of the

Gorgonopsinae, all these genera were included in the Rubidgeinae by Sigogneau (1970) and Sigogneau-Russell (1989). Autapomorphic characters of the Rubidgeinae given by Gebauer (2007) include: considerable broadening of the posterior of the skull; supraorbital thickening; intertemporal width thicker than the interorbital; thickening of the suborbital, postorbital and zygomatic arches; the posterior margin of the postorbital is orientated anteriorly; and the posterior of the zygomatic arch extends ventrally.

Gebauer (2007) once again synonymised *Pravoslavlevia* with *Inostrancevia* (*sensu* Pravoslavlev 1927), such that she considered the Inostranceviinae to be represented by the single Russian genus *Inostrancevia*. Inostranceviinae is considered as the sister taxon to the Rubidgeinae by Gebauer (2007). Gebauer (2007) felt that the “*peculiar character states*” (p. 243) shown in *Inostrancevia* warranted its separation from the other non-Rubidgeinae taxa, thus placing it as the sole genus of the subfamily Inostranceviinae. Inostranceviinae and the remaining gorgonopsian genera not assigned to the Rubidgeinae, were considered to represent successive outgroups of the Rubidgeinae by Gebauer (2007) (Figure 1.2).

1.3 Genera of the Rubidgeinae

Sigogneau (1970) considered the following genera to be members of the ‘subfamily’ Rubidgeinae; *Broomicephalus* (1 species), *Clelandina* (2 species),

Dinogorgon (3 species), *Prorubidgea* (5 species), *Rubidgea* (3 species) and *Sycosaurus* (3 species). Sigogneau-Russell (1989) later included *Niuksenitia* (1 species) as a member of the subfamily, but this taxon has subsequently been identified as a burnetiamorph biarmosuchian (Ivakhnenko *et al.* 1997; Sidor *et al.* 2004).

The posterior expansion of the skull observed in the members of the Rubidgeinae was interpreted by Sigogneau-Russell (1989) to correspond to an increase in size of the external adductor muscles needed to prevent jaw disarticulation when the jaws were opened to their full extent in order to accommodate the large canines. Thickened postorbital bars are likely to also be associated with an increase in the size of the jaw musculature, as they would allow for greater forces to be exerted upon the arches by the jaw muscles (Sigogneau-Russell 1989). The anterior positioning of the transverse pterygoid apophyses would have allowed for a larger surface area for attachment of the internal adductor muscles (Sigogneau-Russell 1989).

Most specimens considered members of the Rubidgeinae by Sigogneau (1970) and Sigogneau-Russell (1989) were retained by Gebauer (2007). Her taxonomic revision led to several genera of the Rubidgeinae being synonymised, and her phylogenetic analysis placed some genera (*Aelurognathus*) considered as belonging to the Gorgonopsinae by Sigogneau (1970) and Sigogneau-Russell (1989), as sister taxa to genera of the Rubidgeinae *sensu* Sigogneau (1970) and Sigogneau-Russell (1989).

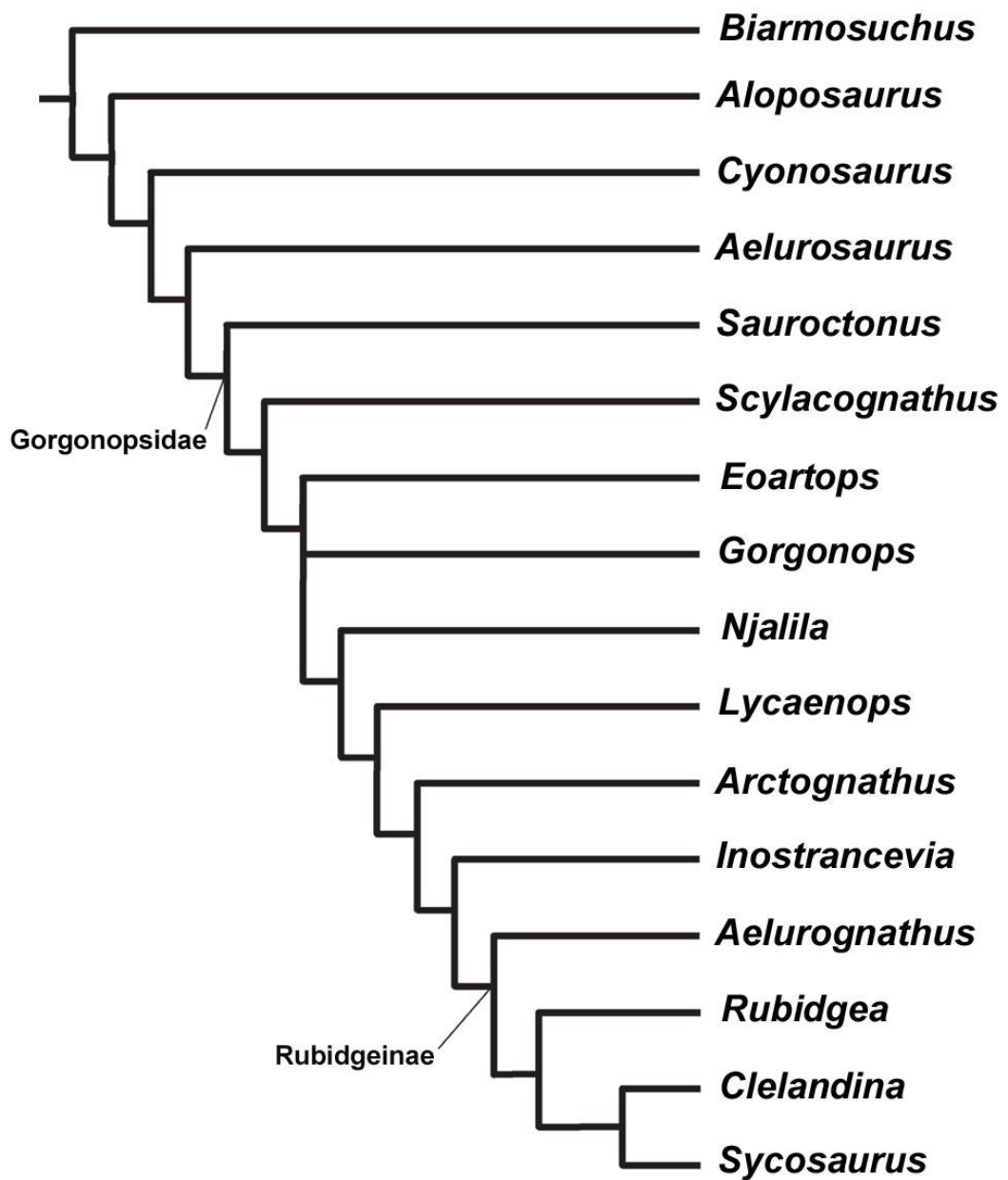


Figure 2.2 Cladogram of the Gorgonopsia. *Biarmosuchus* represents an outgroup.

Modified from Gebauer (2007).

The only species of *Broomicephalus* Brink & Kitching 1953, *B. laticeps* (= *Rubidgea laticeps* Broom 1940, = *Dinogorgon laticeps* Watson & Romer 1956), was synonymised with *Clelandina* Broom 1948. RC 101 and RC 33, respectively the type and referred specimen of *B. laticeps*, are considered by Gebauer (2007) as the holotype and referred specimen of *C. laticeps*. The two species previously attributed to *Clelandina*, *C. rubidgei* Broom 1948 and *C. scheepersi* (= *Dracocephalus scheepersi* Brink & Kitching 1953), remained unchanged. Following Gebauer's (2007) revision, *Clelandina* now comprises four specimens allocated to three species, *C. rubidgei*, *C. laticeps* and *C. scheepersi*.

Dinogorgon Broom 1936 was synonymised with *Rubidgea* Broom 1938 by Gebauer (2007), but *Dinogorgon* has priority. Sigogneau (1970) regarded the possibility of the two genera as being congeneric, but avoided synonymising them as it would have resulted in the genus being based upon the incomplete specimen of *D. rubidgei* (RC 1). Gebauer (2007) considered RC 1 too incomplete for it to be identified to species level and designated it as *Dinogorgon* sp. By doing so Gebauer (2007) was able to negate the law of priority as set out by the I.C.Z.N. and was able to sink *Dinogorgon* into *Rubidgea*, and not *vice versa*. Accordingly *D. quinquemolaris* von Huene 1950 (= *D. oudebergensis* Brink & Kitching 1953) is now considered to be *R. quinquemolaris*, and *D. pricei* (= *Tigrisaurus pricei* Broom & George 1950) is now considered *R. pricei*. The three species of *Rubidgea* recognised by Sigogneau (1970) and Sigogneau-Russell (1989); *R. atrox* Broom 1938, *R. platyrhina* Brink & Kitching 1953 and *R. majora* Brink & Kitching 1953, were all placed into *R. atrox* by Gebauer (2007). *Rubidgea* is still

represented by only three species, but the number of specimens attributed to the genus has risen from three to seven.

Although originally considered to belong in the Gorgonopsinae by Sigogneau (1970) and Sigogneau-Russell (1989), members of the genus *Leontocephalus* Broom 1940 were synonymised with *Sycosaurus* Haughton 1924 by Gebauer (2007). Gebauer (2007) also included the recently re-described *Ruhuhucerberus terror* Maisch 2002 into *Sycosaurus* in her revision. *L. cadlei* Broom 1940 and *L. rubidgei* Sigogneau 1970 are now both considered as *Sycosaurus* sp., while *L. intactus* Sigogneau-Russell 1989 and *R. terror* are now *S. intactus* and *S. terror* respectively. *S. vanderhorsti* Broom & George 1950 was synonymised with the lectotype *S. laticeps* Haughton 1924, while *L. haughtoni* von Huene 1950 was synonymised with *S. kingoriensis* von Huene 1950. The number of species increased in number from three to four and the number of specimens included in the genus increased from three to eight.

The genus *Aelurognathus* will be dealt with in more detail in the following section, giving a brief overview of the genus as well as summarising the taxonomic history of each species in more detail. Specimens mentioned in Table 1 were assigned to *Aelurognathus* by Sigogneau (1970) and Sigogneau-Russell (1989), but are now considered specimens of *Lycaenops* by Gebauer (2007) and will not be dealt with in further detail. A summary of the revisions by Sigogneau (1970), Sigogneau-Russell (1989) and Gebauer (2007) for taxonomy of African gorgonopsian genera is provided in Appendix A.

1.4 The Genus *Aelurognathus*

In both Sigogneau (1970) and Sigogneau-Russell (1989), *Aelurognathus* was included in the Gorgonopsinae. Sigogneau-Russell (1989) gave the following generic diagnosis: heavy skull; long, rounded snout, which is higher than wide; high temporal opening; small orbit; wide interorbital region; wide postorbital and suborbital bars; slender zygomatic arch; narrow participation of the frontal to the orbital margin; long postfrontal; high occiput; low paroccipital process; anteriorly situated transverse apophysis of the pterygoid; fifth nerve foramen not enclosed; thick and massive dentary; and heavy limbs.

The genus was included in the Rubidgeinae after Gebauer's (2007) phylogenetic analysis, and the following diagnosis of the genus was provided: heavily built skull with a snout that is higher than it is wide and convex dorsally. The orbit is small and the temporal foramen is situated high. The septomaxilla has a large posterior extension and the maxilla has a well defined maxillary ridge, anterior to where the maxilla meets the jugal. The postorbital and suborbital bars are robust, while the zygomatic arch is more slender and curves ventrally.

Currently the genus contains six species including: *A. tigriiceps* (5 specimens), *A. kingwilli* (1 specimen), *A. ferox* (5 specimens), *A. maccabei* (1 specimen), *A. alticeps* (2 specimens) and *A. brodiei* (2 specimens).

1.4.1 *Aelurognathus tigriceps*

The holotype of *Aelurognathus tigriceps*, SAM-PK-2342, was described by Broom & Haughton (1913) as *Scymnognathus tigriceps*. SAM-PK-2342 was found on the farm Dunedin, Beaufort West and comprises a crushed and poorly preserved skull with articulated lower jaw and associated postcranial elements. Haughton established the genus *Aelurognathus* in 1924, making *Aelurognathus* (*Scymnognathus*) *tigriceps* the type species. Haughton separated *A. tigriceps* from the genus *Scymnognathus* on the basis that the snout is not as rounded as seen in *S. whaitsi* (= *Gorgonops whaitsi*) Broom 1912.

Haughton described SAM-PK-4334 as the first referred specimen of *Scymnognathus* (*Aelurognathus*) *tigriceps*? in 1918. SAM-PK-4334 is smaller than the SAM-PK-2342, and its locality is uncertain. In 1970 Sigogneau added the previously undescribed specimen, SAM-PK-10071, to *A. tigriceps*. SAM-PK-10071 lacks the posterior portion of the skull and comes from the same provenance as SAM-PK-2342. It is not known if the two specimens were collected from the same outcrop.

SAM-PK-7847 was collected in Malawi, and initially described by Haughton (1926) as *Aelurognathus nyasaensis*. Haughton (1926) wrote that “*the general appearance* [of SAM-PK-7847 is] ...*reminiscent of that of Aelurognathus*” (p. 73) and most likely created the new species, *A. nyasaensis*, due to the specimen having a different number of maxillary postcanine teeth to that of the known

South African species. Sigogneau (1970) renamed the specimen *A. cf. tigriceps*, but later Sigogneau-Russell (1989) resurrected the species as *Aelurognathus nyassaensis* [sic] on the basis that the postorbital bar and zygomatic arch were larger than that of *A. tigriceps*. Sigogneau-Russell also acknowledged that SAM-PK-7847 shared these characters with the Rubidgeinae as at this time *Aelurognathus* was still considered a member of the Gorgonopsinae. Gebauer (2007) finally synonymised SAM-PK-7847 with *A. tigriceps*, regarding the differences seen by Sigogneau-Russell (1989) as individual variation.

The most recent specimen to be referred to *A. tigriceps* was SAM-PK-2672 (Gebauer 2007). Haughton (1915) described SAM-PK-2672, from Dunedin, Beaufort West, as *Scymnognathus serratidens*. The description of the locality in Haughton's (1915) paper is identical to that provided by Broom & Haughton (1913) for the holotype of *A. tigriceps* (SAM-PK-2342). Haughton (1915) noted that despite being a smaller specimen, the "general shape" (p. 88) of SAM-PK-2672 was similar to the type of *S. tigriceps* (= *A. tigriceps*). The differences noted by Haughton (1915) included the more concave antorbital depression of SAM-PK-2672 and that all the teeth of SAM-PK-2672 have serrations on the posterior margin, while the teeth of SAM-PK-2342 do not. Haughton (1915) noted that the absence of serrations on the incisors and canines of SAM-PK-2342 may have been a result of the teeth being worn. In 1924 Haughton reassigned SAM-PK-2672 to the genus *Aelurognathus* and provided a description of the palate.

Broom (1932) commented that *A. serratidens* (SAM-PK-2672) may represent a juvenile form of *A. tigriceps* (SAM-PK-2342), since the specimens were found on the same farm. Broom (1932) noted that the pineal opening of SAM-PK-2672 was larger than that of SAM-PK-2342 and kept the two specimens as separate species. Sigogneau (1970) and Sigogneau-Russell (1989) also remarked on the possibility of SAM-PK-2672 representing a juvenile specimen of *A. tigriceps*, but refrained from synonymising the two taxa on account that SAM-PK-2672 was considered to be sufficiently anatomically different from the referred specimen (SAM-PK-4334), which is a similar size to SAM-PK-2672. Finally Gebauer (2007) synonymised *A. serratidens* with *A. tigriceps*, writing that the difference in size of the preparietals was insufficient to recognise the two species as being separate.

1.4.2 *Aelurognathus maccabei*

Described by Broom in 1940, RC 34 is the only representative of the species and consists of a well preserved and almost completely prepared skull with tightly occluded lower jaw and several cervical vertebrae. Broom's (1940) description of RC 34 likened the overall shape of skull to that of *Scymnognathus* (= *Gorgonops*) *whaitsi*, and noted the well developed preparietal, contribution of the frontal to the orbital margin and the presence of five postcanine teeth. Broom (1940) considered these characters to be sufficient to differentiate RC 34 from the known specimens of *Gorgonopsia*, creating the taxon *Prorubidgea maccabei*, with RC 34 the holotype.

The assignment of RC 34 to *Prorubidgea maccabei* remained unchanged during the taxonomic revisions of Sigogneau (1970) and Sigogneau-Russell (1989), although additional more detailed descriptions of the specimen were provided. Both of these discuss the possibility that *P. maccabei* was more closely related to *Aelurognathus* as opposed to *Scymnognathus* (= *Gorgonops*) as suggested by Broom (1940). Gebauer (2007) noted additional similarities between *Aelurognathus* and *Prorubidgea* that lead to synonymisation of the two genera. RC 34 was made the holotype of *Aelurognathus maccabei* on the basis of its elongated snout, slender lower jaw and broad postorbital bar.

1.4.3 *Aelurognathus brodiei*

Initially named *Sycosaurus brodiei* by Broom (1941), TMP 1493 is a medium sized, poorly preserved skull. The right of the skull has been weathered and the dorsal region of the snout has been reconstructed with plaster. Broom wrote that TMP 1493 resembled *Prorubidgea* (= *Aelurognathus*) *maccabei*, being similar in size and also having five postcanine teeth on the maxilla. Broom (1941) however felt that absence of a preparietal and the meeting of the postfrontal with the prefrontals, to exclude the frontal from contacting the supraorbital margin, meant that the TMP 1493 could not belong to the genus *Prorubidgea*. Instead Broom placed the TMP 1493 in the genus *Sycosaurus*, as TMP 1493 shared the absence of a preparietal and participation of the frontal to the orbital margin, two traits that Broom regarded as diagnostic, with *Sycosaurus laticeps*.

Sigogneau (1970) compared TMP 1493 to specimens of *Arctops? ferox* and *Prorubidgea*, finally noting that the cranial features and dimensions of TMP 1493 were too dissimilar from a referred specimen of *Arctops? ferox* (TMP 132) for TMP 1493 to be placed in *Arctops*. Sigogneau (1970) wrote that the absence of preparietal and supraorbital frontal did not have generic value and considered TMP 1493 a species of *Prorubidgea* morphologically intermediate to the three species; *P. maccabei*, *P. robusta* and *P. alticeps*. As already discussed, Gebauer (2007) felt that *Prorubidgea* and *Aelurognathus* were congeneric, and as such TMP 1493 was made the holotype of *Aelurognathus brodiei*.

There is a single specimen referred to *Aelurognathus brodiei*, BP/1/2190, by Gebauer (2007). Described as *Prorubidgea robusta* by Brink & Kitching (1953), noting several similarities between BP/1/2190 and *Aelurognathus* (= *Prorubidgea*) *maccabei* (RC 34). BP/1/2190 was placed in the new species *P. robusta* as the position of the nasofrontal suture and shape of the postfrontals and prefrontals differed from those of *A. maccabei*. Brink & Kitching (1953) also wrote that the proportions of the orbit and temporal opening of BP/1/2190 differed from those of *A. maccabei*, and that these differences were too large to be as a result of variation in age or sex.

Prorubidgea robusta was recognised as a valid taxon by Sigogneau (1970), though the diagnosis of the species was amended. Sigogneau (1970) did not agree with Brink & Kitching's (1953) interpretation of a large preparietal, considering it to be absent. Sigogneau (1970) also considered BP/1/2190 to most closely

resemble *A. maccabei*. In contrast, Gebauer (2007) considered BP/1/2190 to more closely resemble *A. brodiei* (TMP 1493) as both specimens have a short lacrimal, broad postorbital bar and lack a preparietal, leading Gebauer (2007) to synonymise the two species.

1.4.4 *Aelurognathus kingwilli*

First described by Broom (1948) RC 60 is a nearly complete skull that has been subjected to extensive lateral compression. Broom (1948) compared RC 60 to *Aelurognathus tigriceps* (SAM-PK-2342), but did not feel that it could be referred to the genus as RC 60 has three maxillary postcanine teeth and no preparietal, while the type for *A. tigriceps* has four maxillary postcanine teeth and a large preparietal present. Broom also compared RC 60 to *Broomisaurus* (= *Leontocephalus*) *rubidgei*, but felt that despite RC 60 having the same number of maxillary postcanines as *Broomisaurus*, it could not belong to the genus as it lacked a preparietal, which is present in *B. rubidgei*. Based on having three maxillary postcanine teeth and no preparietal, Broom (1948) created the genus *Tigricephalus* for RC 60, naming it *Tigricephalus kingwilli*.

In Sigogneau's (1970) work, RC 60 was compared with specimens of *Lycaenops ornatus*, *Lycaenops angusticeps* and *Arctops? ferox*. Sigogneau (1970) considered RC 60 to belong to *Lycaenops*, despite the thickened suborbital bar, broad skull roof, shape of the zygomatic arch and angle of the occiput being similar to *A.?*

ferox. Sigogneau (1970) hesitated to synonymise the two taxa as she did not feel that the specimens of *A.?* *ferox* adhered to the diagnosis for *Lycaenops*, while RC 60 did. As such RC 60 was redescribed as *Lycaenops kingwilli* and *Arctops?* *ferox* remained unchanged by Sigogneau (1970).

Characters used by Sigogneau (1970) to define *L. kingwilli* as a separate species were considered by Gebauer (2007) as only good enough to describe the specimen to the generic level. Gebauer (2007) also felt that these characters were more characteristic of the genus, *Aelurognathus*, and that in fact the specimen showed no characters observed in *Lycaenops*, except those common to the two genera. As a result Gebauer (2007) reassigned the specimen to *Aelurognathus*.

1.4.5 *Aelurognathus ferox*

First described by Broom (1948) as *Smilesaurus ferox*, the holotype (RC 62) consists of a medium to large sized skull with attached lower jaw and some postcranial elements, which were omitted from Broom's (1948) description. The skull has undergone some lateral compression, with the jugal, squamosal and articular of the right side being damaged and both postorbital bars are incomplete. The occipital region and palate of the specimen are not visible due to the presence of several articulated cervical vertebrae. Broom (1948) felt that RC 62 represented a new taxon, as it had only two maxillary postcanines and he considered the structure of the jaw to be different from any previously described gorgonopsian.

While Broom (1948) thought that RC 34, *Aelurognathus* (=Prorubidgea) *maccabei* represented a close relative to RC 62, in 1970, Sigogneau interpreted RC 62 to more closely resembled the Gorgonopsinae genus, *Arctops*, renaming RC 62 *Arctops? ferox*. Sigogneau (1970) also assigned four additional specimens to *A.? ferox*, the previously described specimens, RC 81 and RC 82, and two previously undescribed specimens, BP/1/2465 and TMP 132.

Another large gorgonopsian, RC 81, was described by Broom in 1948, and in this work Broom noted the close morphological similarities between RC 81 and RC 62. Broom stated that the similarities were sufficient for the two specimens to represent the same genus, but as “*the proportions of the bone differ considerably,*” (p. 602), felt that RC 81 represented a different species. RC 81 was named *Smilesaurus maccabei* by Broom (1948).

1.4.6 *Aelurognathus alticeps*

According to Gebauer’s (2007) taxonomic revision there are two specimens currently assigned to *A. alticeps*. The first specimen, BP/1/813, was originally described as *Lycaenops alticeps* by Brink & Kitching (1953). Found in *Cistecephalus* AZ beds (Brink & Kitching 1953; Smith & Keyser 1995b) on the farm Hoeksplaas, Murraysburg District. BP/1/813 displays slight lateral compression. The zygomatic arch and postorbital bar of both sides have been reconstructed. Both angulars of the lower jaw are incomplete, as is the posterior

ramus of the left dentary. Brink & Kitching (1953) compared the skull with other members of the genus *Lycaenops*, as they felt it resembled the genus superficially in structure, but differed in the proportions of the skull. This new skull showed a new suite of characters for the genus, such the nasal being as broad anteriorly as it is posteriorly and narrow in the middle. The name of BP/1/813 remained unchanged until 2007, when Gebauer synonymised *Prorubidgea* with *Aelurognathus*, thus BP/1/813 became *Aelurognathus alticeps*.

Manten (1958) described BP/1/1566 as a new taxon, *Prorubidgea brinki*. In this description, Manten compared BP/1/1566 extensively with RC 34, the holotype of *Aelurognathus maccabei* (= *Prorubidgea maccabei*), but not with BP/1/813. Several differences between BP/1/1566 and RC 34 were noted by Manten (1958) including longer nasals and shorter frontals in BP/1/1566.

Sigogneau (1970) also compared BP/1/1566 to RC 34, and like Manten (1958), considered BP/1/1566 to be of the same genus, but a different species. In contrast to Manten (1958), Sigogneau compared BP/1/1566 to BP/1/813, noticing that despite the difference in size, the two specimens shared certain morphological characters. These included small diameter of the orbit, large temporal openings and a narrow intertemporal region. As such, Sigogneau (1970) felt that BP/1/1566 shared sufficient characters with BP/1/813 for it to be renamed *Prorubidgea alticeps*? Upon further investigation, Sigogneau-Russell (1989) determined the breadth of the intertemporal region of BP/1/813 to be indeterminable, either due to incomplete preservation or lateral compression. Sigogneau-Russell (1989) also

reconsidered her 1970 renaming of BP/1/1566, resurrecting the name *Prorubidgea brinki*. No reason for this change in nomenclature is provided by Sigogneau-Russell (1989), with the revised diagnosis of *P. brinki* being almost identical to that of *P. alticeps*. Due to the numerous morphological similarities between BP/1/813 and BP/1/1566, as well as the apparent lack of justification by Sigogneau-Russell (1989) to resurrect *P. brinki*, Gebauer (2007) considered both specimens as representatives of *P. alticeps*.

1.5. Summary

From the taxonomic histories of the 16 specimens assigned to *Aelurognathus* by Gebauer (2007) it can be seen that many of the taxa have been compared to one another at some point in earlier studies. This outline also provides an insight into how convoluted the taxonomy of the Gorgonopsia has been as a result of too much taxonomic weight being placed on conservative cranial morphology.

In view of the fact that the genus *Aelurognathus* has 16 specimens and six described species, this study was undertaken in order to better understand the degree of morphological variation among species, and to utilise this information to possibly refine the taxonomy of the genus. As *Aelurognathus* represents the genus of Rubidgeinae with the largest number of referred specimens and species, it will be used to explore the degree of morphological variation that can occur within a single genus.

From the small number of specimens of *Aelurognathus* available it appears to that too many species are currently recognised. This may be due to the fact that specimens from different collections have not previously been studied together and compared directly with one another. Accordingly for this study most of the specimens were loaned to the Bernard Price Institute, where they were able to be studied alongside one another.

CHAPTER TWO - MATERIAL & METHODOLOGY

2.1 Specimens Examined

Gebauer (2007) assigned a total of 16 specimens to *Aelurognathus* (Table 2.1), which are all housed in South African collections. All specimens were examined except for TMP 132, which could not be located. The following South African palaeontological collections were visited in order to study specimens of *Aelurognathus*: Bernard Price Institute for Palaeontological Research (BP), Johannesburg; Rubidge Collection (RC), Wellwood, Graaff-Reinet; Iziko: South African Museum (SAM), Cape Town and the Ditsong: National Museum (TMP), Pretoria. Selected specimens were taken on loan for further preparation.

2.2 Methods

This study used both qualitative (morphological comparisons) and quantitative (statistical techniques) methods in order to elucidate differences/ similarities between the species of *Aelurognathus* as defined by Gebauer (2007). In addition, specimens whose localities were known were recorded on a digital map of South Africa.

Table 2.1 List of specimens assigned to *Aelurognathus* by Gebauer (2007).

Collection number	Alternate number	Current name	Synonym(s)
BP/1/813	BPI 261 ^a	<i>A. alticeps</i>	<i>Lycaenops alticeps</i> (Brink & Kitching 1953); <i>Prorubidgea alticeps</i> (Sigogneau 1970)
BP/1/1566	BPI 289 ^a	<i>A. alticeps</i>	<i>Prorubidgea brinki</i> (Manten 1958); <i>Prorubidgea alticeps?</i> (Sigogneau 1970)
BP/1/2190	BPI 249 ^a	<i>A. brodiei</i>	<i>Prorubidgea robusta</i> (Brink & Kitching 1953)
BP/1/2465	BPI 226 ^a	<i>A. ferox</i>	<i>Arctops? ferox</i> (Sigogneau 1970)
RC 34	-	<i>A. maccabei</i>	<i>Prorubidgea maccabei</i> (Broom 1940) <i>Prorubidgea pugnax</i> ^b (Broom 1940)
RC 60	-	<i>A. kingwilli</i>	<i>Tigricephalus kingwilli</i> (Broom 1948); <i>Lycaenops kingwilli</i> (Sigogneau 1970)
RC 62	-	<i>A. ferox</i>	<i>Smilesaurus ferox</i> (Broom 1948); <i>Arctops? ferox</i> (Sigogneau 1970)
RC 81	-	<i>A. ferox</i>	<i>Smilesaurus maccabei</i> (Broom 1948); <i>Arctops? ferox</i> (Sigogneau 1970)
RC 82	-	<i>A. ferox</i>	<i>Pardocephalus wallacei</i> (Broom 1948); <i>Arctops? ferox</i> (Sigogneau 1970)
SAM-PK-2342	SAM 3342 ^c	<i>A. tigriceps</i>	<i>Scymnognathus tigriceps</i> (Broom & Haughton 1913)
SAM-PK-2672	SAM 2792 ^d	<i>A. tigriceps</i>	<i>Scymnognathus serratidens</i> (Haughton 1915); <i>Aelurognathus serratidens</i> (Haughton 1924))
SAM-PK-4334	-	<i>A. tigriceps</i>	<i>Scymnognathus tigriceps?</i> (Haughton 1918)
SAM-PK-7847	-	<i>A. tigriceps</i>	<i>Aelurognathus nyasaensis</i> (Haughton 1926); <i>Aelurognathus cf. tigriceps</i> (Sigogneau 1970); <i>Aelurognathus nyassaensis</i> (Sigogneau-Russell 1989) <i>Aelurognathus nyassicus</i> ^e (Gebauer 2007)
SAM-PK-10071	-	<i>A. tigriceps</i>	-
TMP 132	-	<i>A. ferox</i>	<i>Arctops? ferox</i> (Sigogneau 1970)
TMP 1493	TMP 149 ^f	<i>A. brodiei</i> ^g	<i>Sycosaurus brodiei</i> (Broom 1941); <i>Prorubidgea brodiei</i> (Sigogneau 1970)

a Previous numbering system used by the BP, appearing in older literature.

b Labeled *P. pugnax* in Figures 11 & 12, p. 170 of Broom (1940).

c Number used by Sigogneau-Russell (1989), p. 66 and Gebauer (2007), p. 50 & 157.

d Number used by Sigogneau (1970), p. 168; Brink (1986), J213A211A6; Sigogneau-Russell (1989), p. 67 and Gebauer (2007), p. 157, 166-168 & 184.

e Name appears in Gebauer (2007), p. 225.

f Number appears in Gebauer (2007), p. 187.

g Spelt *P. brodiei* in Sigogneau-Russell (1989), p. 107 and *A. brodiei* in Gebauer (2007), p. 158, 183 & 187.

2.2.1 Morphology

Morphological differences between all 15 examined specimens were noted and compared with one another. Brief descriptions of the holotype of each of the six species recognised by Gebauer (2007) are provided in Chapter 3. Notes where the referred specimens may differ from the description of the type are provided where necessary.

2.2.2 Measurements

In order to test for allometric patterns in the chosen 16 skulls of *Aelurognathus*, a list of approximately 70 measurements (Appendix B) concerning the cranium and mandible was established based on measurements used in previous studies dealing with ontogeny and relative growth regarding both extinct and extant synapsid taxa (Sigogneau 1970; Grine *et al.* 1978; Tollman *et al.* 1979; Abdala & Giannini 2000, 2002; Giannini *et al.* 2004; Flores *et al.* 2006).

Measurements were taken to the nearest millimetre, using a sliding vernier calliper. Each specimen was measured at least three times in order to minimise error (Simpson *et al.* 1960). This was repeated for all measurements. In order to further account for error each replication of the measurements per specimen was taken on a different day. Replicates of each measurement were averaged together,

following Dodson (1975), prior to being used for statistical analyses. A table of the data used in the statistical analyses appears in Appendix C.

2.2.3 Univariate analysis

Statistical analysis of the measurements was undertaken using PAST v 2.02 (Hammer *et al.* 2001). Univariate analyses were performed on each measurement to determine any numerical relationships that may exist between the different specimens used in this study. The following descriptive statistics are reported in tabular form for each species, as well as a collective sample under the heading ‘Total’; sample size (n), number of specimens missing/ excluded from the sample (# missing), total sum of values (Sum), average value (Average) maximum recorded measurement (Max. val.), minimum recorded value (Min. val.), range of recorded values (Range), variance (Var.), standard deviation (Std. dev.) and the standard error (Std. error).

2.2.4 Bivariate Allometry

A total of 27 measurements of the skull, intended to represent the shape of the skull in all relevant dimensions, were used in two separate analyses of allometry to investigate growth responses of different parts of the skull to the overall increase in size. Most of these measurements have been used in previous

allometric studies of extinct (Abdala & Giannini 2000, 2002) and extant (Flores *et al.* 2006) tetrapod taxa. Only measurements of the skull were used as many of the specimens lack associated postcranial material. All measurements were taken using the procedure described above. When possible, symmetrical variables (*e.g.* orbit diameter) were measured for both sides of the skull. In such instances, if no taphonomic distortion was evident, the measurements were averaged as per Dodson (1975). Specimens measured varied greatly in quality and completeness of preservation. If any distortion was exhibited on a specimen and was thought to possibly affect the outcome of the analyses, the measurement was not used.

During the analyses, previous taxonomic assignments of specimens were ignored. For visual purposes the data points are labelled in the figures accompanying the results (Chapter 4.3). All specimens were treated as single taxon, representing a null hypothesis of there being only one species of *Aelurognathus*. Thus, if all specimens are adequately described by the allometry functions (without outliers, systematic trends in residuals or size gaps), they may be considered a growth series of a single taxon.

Initially only specimens for which the total skull length (Variable 2, Appendix B) was measurable were included in the analysis of allometry as this measurement was used as the independent variable (Simpson *et al.* 1960; Radinsky 1981a, b; Emerson & Bramble 1993; Abdala & Giannini 2000, 2002; Giannini *et al.* 2004). Due to incomplete preservation the total skull length was recorded for only nine of the total specimens measured (Table 2.2). Sample size (*n*) for each analysis

ranged between 9 and 7, as only variables that were measured in 75% (n = 7) or more of the specimens were considered. Of the total 27 variables, only 20 had a sample size of 7 or more (Figure 2.1).

Table 2.2 List of specimens included in the allometric analyses. TL: total skull length (Variable 2), PL: prepineal skull length (Variable 6), PC: number of maxillary postcanines.

Specimen	Taxon	TL	PL	PC
RC 81	<i>A. ferox</i>	343	321	2
BP/1/2465	<i>A. ferox</i>	300	280	2
RC 62	<i>A. ferox</i>	299	255	2
RC 60	<i>A. kingwilli</i>	272	235	3-4
SAM-PK-2342	<i>A. tigriceps</i>	264	241	4
RC 34	<i>A. maccabei</i>	260	234	4-5
SAM-PK-7847	<i>A. tigriceps</i>	-	230	1
BP/1/2190	<i>A. brodiei</i>	-	212	3-5
BP/1/1566	<i>A. alticeps</i>	237	198	4-5
SAM-PK-2672	<i>A. tigriceps</i>	-	195	4
SAM-PK-10071	<i>A. tigriceps</i>	203	188	2
BP/1/813	<i>A. alticeps</i>	-	185	4-5
SAM-PK-4334	<i>A. tigriceps</i>	195	184	2

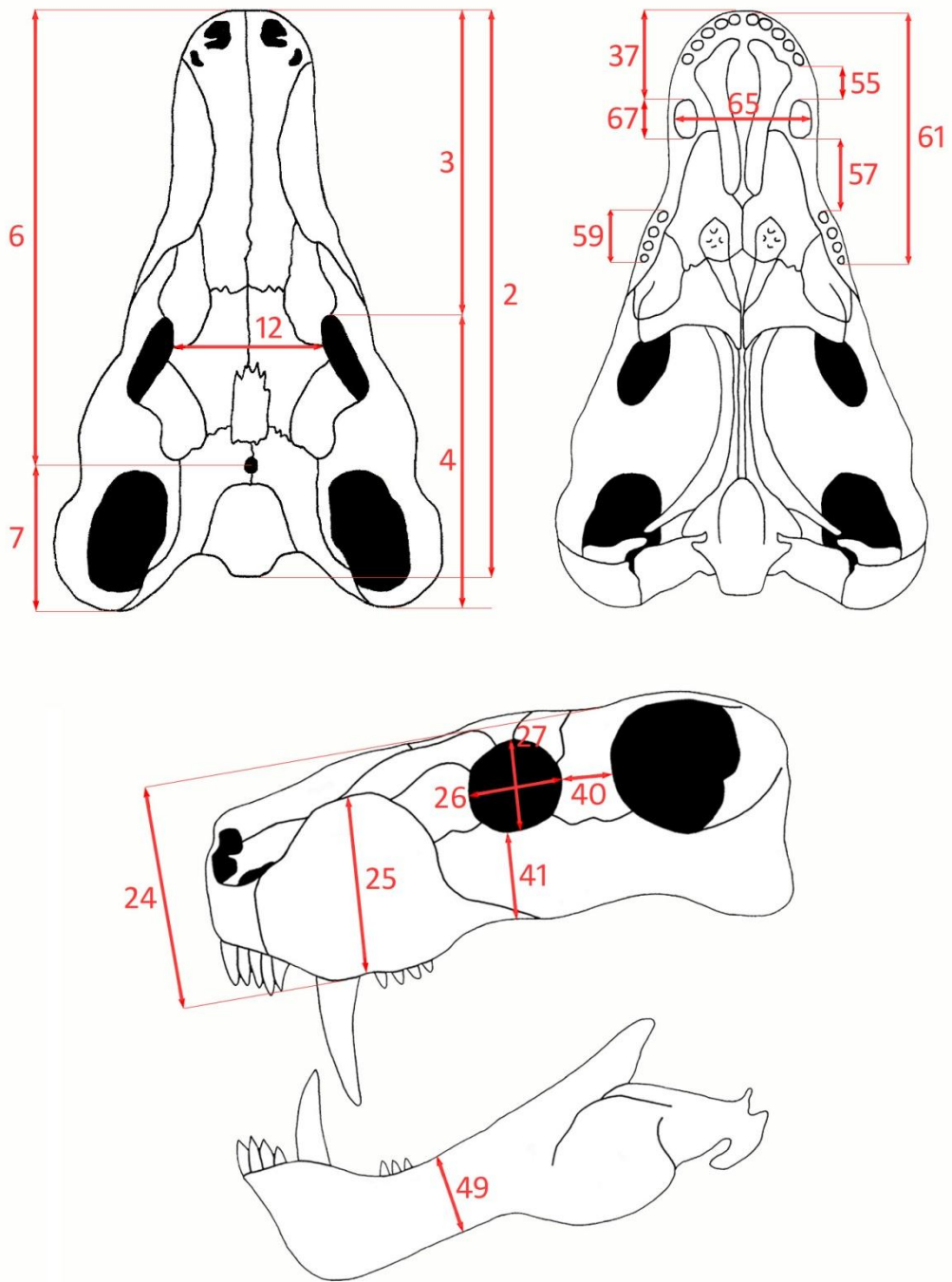


Figure 2.1 Illustration of the skull of *Aelurognathus* showing measurements used in the allometric analysis. Redrawn after Gebauer (2007).

Due to the low number of specimens for which the total skull length was preserved a second analysis of allometry was undertaken using the prepineal skull length (Variable 6, Appendix B). Prepineal skull length was chosen as an alternative independent variable as in many specimens, it was the region of the squamosals which was damaged preventing accurate measurement of the total skull length. Dodson (1976) used a similar approach in his work on the skull of *Protoceratops*, where the bony frills of the specimens were seldom completely preserved. Using the prepineal skull length increased the number of specimens included in the analysis to 13. Again, only variables which could be measured in 70% ($n = 10$) or more of the specimens are considered (Figure 2.1). The exception being the inclusion of Variable 2 ($n = 9$) for comparative purposes.

The independent variable is assumed to reflect overall size (Simpson *et al.* 1960; Radinsky 1981a, b; Emerson & Bramble 1993; Abdala & Giannini 2000, 2002; Giannini *et al.* 2004). The relation of each cranial variable with regard to the length of the independent variable was studied using the allometry equation;

$$\log y = \log b_0 + b_1 \log x + \log e \quad [1]$$

which is derived from the power growth equation (Huxley 1932, Alexander 1985);

$$y = b_0 x^{b_1} e \quad [2]$$

by the calculation of the base 10 logarithm in both members. In the equation b_0 is the y -intercept, b_1 the slope of the line (coefficient of allometry) and e represents an error term that is assumed to be multiplicative (i.e. it may interact with the independent term, for instance, by increasing variance with size). Significance of slopes was assessed using one-tailed t -tests. Deviations from isometry (i.e. an unequal rate of change of the independent and dependent variables) were evaluated with one-tailed t -tests. This was accomplished by setting the null coefficient equal to the value expected under geometric similarity, i.e. unity for linear measurements (see Alexander 1985). ‘Positive’ and ‘negative’ coefficients of allometry are significantly greater or less than those expected by isometry, i.e. statistically different from unity (Emerson & Bramble 1993).

The analysis described above meets ordinary least squares criteria, assuming among other points, that (1) there is a dependence relationship, and (2) the independent variable are measured without error. Although the first assumption is more likely to be met, since all variables are expected to change as a function of overall size, the second assumption is certainly less realistic. Therefore ordinary least squares (LS) parameter estimation has been complemented by computing coefficients using reduced major axis (RMA). This is an alternative approach for these types of data, since RMA does not assume a dependency relationship between variables, and allows for variation in both x - and y -axes (Kermack & Haldane 1950).

Since least squares regression only minimises error with regard to the y-variable, while RMA and MA regression techniques minimise error for both variables simultaneously. As a result, the coefficients of allometry calculated using RMA and MA may be considered as better approximations of the true coefficient of allometry for these relationships (Radinsky 1981a, b; Niklas 1994). All data for the allometric analyses were log transformed, such that the relationships could be converted to linear relationships.

2.2.5 Biostratigraphy

Using the Karoo vertebrate GIS database established by Nicolas (2007), the known localities of specimens identified as *Aelurognathus* by Gebauer (2007) were plotted onto the vertebrate biozone map of South Africa of van der Walt *et al.* (2010) using ARC-GIS (ESRI). In most cases only the name of the farm is known, and not the exact co-ordinates of the outcrop from which the fossil was recovered.

CHAPTER THREE - MORPHOLOGICAL DESCRIPTIONS

In this chapter a description of the skull morphology for the holotype of each species of *Aelurognathus*, as defined by Gebauer (2007) is presented. Each description also highlights notable differences observed between the morphology of the type and the referred specimens.

3.1 *Aelurognathus tigriceps*

Due to the poor state of preservation of the holotype (SAM-PK-2342), many of the cranial sutures are not discernible on the dorsal surface of the cranium, particularly the anterior snout and interorbital and intertemporal regions where the bone is damaged (Figure 3.1).

In dorsal view, the suture between the septomaxilla and nasal are only partially visible. As mentioned by Broom & Haughton (1913), the septomaxilla is large, and extends back to the level of the canine. The contact between the nasal and frontal is not clearly visible, but it appears that the nasal would have reached the anterior border of the orbital margin. The frontal contributes to the dorsal margin of the orbit. An elongated preparietal is present and is surrounded by the frontals and parietals. While Sigogneau (1970: Figure 92) figured parietals not extending anteriorly beyond the temporal fenestra, Gebauer (2007: Figure 42A) shows the parietals reaching far beyond the temporal fenestrae and to the posterior limit of



Figure 3.1 SAM-PK-2342, *Aelurognathus tigriiceps* (Broom & Haughton 1913). Lateral view (top), dorsal view (bottom left), ventral view (bottom right). Scale bars equal 5 cm.

the interorbital space. My observations of the material support Sigogneau's (1970) interpretation. The parietal does not extend beyond the border of the temporal fenestra, even at its most anterior point where it meets the frontal adjacent to the preparietal. Behind the preparietal a prominent pineal opening is present, and is situated between the temporal fenestrae, as figured in Sigogneau (1970).

When viewed laterally, the snout of SAM-PK-2342 is deepest at the diastema behind the canine. The orbit is small and round, and the temporal foramen is large. Of the cranial arcadia, the suborbital bar is the thickest, being twice as thick as the postorbital and zygomatic bars. Five conical incisors are present on the premaxilla. The maxilla forms the largest component of the antorbital region. A long posterior process of the maxilla extends posteriorly beyond the orbit and terminates below the postorbital bar. This process of the maxilla forms the ventral margin of the suborbital bar. The maxilla bears a large canine and four small, conical postcanines. Broom & Haughton (1913) noted that the suture between the lacrimal and prefrontal was not clear, but inferred that both bones would have been large. The contact between the lacrimal and jugal is not clear. The jugal forms the majority of the suborbital bar, extending posteriorly to make contact with the squamosal, which together form the ventral margin of the temporal foramen.

Sigogneau (1970) noted the heavy appearance of the skull, mentioning the long snout with a rounded dorsal contour, high temporal opening, small orbit, thick suborbital bar, slender zygomatic arch, relatively thick postorbital bar, moderate

intertemporal width, long and narrow postfrontal, constriction of the postorbital posteriorly, long prefrontal, posteriorly situated nasofrontal suture, small supraorbital portion of the frontal, square lacrimal, vertical occiput, tall interparietal, diagonal paroccipital process, long basisphenoid fossa, anteriorly situated transverse apophyses without teeth, and narrow ectopterygoid.

The first specimen allocated to *Scymnognathus tigriceps* as a referred specimen by Haughton (1918) was SAM-PK-4334. Sigogneau (1970) confirmed this suggestion and pointed out that SAM-PK-4334 resembled SAM-PK-2342 in most characters. In 1970, Sigogneau also referred an undescribed specimen, SAM-PK-10071, to *A. tigriceps*.

Aelurognathus nyasaensis (SAM-PK-7847) was described by Haughton (1926). The specimen is large and incomplete (Figure 3.2), with the posterior portion of the skull having been weathered away. Haughton (1926) mentioned that it differed from *A. tigriceps* in having a single postcanine tooth. Haughton also described the skull as having a snout that was higher than wide, an elongated lacrimal, presence of a preorbital fossa, slight protrusion of the prefrontal over the orbital margin, a narrow nasal, participation of the frontal in the formation of the supraorbital margin, a small preparietal, and a large lower jaw with a deep mandibular symphysis. Sigogneau (1970) considered SAM-PK-7847 to closely resemble *A. tigriceps*, referring to it as *Aelurognathus cf. tigriceps*. Sigogneau (1970) did not synonymise the two taxa however, as she interpreted the postorbital bar of SAM-PK-7847 to be broader than that of *A. tigriceps*. In 1989, Sigogneau-Russell

resurrected the species as *Aelurognathus nyassaensis* [sic], based on its overall more robust appearance.



Figure 3.2 SAM-PK-7847, *Aelurognathus tigriceps* (= *A. nyassaensis* Haughton 1926). Lateral view. Scale bar equals 5 cm.

Haughton (1915) initially described SAM-PK-2672 as a new species, *Scymnognathus serratidens*. The specimen is poorly preserved, with much of the skull posterior of the postorbital bar missing (Figure 3.3). Haughton (1915) noted the small size of the SAM-PK-2672, and went on to describe the specimen as having four postcanines, a small contribution by the frontal to the supraorbital margin, a large preparietal, separated from the parietal foramen, a preorbital fossa,



Figure 3.3 SAM-PK-2672, *Aelurognathus tigriceps* (= *A. serratidens* Haughton 1915). Lateral view. Scale bar equals 5 cm.

long nasals, a weak mandibular symphysis and a ridge on top of the snout. In 1924 Haughton provided figures of the lateral, dorsal and ventral views and added a description of the palate. The palate was interpreted as having a deep and narrow palatal fossa, no teeth on the palatines, teeth present on the pterygoid tuberosities, long choanae and massive transverse apophyses. In 1924 Haughton renamed SAM-PK-2672 as *Aelurognathus serratidens*.

Broom (1932) considered *A. tigriceps* and *A. serratidens* to be closely related, with the latter possibly representing a juvenile individual of *A. tigriceps*. Despite

this, Broom felt that the disparity in sizes of the pineal opening was too great to warrant the synonymisation of the two taxa. Sigogneau (1970) too mentioned that SAM-PK-2672 shared a number of attributes with *A. tigriceps*, reiterating Broom's (1932) suggestion of it being a younger individual. However, Sigogneau (1970) did not unite the two taxa, as SAM-PK-2672 did not correspond well with SAM-PK-4334, a similarly sized specimen of previously referred to *A. tigriceps* by Houghton (1918)

3.2 *Aelurognathus maccabei*

This species was first described as *Prorubidgea maccabei* by Broom 1940 and is represented only by specimen RC 34, which consists of a well preserved and almost completely prepared skull with tightly occluded lower jaw and several cervical vertebrae (Figure 3.4).

The right premaxilla and region of the nares have been damaged, and as a result the roots of the incisors are visible. A small region of the maxilla has been filled using plaster. The maxilla is at its deepest behind the large canine, where the dorsal border is at the same height as the dorsal border of the orbit. Five small postcanines are present. A prominent maxillary ridge is present above the last two postcanines in the series, and extending posteriorly along the posterior process of the maxilla. The posterior process of the maxilla extends well beyond the anterior margin of the orbit, but does not reach the posterior orbital margin. The

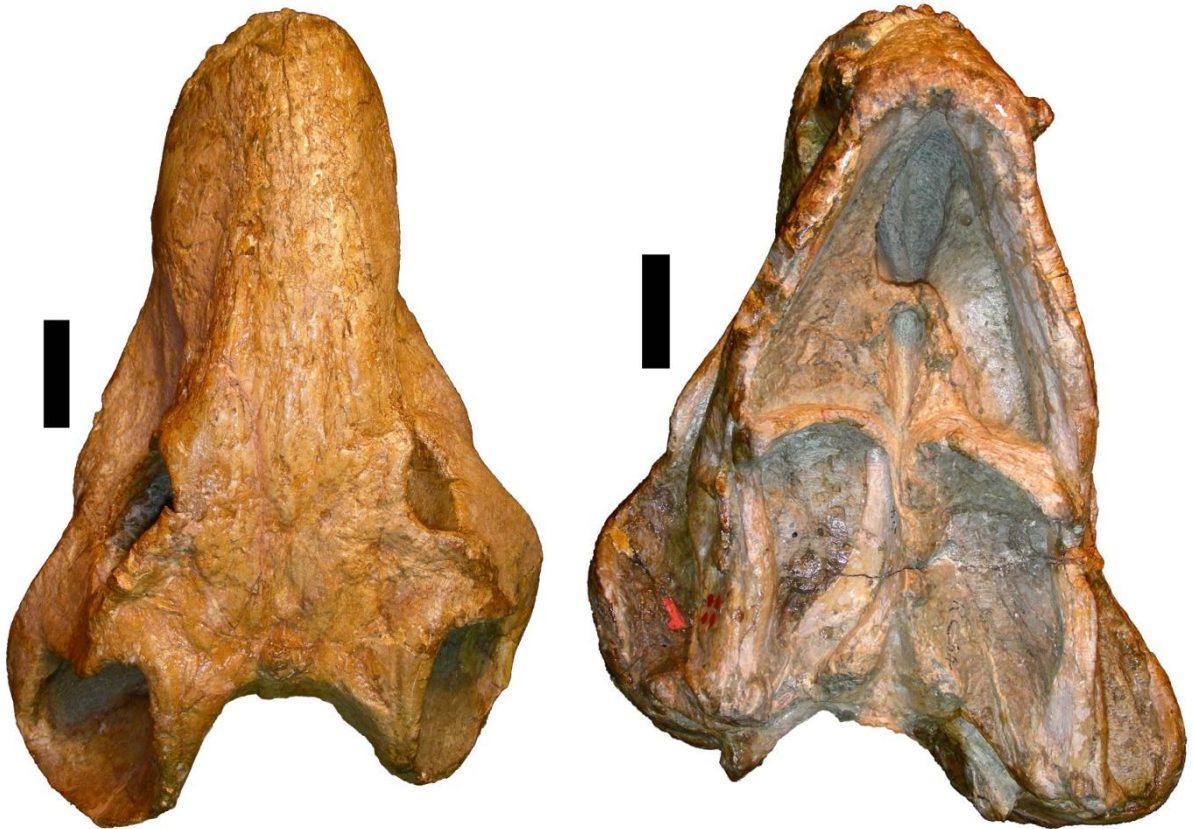


Figure 3.4 RC 34, *Aelurognathus maccabei* (= *Prorubidgea maccabei* Broom 1940). Lateral view (top), dorsal view (bottom left), ventral view (bottom right).

Scale bars equal 5 cm.

postfrontal is a long narrow bone that forms the anterior boundary of the orbit along with the small, rectangular lacrimal. The jugal and posterior process of the maxilla, form the suborbital bar which is the thickest of the cranial arches. The jugal meets the squamosal, below the ventral limit of the temporal fenestra. From the anterior portion of the temporal fenestra, the squamosal begins to widen ventrally, until it reaches its thickest point below the temporal fenestra. The postorbital bar is made up entirely by the postorbital. A noticeable constriction of the postorbital is seen in lateral view (Figure 3.4).

In dorsal view, the extent of lateral distortion of the specimen becomes evident (Figure 3.4). The left postorbital region has been compressed, while the right was stretched and the midline of the snout is displaced towards the left. The skull roof is wide and flat, with the interorbital distance being slightly narrower than the intertemporal distance. Anteriorly the nasals have been damaged, but their transverse posterior sutural boundary with the frontal is clearly visible and is situated antero-dorsally to the orbit in line with a noticeable constriction in the region of the lacrimals. This antorbital depression appears to be a natural feature of the specimen and not due to compression. At this level a protuberance of the maxillary ridge and jugal is visible. The frontal is long and narrow, extending posteriorly to meet with the parietal in line with the anterior end of the temporal fenestra. A small lateral protrusion of the frontal extends to form part of the orbital margin. The postorbital forms almost as much of the skull roof as the frontal. Posterior to the frontal and postorbital is a narrow contribution of the parietal to the skull roof. A slight depression is present on the skull roof where

Broom (1940) figured the suture between a very large preparietal and the parietal. Broom interpreted the preparietal as being large, but Brink & Kitching (1953), Manten (1958) and Sigogneau (1970) have all interpreted the preparietal as being much smaller than that figured by Broom (1940). The pineal opening is posteriorly positioned on a chimney behind the anterodorsal extent of the temporal fenestrae and close to the nuchal crest.

3.3 *Aelurognathus brodiei*

The holotype of *Aelurognathus brodiei* (TMP 1493), consists of a large, weathered and laterally compressed skull with lower jaw preserved in articulation (Figure 3.5). The palate and occiput have not been prepared due to the occluded jaws.

In his original description of the species Broom (1941) noted that the overall size and shape of the specimen was very similar to “*Prorubidgea*” *maccabei* (RC 34) and that both specimens had five postcanines in the maxilla. Broom (1941) did not assign TMP 1493 to the genus *Prorubidgea* however, as he felt that the lack of a preparietal and exclusion of the frontal from the orbital margin meant that the new specimen was more closely related to “*Sycosaurus laticeps*” (SAM-PK-4022), and accordingly described the specimen as the holotype of *Sycosaurus brodiei*.

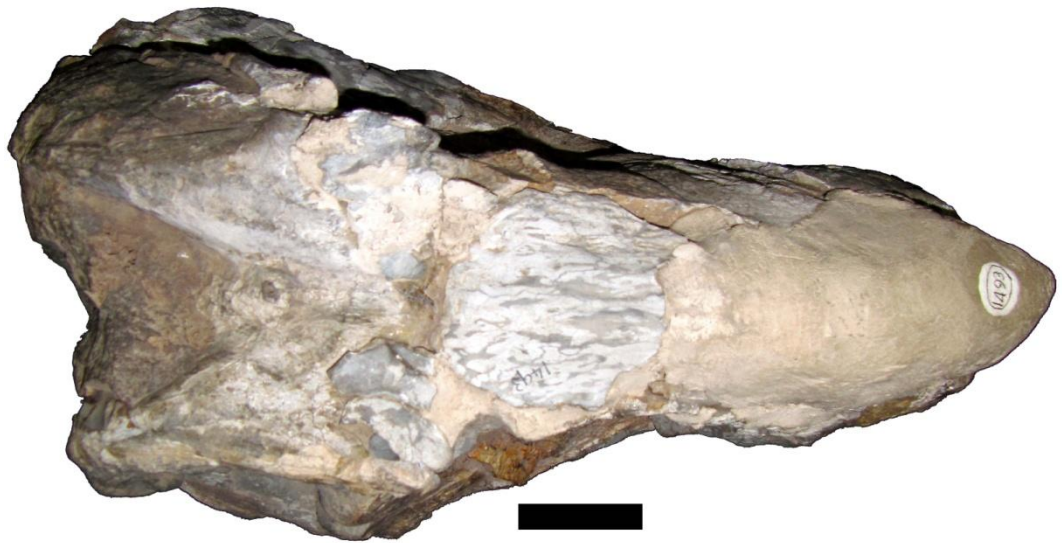
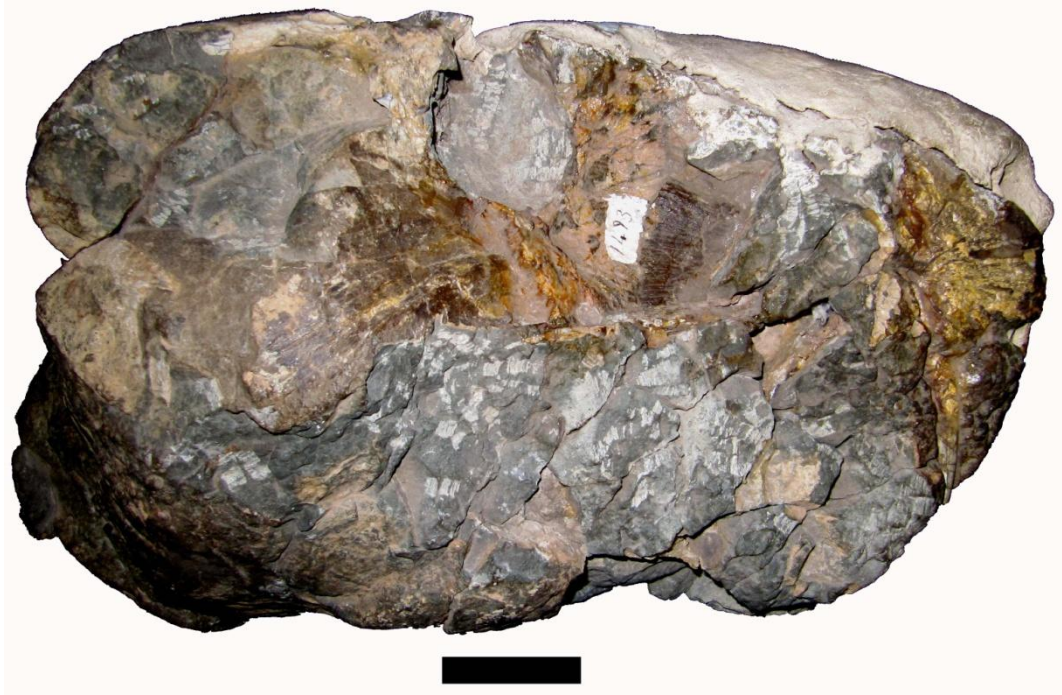


Figure 3.5 TMP 1493, *Aelurognathus brodiei* (= *Sycosaurus brodiei* Broom 1941). Lateral view (top), dorsal view (bottom). Scale bars equal 5 cm.

Due to weathering, much of anterior of the snout has been damaged and the anterior end of the nasals and septomaxilla are absent. The premaxillae have been eroded away, but traces of five incisors are partially preserved. According to Broom (1941), only impressions of the anterior two thirds of the nasals were preserved. The snout has subsequently been reconstructed using plaster, making it impossible to determine the shape of the nasals. Broom's illustration (1941, Figure 4) indicates that the nasals were narrowest in the middle, a characteristic in other members of *Aelurognathus*. The maxilla is a large bone and is deepest at the first postcanine. A posterior process of the maxilla extends to form part of the suborbital bar, and does not pass the posterior border of the orbit. Four postcanine teeth are visible on the left maxilla, with serrations on the distal edge of the first postcanine visible. Broom (1941) wrote that there were five postcanine teeth, with the second having fallen out prior to preservation. There is a diastema between the first and second observable postcanines, which is sufficiently large for another postcanine to have fitted.

The long, narrow prefrontal contacts the maxilla via a diagonal suture at the level of the second visible postcanine. The interorbital region has also been reconstructed using plaster so that the sutures of the postfrontal are obscured. Broom (1941) figured the posterior end of the prefrontal as meeting the postfrontal, thus excluding the frontal from the dorsal margin of the orbit, a feature which has been verified by the current research. The lacrimal is a small, square bone surrounded by the prefrontal dorsally, maxilla anteriorly and the jugal ventrally and posteriorly forming the anterior margin of the orbit. Between the

lacrimal and jugal is a horizontal suture. The jugal extends from the lower third of the orbital rim ventrally to meet the dorsal side of the posterior process of the maxilla, before continuing posteriorly beyond the postorbital bar until it reaches the squamosal below the temporal fenestra. The anterior portion of the squamosal forms a process surrounded by the jugal both dorsally and ventrally.

The cranial arcadia are roughly uniform in thickness, except for the postorbital bar, which exhibits a noticeable decrease in thickness at its dorsal and ventral extents. The suborbital bar is slightly thicker than that of the zygomatic, which is the same thickness as the postorbital bar at its broadest point.

When viewed from above, the extent of the lateral compression that the skull has suffered is evident, especially in the posterior intertemporal region (Figure 3.5). The transverse nasofrontal suture is anterior to the orbital margin. The interorbital region has been damaged, but a small portion of the midline suture between the frontals can be made out at the posterior level of the orbital border. This suture extends posteriorly up to the pineal opening. A short parietal forms the central portion of the skull roof behind the frontal. The pineal opening is situated on an elevated chimney at the posterior end of the parietal close to the nuchal crest.

3.4 *Aelurognathus kingwilli*

RC 60 was described by Broom as *Tigricephalus kingwilli* in 1948. The specimen consists of a relatively well preserved, but laterally compressed skull and lower jaw. The right of the specimen is complete (Figure 3.6), but the squamosal, part of the jugal, postorbital, as well as part of the lower jaw of the left is missing.

The prominent features of the skull, when viewed from the side, are the deep, rounded snout, large orbit and a postorbital bar that is narrower than the zygomatic and suborbital bars. While the depth of the snout may be exaggerated due to lateral compression, it does not appear out of proportion when compared to other members of the genus (e.g. RC 34). Five serrated incisors are borne on each premaxilla. A slender septomaxilla is present and extends posteriorly to midway of the diameter of the canine. Between the septomaxilla and maxilla lies a prominent septomaxillary foramen. The maxilla forms a major portion of the snout. A process of the maxilla protrudes posteriorly, until half way along the length of the orbit, where this process forms a prominent maxillary ridge. This ridge extends anteriorly until it reaches to be in line with the last postcanine. Each maxilla has a single, large canine. The right maxilla bears four postcanines, while the left has only three postcanines. A cavity on the left maxilla indicates the position of where the fourth postcanine once sat. The posterior end of the maxilla contacts the prefrontal, lacrimal and jugal. The prefrontal is a square bone that makes up the upper portion of the anterior orbital margin. Below the prefrontal is a smaller lacrimal which contributes to the middle portion of the anterior orbital

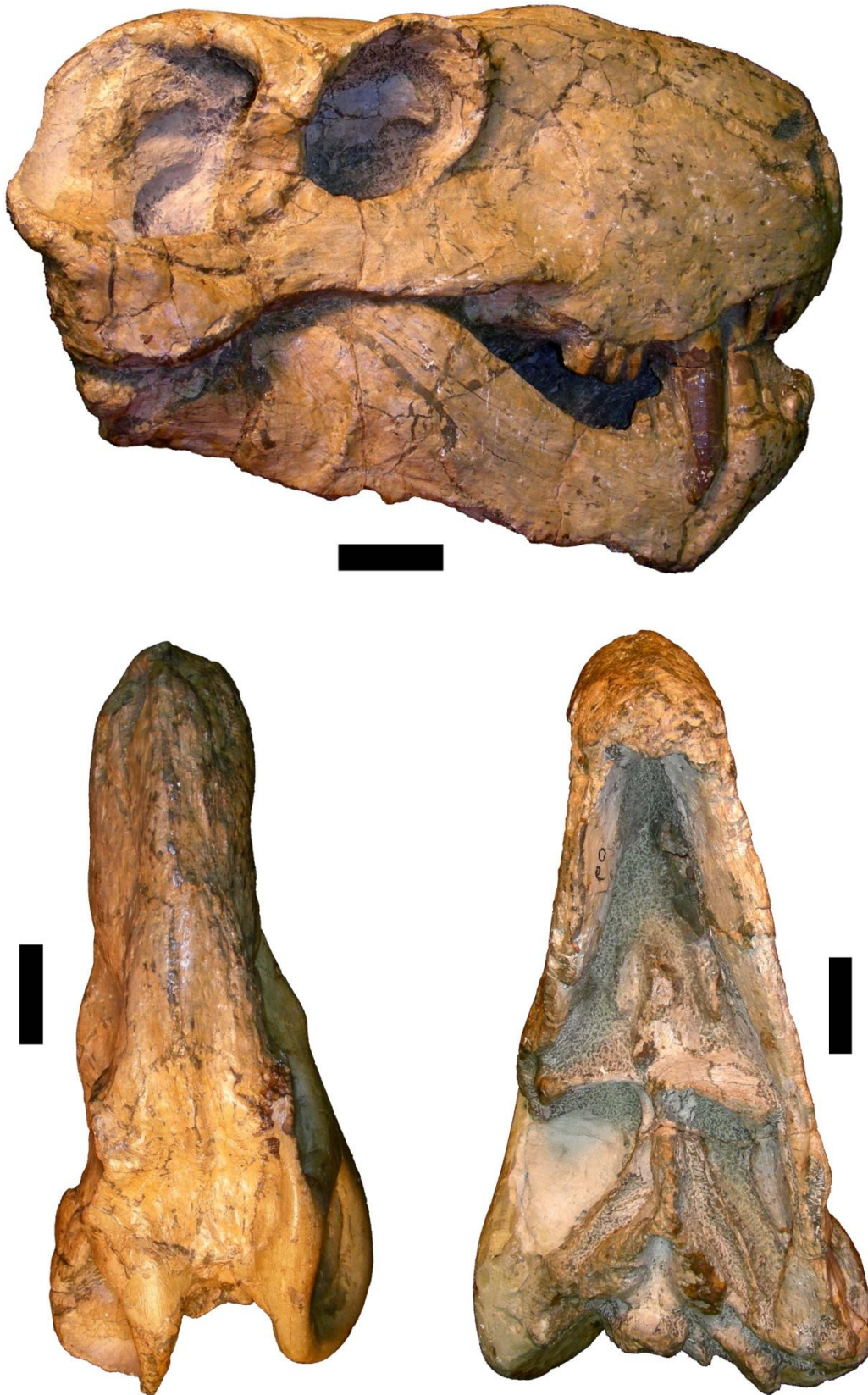


Figure 3.6 RC 60, *Aelurognathus kingwilli* (= *Tigricephalus kingwilli* Broom 1948). Lateral view (top), dorsal view (bottom left), ventral view (bottom right). Scale bars equal 5 cm.

margin. The ventral border of the lacrimal is bounded by the jugal. The jugal forms the lower anterior portion and ventral margin of the orbit. Extending from its contact with the maxilla, the jugal meets the squamosal below the temporal opening. A small participation of the jugal in the formation of the temporal opening can be seen.

In dorsal view the extent of the lateral compression is more evident (Figure 3.6), especially with regard to the anterior end of the snout. The nasal extends posteriorly from the naris to near the level of the anterior orbital margin where it contacts the frontal. The frontal is an elongated and narrow bone.

Broom (1948: p. 599) noted that there was no preparietal bone present on the skull roof, and that the pineal foramen was “*remarkably small for so large a skull,*” which he estimated to have a length of 320 mm. The lateral view of the skull was figured and described by Broom (1948: p. 599) as “*typically Gorgonopsian, with a powerful deep snout and very strong suborbital and temporal arches.*”

Broom (1948) compared this specimen to others, at the time, assigned to *Aelurognathus*, but did not feel that it could be referred to the genus as it had only three maxillary postcanine teeth and no preparietal, while the type for *Aelurognathus* had four postcanine teeth and a large preparietal. Sigogneau-Russell (1989) thought that Broom had counted the number of postcanine teeth on the maxilla incorrectly, and that it instead had four.

Sigogneau (1970) included the *Lycaenops* a new combination, *Lycaenops kingwilli*. Characters used by Sigogneau (1970) to define *L. kingwilli* as a separate species were considered by Gebauer (2007) as only good enough to describe the specimen to the generic level. Gebauer (2007) also felt that these characters were more characteristic of the genus, *Aelurognathus*, and that the specimen showed no characters observed in *Lycaenops*, except those common to the two genera. As a result Gebauer (2007) reassigned the specimen to *Aelurognathus*.

3.5 *Aelurognathus ferox*

This species is represented by several specimens, of which the holotype (RC 62), consists of a large, laterally compressed skull with attached lower jaw and isolated postcranial elements (Figure 3.7). The zygomatic and postorbital of both sides of the skull, and the right postfrontal, squamosal and quadrate are damaged. Reconstructions of the missing or damaged bones have been made using plaster.

The nasal is broad on either end, with a slight narrowing in the middle. The prefrontal and postfrontal are both large and form a large part of the anterior and dorsal regions of the orbital margin respectively. There is also a slight contribution of the frontal to the border of the orbit. Broom (1948: p. 600) felt that a large preparietal was present, although he did write that, “*the posterior borders cannot be very clearly made out.*” Sigogneau (1970) interpreted the preparietal as being absent. A large pineal foramen, surrounded by a thickening of bone is

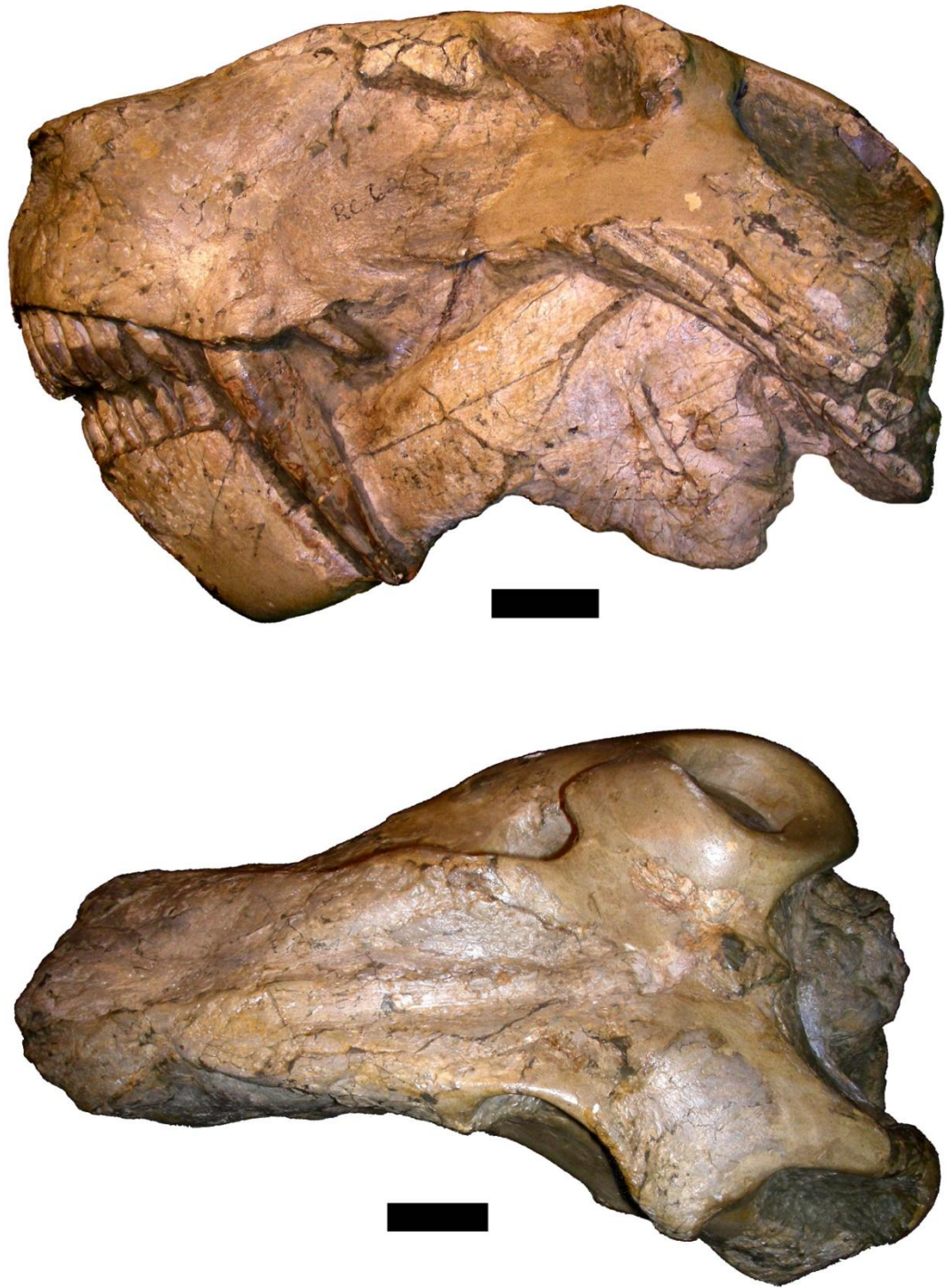


Figure 3.7 RC 62, *Aelurognathus ferox* (= *Smilesaurus ferox* Broom 1948).
Lateral view (top), dorsal view (bottom). Scale bars equal 5 cm.

present. The interparietal lies entirely on the occipital face, a feature which differs in some of the referred specimens (e.g. RC 81) possibly due to distortion of the skull. Two postcanines are present on the large maxilla. The jugal is large and a prominent component of the strong suborbital arch. Much of the occipital and all of the palate are obscured by the articulated postcranial elements.

RC 81 is larger than RC 62, and at a glance has a similar morphology (Figure 3.8). Differences include a relatively narrower nasal, and the expansion of the interparietal onto the dorsal surface of the skull. Another referred specimen, RC 82, is smaller and less complete than the holotype, with the dorsal surface of the skull missing (Figure 3.9). It comes from a similar locality as the type and has only one postcanine.



Figure 3.8 RC 81, *Aelurognathus ferox* (= *Smilesaurus maccabei* Broom 1948).

Lateral view (top). Scale bar equals 5 cm.



Figure 3.9 RC 82, *Aelurognathus ferox* (= *Pardocephalus wallacei* Broom 1948). Lateral view (top). Scale bar equals 5 cm.

3.6 *Aelurognathus alticeps*

The holotype of the species, BP/1/813, is a small skull with attached lower jaw described by Brink & Kitching (1953: p. 22) as being in “*a fair condition of preservation.*” The skull however has clearly been subjected to lateral compression and lacks much of the posterior region (Figure 3.10).

The anterior and posterior widths of the nasal are approximately the same, but there is a slight narrowing in the middle. The suture between the nasal and frontal is straight and located anterior to the orbit. A small portion of the frontal participates in the formation of the orbital margin. Neither the postfrontal nor

postorbital are well preserved. A preparietal is present and is situated well anterior to a reconstructed pineal foramen on the specimen. As a result of damage to the posterior part of the skull, the postorbital bar is missing on both sides, but has been reconstructed based on the thickness of the remains of the ventral portion of the left postorbital bar.

When viewed laterally, the maxilla is deep and the snout rounded anteriorly. There are four postcanines on the maxilla, which are not as large and robust as the incisors. A short lacrimal lies in front of the small orbit. Despite much of the posterior region being damaged, the occiput is partially preserved. The occiput is high and narrow, and Sigogneau (1970) interpreted it as having a slight posterior inclination.

BP/1/1566 is larger and better preserved than the holotype and comprises a skull with lower jaw preserved in articulation (Figure 3.11). The overall morphology of the specimen is the same as that of the holotype with the addition of the following characters due to the preservation of the posterior region of the skull: a small preparietal situated anterior to the pineal opening, near the nuchal crest and surrounded by a thickened ring of bone, short, broad fused parietals, and a pronounced expansion of the squamosal ventrally (Mantel 1958).



Figure 3.10 BP/1/813, *Aelurognathus alticeps* (= *Prorubidgea alticeps* Brink & Kitching 1952). Lateral view (top), dorsal view (bottom left), ventral view (bottom right). Scale bars equal 5 cm.

The occipital face tilts forwards, and has a distinct median ridge leading from the foramen magnum to the nuchal crest. The exoccipitals are large and almost completely enclose the foramen magnum. This specimen clearly has five postcanines, whereas the holotype has only four. Manten (1958) notes that the fifth postcanines of BP/1/1566 are smaller and appear to be immature.

3.7 Summary

Table 3.1 contains a summary of morphological descriptions laid out in this chapter. There is very little intraspecific variation with regard to the characters of the preparietal and inclusion of the frontal on the supraorbital margin. Differences in the cranial sutures at the intraspecific level are considered to be within the range of expected individual variation, as demonstrated by Cunningham (1866, 1896) and Keyser (1975). The most noticeable observed difference between specimens of the same species is in the number of postcanine teeth. The largest range being that of *Aelurognathus tigriceps*, which varies from 1 - 4 maxillary postcanines. Such variation is also considered to be within the range of individual variation, and has been shown to be the case in several instances within the Therapsida (Kermack 1956; Crompton 1963; Brink 1977)

At the interspecific level of variation on the skull roof, three distinct morphotypes are evident. Morphotype I (*Aelurognathus tigriceps*, *Aelurognathus maccabei* and *Aelurognathus alticeps*) displays a prominent preparietal and contribution by the

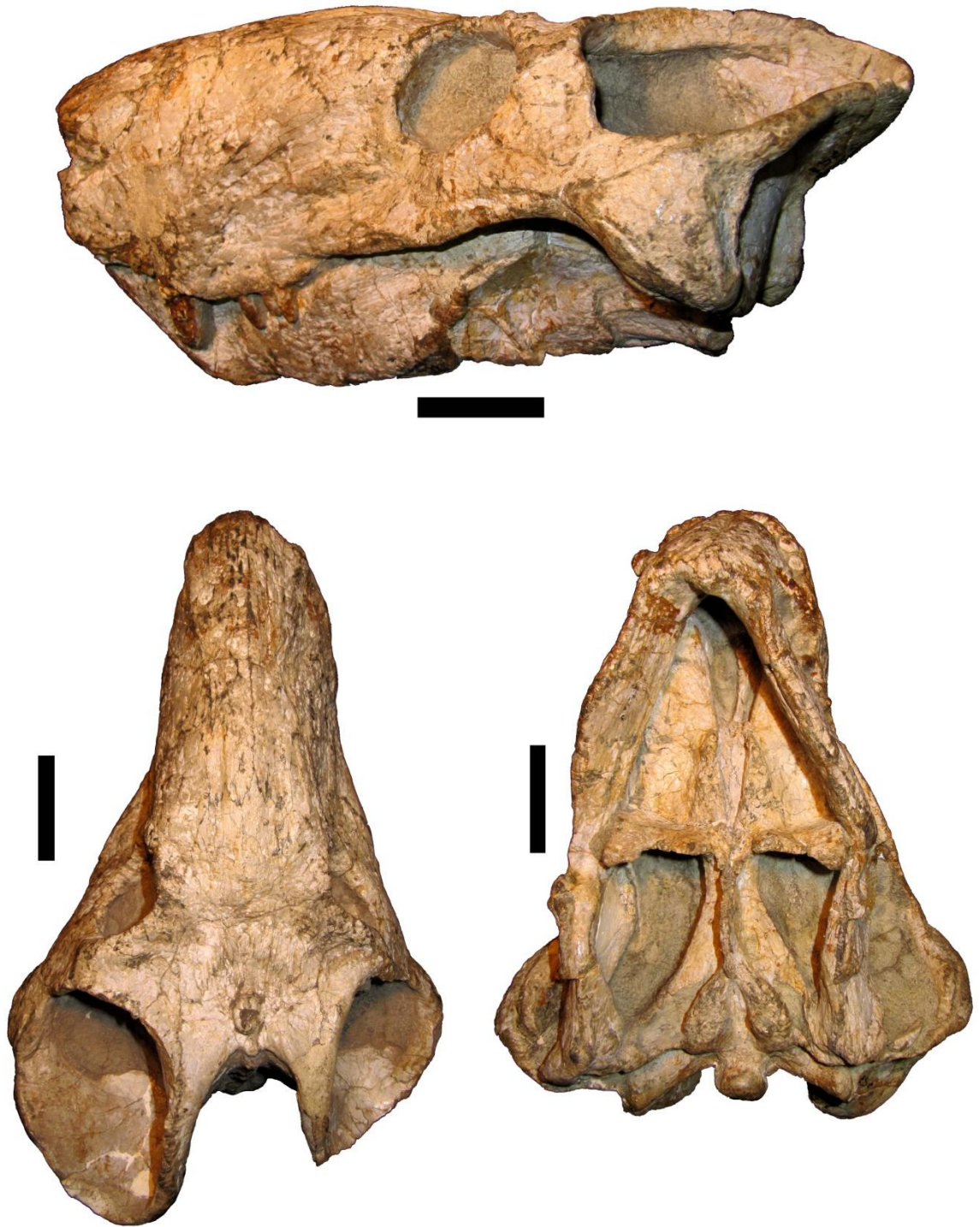


Figure 3.11 BP/1/1566, *Aelurognathus alticeps* (=Prorubidgea alticeps Manten 1958). Undistorted lateral view (top), dorsal view (bottom left), ventral view (bottom right). Scale bars equal 5 cm.

frontal (of variable size, *sensu* Haughton 1915) to the supraorbital margin. Morphotype II (*Aelurognathus kingwilli* and *Aelurognathus ferox*) lacks a preparietal, but has a contribution of the frontal to the supraorbital margin. Morphotype III (*Aelurognathus brodiei*) lacks both a preparietal and participation of the frontal to the supraorbital margin.

Due to the apparent plasticity of the shape and size of the preparietal, differences in the extent to which the frontal contributes to the supraorbital margin, as well as the large disparity in size of the specimens studied, the hypothesis that the sample may represent a growth curve was established. Several techniques were used, as laid out in Chapter 2.2, the results of which are discussed in the following chapter.

Table 3.1 Summary of observed morphological characters in *Aelurognathus* that have previously been used to diagnose taxa.

Taxon/ Morphotype	Specimen	Preparietal	Supraorbital Frontal	Maxillary Postcanines
<i>A. tigriceps</i> Morphotype I	SAM-PK-2342	present	present	4
	SAM-PK-4334	present	present	2
	SAM-PK-10071	?	?	2
	SAM-PK-7847	present	present	1
	SAM-PK-2672	present	present	4
<i>A. maccabei</i> Morphotype I	RC 34	present	present	4-5
<i>A. brodiei</i> Morphotype III	TMP 1493	absent	absent?	4-5
	BP/1/2190	absent	absent?	3-5
<i>A. kingwilli</i> Morphotype II	RC 60	absent	present	3-4
<i>A. ferox</i> Morphotype II	RC 62	absent	present	2
	RC 81	absent	present	2
	RC 82	?	?	1
	BP/1/2465	absent	present?	2
	TMP 132	?	?	2-3
<i>A. alticeps</i> Morphotype I	BP/1/813	present	present	4-5
	BP/1/1566	present	present	4-5

CHAPTER FOUR - STATISTICAL & ALLOMETRIC ANALYSES

4.1 Introduction

The morphological descriptions provided in Chapter 3 suggest that all the specimens examined may belong to a single species, which shows some individual variation. This variation may possibly be attributed to ontogeny. To test this hypothesis, relationships between different dimensions of the skull were explored using both univariate and bivariate allometric statistical methods as set out in Chapter 2.

Due to the small sample sizes ($6 < n \leq 15$), and the fact that some specimens exhibit a high degree of distortion, the results of these statistical tests should be considered with caution, and interpreted in conjunction with the morphological descriptions.

4.2 Results of Univariate Analyses

In this section the results of the univariate analyses are discussed. For each measurement, a table (Tables 4.1-4.12 & Tables D1-D15) providing summary statistics and a plot showing the average values for each taxon is provided (Figures 4.1-4.12 & Figures D1-D15). Summary statistics presented in Tables 4.1-4.12 & Tables D1-D15 only show results for species that were represented by two

or more specimens in the analyses. Measurements that displayed a continuous range when plotted will be dealt with collectively, while measurements for which no continuum was evident will be discussed individually.

4.2.1 Measurements with continuous range

For these measurements, the point representing the average value for each species falls within the range of the standard error for the other described *Aelurognathus* species. For instance in Figure 4.1, a plot of the total skull length (Variable 1), the values for both *A. kingwilli* and *A. maccabei* (species based on only the holotype) fall within the upper limit of *A. ferox*, while the value for *A. brodiei* falls within the lower limit of *A. ferox*. The average values for *A. tigriiceps* and *A. alticeps* fall out of the lower limit of *A. ferox*, but *A. tigriiceps* and *A. alticeps* lie within the lower and upper limits of one another respectively. In addition to this, the upper limit of *A. tigriiceps* overlaps with the lower limit of *A. ferox*, providing an unbroken continuum, across all taxa size for the total skull length (Variable 1). Similar conditions apply to the measurements listed below (Variable numbers correspond to the list of measurements in Appendix B. Accompanying Figures and Tables are included as Appendix D);

Skull length (Variable 2, Figure D1); Prepineal skull length (Variable 6, Figure D2); Postpineal skull length (Variable 7, Figure D3); Intertemporal width (Variable 14, Figure D4); Temporal opening length (Variable 18, Figure D5);

Temporal opening height (Variable 19, Figure D6); Maxilla height (Variable 25, Figure D7); Orbit length (Variable 27, Figure D8); Minimum postorbital bar width (Variable 40, Figure D9); Minimum suborbital bar height (Variable 41, Figure D10); Mandible length (Variable 45, Figure D11); Dentary corpus height (Variable 49, Figure D12); Dentary thickness (Variable 51, Figure D13); Maxillary bicanine breadth (Variable 65, Figure D14); Mesiodistal diameter of maxillary canine (Variable 67, Figure D15).

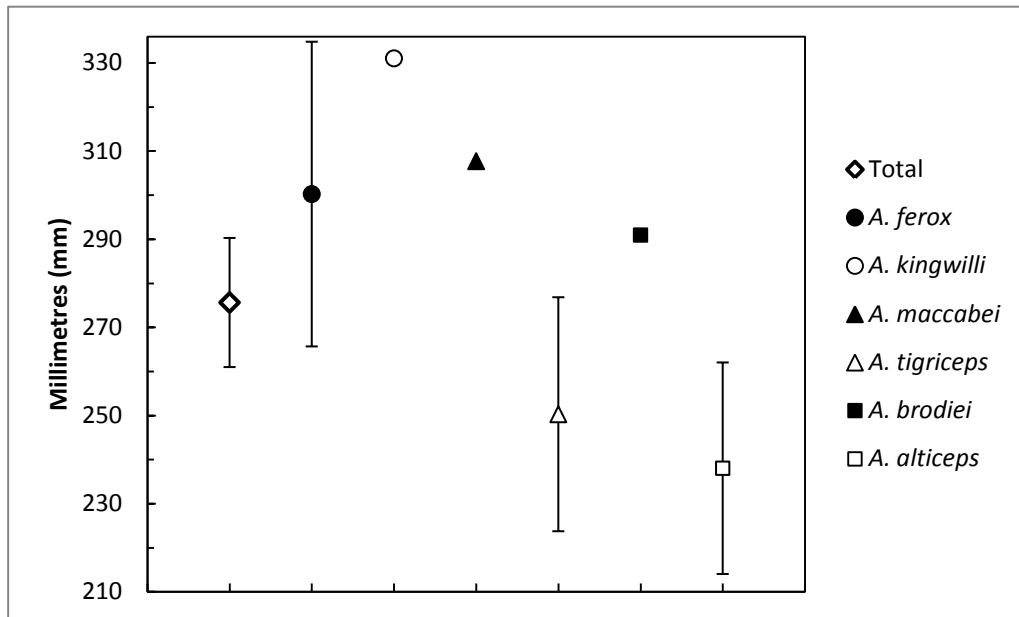


Figure 4.1 Average cell plot of the Total skull length (Appendix B, Variable 1).

Error bars represent \pm one standard error (Table 4.1).

Table 4.1 Summary statistics for Total skull length (Appendix B, Variable 1).

	Total	<i>A. tigriceps</i>	<i>A. ferox</i>	<i>A. alticeps</i>
<i>n</i>	12	4	3	2
# Missing	4	1	2	0
Sum	3307	1001	901	476
Average	276	250	300	238
Max. val.	337	295	337	262
Min. val.	187	187	231	214
Range	151	109	106	48
Var.	2575.172	2819.417	3585.402	1152
Std dev.	50.7462	53.0982	59.8782	33.9411
Std error	14.6492	26.5491	34.5707	24

4.2.2 Measurements without continuous range

A minority of the measurements of the specimens representing different species returned a broken or discontinuous series of values. In these instances the discontinuity may be shown to be due to two factors; 1) reduction of the sample by excluding poorly preserved specimens from the analysis, or 2) presence of strong distortion in some specimens included in the analysis.

By removing specimens, the sample size (n) is reduced, causing the average to be unusually skewed. If large specimens are excluded, then the average will be lower than expected, while the opposite is observed if small specimens are excluded. The closer an excluded specimen may appear to the median, the less effect it has on the average value.

Keyser (1975) wrote that all fossils from the Karoo Beds of South Africa are subjected to some form of distortion, which may be caused by several factors. Distortion of a specimen can often go unrecognised if the overall shape of the fossil remains symmetrical. This is often the case when dealing with cranial material that has been compressed laterally. Distortion in specimens will have a similar result in poorly representing the average for the species. Depending on whether the measurement has been stretched or compressed, the resultant average will be larger or smaller than the real value of the variable. In most cases, distorted measurements were discarded, except for *A. kingwilli* and *A. maccabei*, as each species is represented by only a single specimen. Considering the reduced sample size, measurements without a continuous range were excluded from the allometric analyses. The following measurements are numbered as they appear in Figure 2.1 and Appendix B.

4.2.2.1 Antorbital skull length (Variable 3)

For this measurement, there is a continuous size range, which incorporates all species and specimens, except for *A. alticeps* (Figure 4.2). *Aelurognathus alticeps* is represented by only two specimens (BP/1/813 and BP/1/1566). BP/1/813 is one of the smallest specimens of *Aelurognathus*, while BP/1/1566 is only marginally larger (~6mm) and smaller (~4mm) than the smallest specimens of *A. tigriiceps* and *A. ferox* respectively (Table 4.2). Despite BP/1/1566 being of comparable size to specimens of other species, the average for *A. alticeps* is noticeably low, falling outside of the error range of the next smallest species *A. tigriiceps*.

This could be ascribed to the fact that BP/1/813, one of the smallest specimens in the sample, may represent a very early growth stage of *Aelurognathus* not represented by any other specimen (except perhaps SAM-PK-4334). It is well recorded in extant mammals (as well as some non-mammalian amniotes) that the ‘snout’ of juveniles grows proportionately quicker than the total length of the skull (Reiss 1989). Such a disproportion in the rate of growth of the antorbital region may account for the measurement of *A. alticeps*, and more precisely BP/1/813, being noticeably smaller.

Table 4.2 Summary statistics for Antorbital skull length (Appendix B, Variable 3).

	Total	<i>A. tigriceps</i>	<i>A. ferox</i>	<i>A. alticeps</i>
<i>n</i>	14	5	4	2
# Missing	2	0	1	0
Sum	2166	737	718	230
Average	155	147	180	115
Max. val.	222	188	222	125
Min. val.	105	123	129	105
Range	117	66	93	20
Var.	1121.326	943.0556	1486.316	200
Std dev.	33.48621	30.70921	38.55276	14.14214
Std error	8.949567	13.73358	19.27638	10

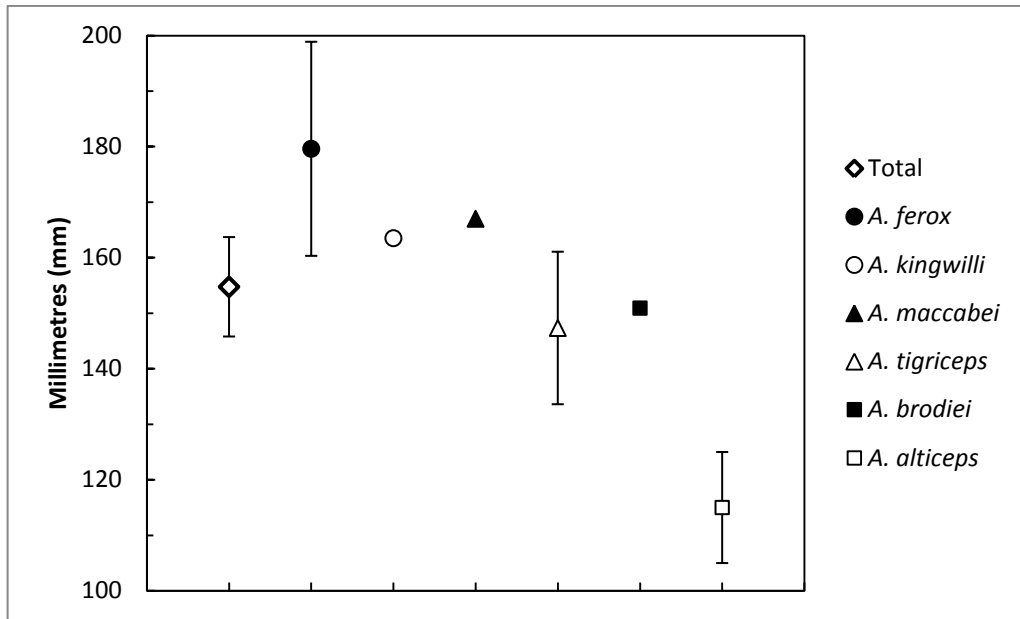


Figure 4.2 Average cell plot of the Antorbital Skull length (Appendix B, Variable 3) Error bars represent \pm one standard error (Table 4.2).

4.2.2.2 Postorbital skull length (Variable 4)

Five of the six species form a continuous range in sizes for the length of the skull posterior to the anterior margin of the orbit. The point for *Aelurognathus kingwilli* (RC 60) lies well above the upper most limit of *A. ferox* and the point of *A. maccabei*.

From Figure 3.6, it can be seen that the antorbital margin of the orbit of RC 60 has been deformed during preservation. The extent of this deformation is sufficient to cast the single specimen of *A. kingwilli* as an outlier in Figure 4.3, but when removed from the analyses, there was no noticeable difference observed in the values of the summary statistics. Thus the extent of deformation in RC 60 was

considered to have little to no effect on the results of the analysis and the specimen was not excluded.

Table 4.3 Summary statistics for postorbital skull length (Appendix B, Variable 4).

	Total	<i>A. tigriceps</i>	<i>A. brodiei</i>	<i>A. ferox</i>	<i>A. alticeps</i>
<i>n</i>	13	4	2	3	2
# Missing	3	1	0	2	0
Sum	1742	474	290	415	251
Average	134	119	145	138	126
Max. val.	160	151	150	154	144
Min. val.	103	103	140	110	107
Range	57	48	10	44	37
Var.	480.9113	480.3333	45.125	604.3333	684.5
Std dev.	21.92969	21.91651	6.717514	24.58319	26.16295
Std error	6.082202	10.95825	4.75	14.19311	18.5

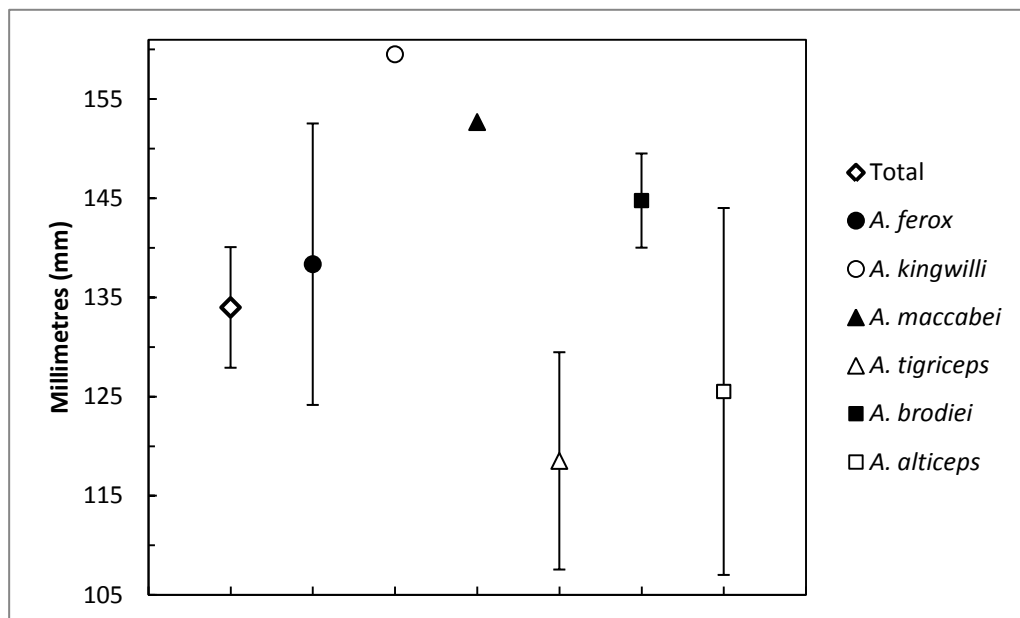


Figure 4.3 Average cell plot for postorbital skull length (Appendix B, Variable 4)

Error bars represent \pm one standard error (Table 4.3).

4.2.2.3 Total postorbital length (Variable 5)

Due to poor preservation, seven specimens were omitted from this analysis of the distance from the anterior border of the orbit to the posterior of the foramen magnum. These excluded specimens are both representatives of *A. brodiei* (TMP 1493 & BP/1/2190), the smaller specimens of *A. ferox* (TMP 132 & RC 82), the smallest specimen of *A. alticeps* (BP/1/813), as well as the two larger specimens of *A. tigriiceps* (SAM-PK-7847 & SAM-PK-2672). The exclusion of TMP 132, RC 82 and BP/1/813 has resulted in the points for *A. ferox* and *A. alticeps* in Figure 4.4 to be plot higher than they should. Similarly the point for *A. tigriiceps* plots lower than expected due to the exclusion of SAM-PK-7847 and SAM-PK-2672. In all three of these species the error bars are not as wide as they should be. The error bars have been reduced in their limits, because of the exclusion of specimens representing the extremes of the size range.

Table 4.4 Summary statistics for total postorbital skull length (Appendix B, Variable 5).

	Total	<i>A. tigriiceps</i>	<i>A. ferox</i>
<i>n</i>	9	3	3
# Missing	7	2	2
Sum	945	266	377
Average	105	89	126
Max. val.	132	98	132
Min. val.	80	80	119
Range	52	18	14
Var.	299.3125	81.33333	45.75
Std dev.	17.30065	9.0185	6.763875
Std error	5.766883	5.206833	3.905125

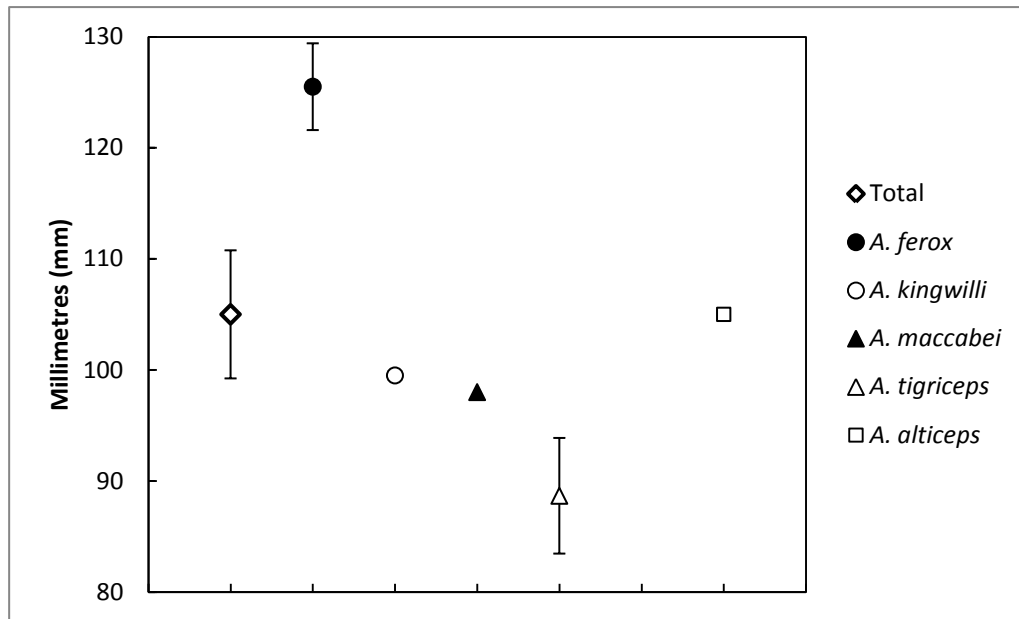


Figure 4.4 Average cell plot of the total postorbital skull length (Appendix B, Variable 5) Error bars represent \pm one standard error (Table 4.4).

4.2.2.4 Interorbital width (Variable 12)

There appear to be two factors affecting the analysis of the skull breadth across the orbits (Figure 4.5). Firstly, *A. ferox* and *A. kingwilli* appear to plot lower than expected. This is most likely due to specimens of these species having been subjected to some form of distortion, resulting in the interorbital widths of these specimens being compacted. Secondly the value for *A. tigriceps* is lower than expected, given that it has the third highest maximum value amongst the species represented (Table 4.5). This low average may be due to the exclusion of SAM-PK-7847, forcing the average to be lower than expected, as well as decreasing the range of the error bars for the species.

Table 4.5 Summary statistics for Interorbital width (Appendix B, Variable 12).

	Total	<i>A. tigriceps</i>	<i>A. brodiei</i>	<i>A. ferox</i>
<i>n</i>	13	4	2	4
# Missing	3	1	0	1
Sum	988	268	168	333
Average	76	67	84	83
Max. val.	89	79	87	89
Min. val.	53	53	81	76
Range	37	27	6	13
Var.	107.067	119.9329	18	31.58333
Std dev.	10.34732	10.95139	4.242641	5.619905
Std error	2.869829	5.475693	3	2.809953

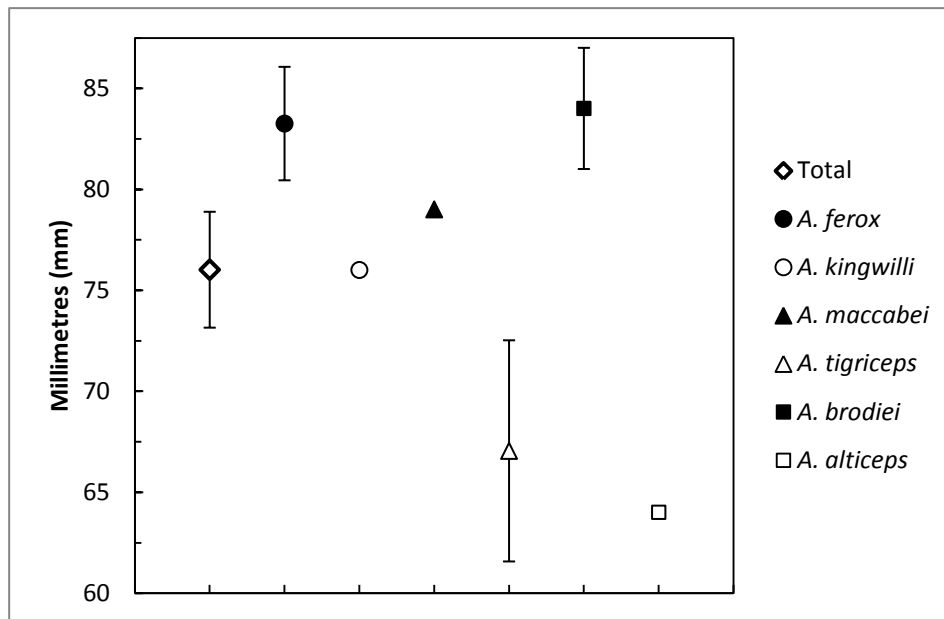


Figure 4.5 Average cell plot of the Interorbital width (Appendix B, Variable 12)

Error bars represent \pm one standard error (Table 4.5).

4.2.2.5 Lateral skull height (Variable 24)

With the exception of *A. ferox*, the data points representing all the other species cluster closely to one another, with *A. kingwilli*, *A. maccabei* and *A. brodiei* all plotting within the error limits of *A. tigriceps*. The point for *A. ferox* lies much higher than those of the other species. This is most likely due to the fact that only the two larger specimens of the species (RC 81 & RC 62) are well enough preserved to be included in the analyses, and resulted in the calculated average being larger than the true average for *A. ferox*.

Table 4.6 Summary statistics for lateral skull height (Appendix B, Variable 24).

	Total	<i>A. tigriceps</i>	<i>A. ferox</i>
<i>n</i>	11	5	2
# Missing	5	0	3
Sum	1179	508	274
Average	107	102	137
Max. val.	154	120	154
Min. val.	75	75	120
Range	79	45	34
Var.	449.1783	365.8556	578
Std dev.	21.19383	19.12735	24.04163
Std error	6.390179	8.554011	17

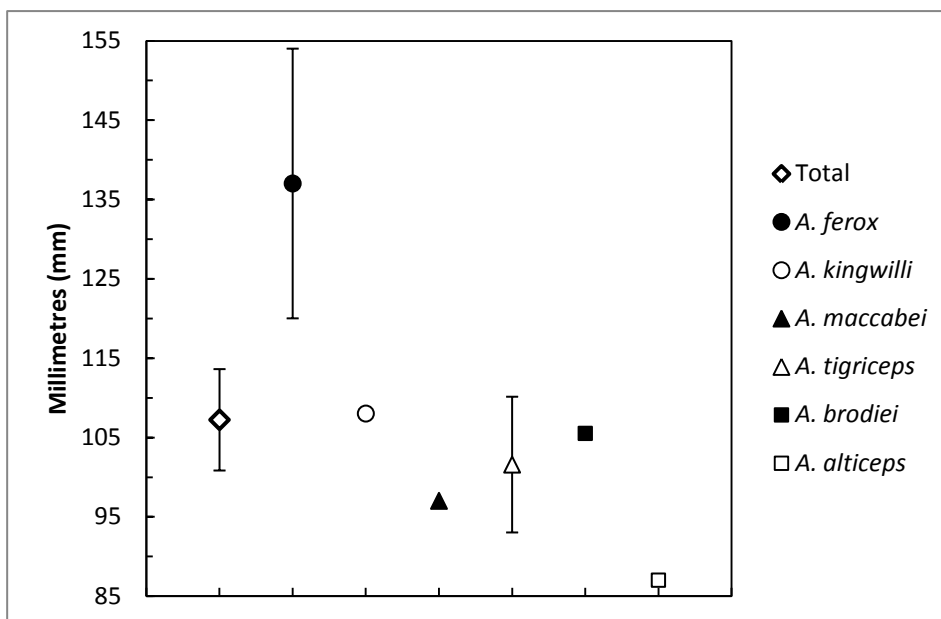


Figure 4.6 Average cell plot of the Lateral skull height (Appendix B, Variable 24)

Error bars represent \pm one standard error (Table 4.6).

4.2.2.6 Orbital length (Variable 26)

Two specimens were excluded from this analysis, a smaller specimen of *A. ferox* (RC 82) and of *A. alticeps* (BP/1/813). While upper and lower limits for the plotted points of *A. ferox* encompass the plotted points of *A. maccabei*, *A. brodiei* and *A. kingwilli*, the points of both *A. tigriceps* and *A. alticeps* plot below the lower limit of *A. ferox*. While the upper limit of *A. tigriceps* only just falls outside of the lower limit of *A. ferox*, the larger specimen of *A. alticeps* plots well below the values of any other taxon (Figure 4.7). This is an unusual result as BP/1/1566 is of comparable size to specimens of the five other taxa, while *A. tigriceps* is considered to be one of the larger taxa.

Interestingly both *A. tigriceps* and *A. alticeps* were identified as representatives of Morphotype I in the preceding chapter. Several diagnoses of *A. tigriceps* have also identified small orbits as characteristic of the species.

This is the only example from the univariate analyses for which the deviation from a continuous range cannot be attributed to either a small sample size or possible error in the measuring of the variable due to deformation.

Table 4.7 Summary statistics for Orbital length (Appendix B, Variable 26).

	Total	<i>A. tigriceps</i>	<i>A. brodiei</i>	<i>A. ferox</i>
<i>n</i>	14	5	2	4
# Missing	2	0	0	1
Sum	685	216	103	216
Average	49	43	52	54
Max. val.	66	47	54	66
Min. val.	30	40	49	30
Range	36	7	5	36
Var.	112.2956	10.75556	12.04959	260.7292
Std dev.	10.59696	3.279566	3.471251	16.14711
Std error	2.832157	1.466667	2.454545	8.073555

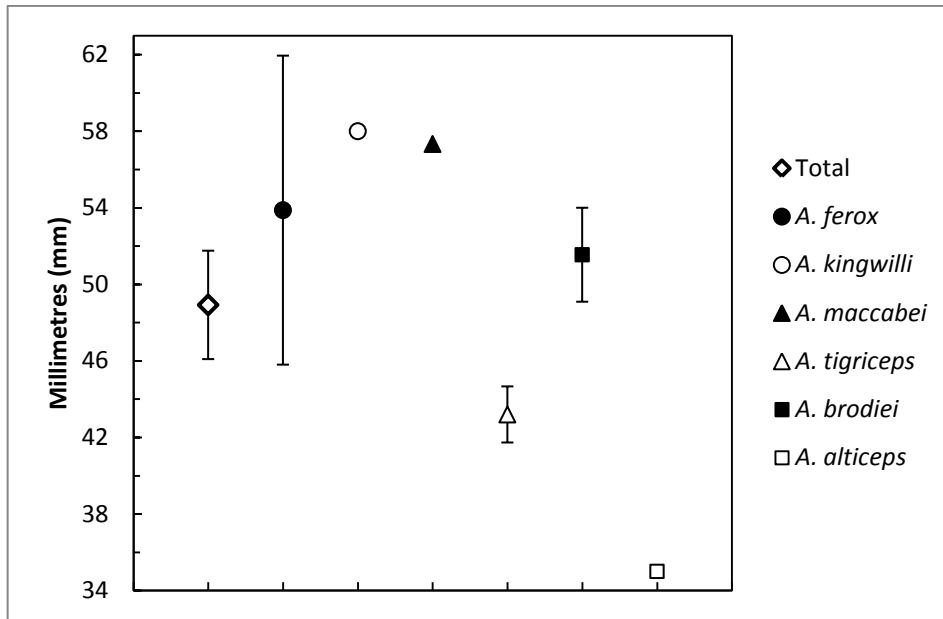


Figure 4.7 Average cell plot of the Orbital length (Appendix B, Variable 26)

Error bars represent \pm one standard error (Table 4.7).

4.2.2.7 Snout-maxillary canine length (Variable 37)

The plotted points of *A. maccabei* and *A. kingwilli* do not fall within the limits of the remaining four, all of which overlap with one another. Both these taxa are of medium size and represented by only a single specimen each. This may account for their values plotting higher than the average values of the other ‘larger’ taxa, which include individuals smaller than both *A. maccabei* and *A. kingwilli*, whose values are less than the largest recorded measurement of RC 62. The length from the tip of the snout to the maxillary canine may be exaggerated for *A. kingwilli*, as the specimen has undergone some lateral compression which may have caused the premaxilla to protrude further forward than would have been seen while the animal was alive.

Table 4.8 Summary statistics for Snout-maxillary canine length (Variable 37).

	Total	<i>A. tigriceps</i>	<i>A. ferox</i>	<i>A. alticeps</i>
<i>n</i>	15	5	5	2
# Missing	1	0	0	0
Sum	1039	346	315	139
Average	69	69	63	69
Max. val.	94	91	94	78
Min. val.	26	50	26	61
Range	68	41	68	17
Var.	444.441	355.5889	985.8765	136.125
Std dev.	21.08177	18.85706	31.39867	11.66726
Std error	5.443289	8.433136	14.04191	8.25

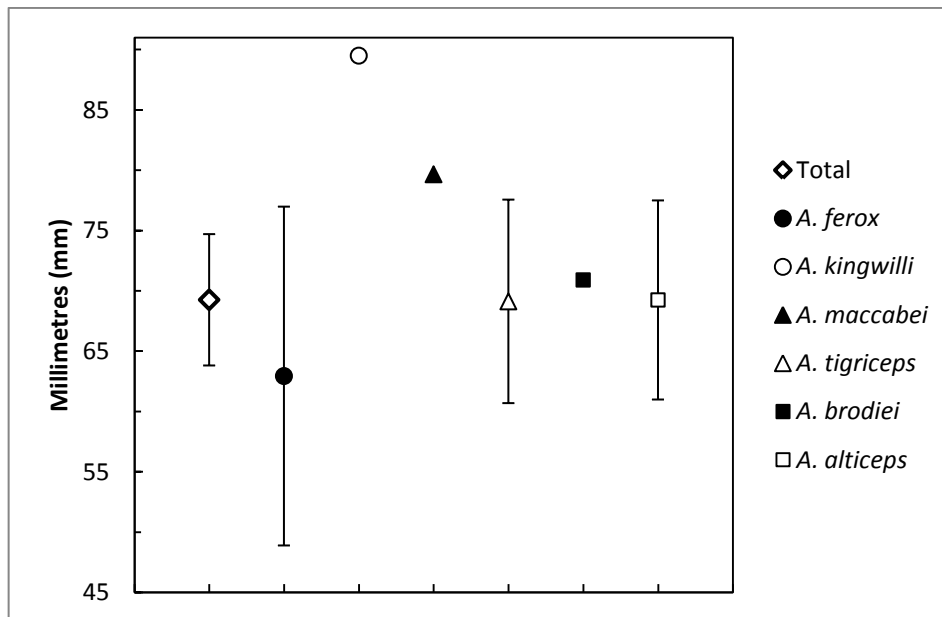


Figure 4.8 Average cell plot of the Snout-maxillary canine length (Appendix B, Variable 37) Error bars represent \pm one standard error (Table 4.8).

4.2.2.8 Minimum height of the zygomatic arch (Variable 42)

Only 2 specimens of *A. tigriceps* were measurable (SAM-PK-2342 and SAM-PK-4334) and their values are very similar (22mm & 23mm), restricting the limits of the error bar, and thus preventing a ‘continuum’ of observed measurements. If the limits of the error bars for *A. tigriceps* were not constricted in this manner, the taxon would almost certainly occupy the space in the plot between the lowermost limit of *A. ferox* and the uppermost limit of *A. alticeps* (Figure 4.9).

Table 4.9 Summary statistics for Minimum height of the zygomatic arch (Variable 42).

	Total	<i>A. tigriceps</i>	<i>A. ferox</i>	<i>A. alticeps</i>
<i>n</i>	10	2	3	2
# Missing	6	3	2	0
Sum	278	45	102	38
Average	28	23	34	19
Max. val.	39	23	39	22
Min. val.	16	22	31	16
Range	23	1	8	7
Var.	47.86091	0.5	15.35905	21.125
Std dev.	6.918158	0.707107	3.919063	4.596194
Std error	2.187714	0.5	2.262672	3.25

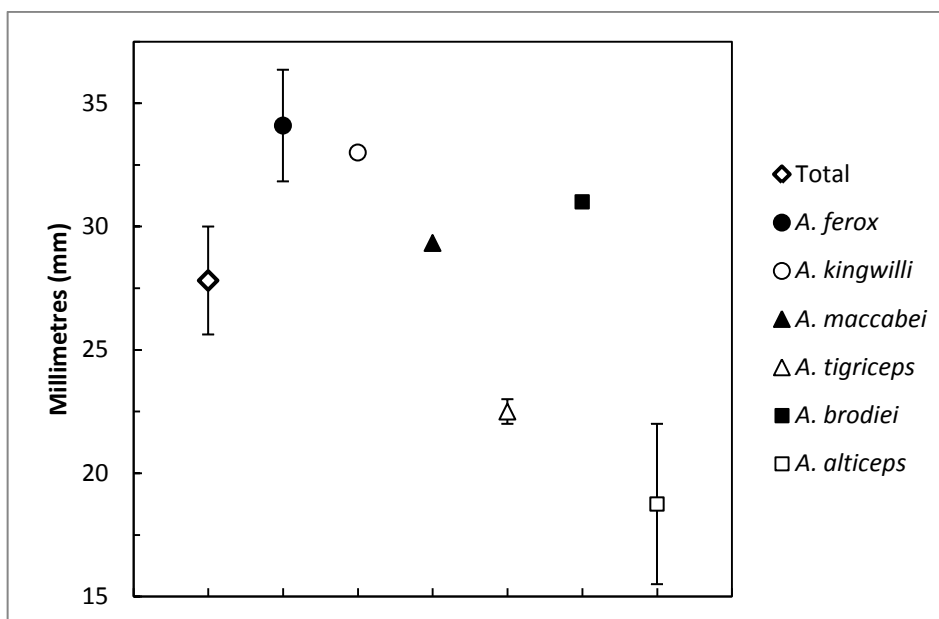


Figure 4.9 Average cell plot of the Minimum height of the zygomatic arch (Appendix B, Variable 42) Error bars represent \pm one standard error (Table 4.9).

4.2.2.9 Diastema between last incisor and canine (Variable 55)

A continuum of measurements is observed for all taxa (Figure 4.10) except for *A. alticeps*, which is represented by one specimen, BP/1/1566. While none of the specimens in the sample represent an individual in the process of replacing an upper canine tooth, it has been shown in other specimens belonging to the Rubidgeinae (e.g. RC 13, Broom 1938) that the replacement canine erupt anteriorly to the existing functional canine. This process would cause a temporary reduction in size of the diastema between the incisors and canines, until such time as the replacement canine had fully erupted and migrated to take the place of the shed canine. Due to this potential variability in the measurement of the diastema between last incisor and canine, due to different stages of canine eruption between

individuals, the fact that *A. alticeps* falls outside of the lower limits of *A. ferox*, *A. tigriceps* and *A. brodiei* is interpreted to be of little importance.

Table 4.10 Summary statistics for Diastema between last incisor and canine (Variable 55).

	Total	<i>A. tigriceps</i>	<i>A. brodiei</i>	<i>A. ferox</i>
<i>n</i>	14	5	2	4
# Missing	2	0	0	1
Sum	256	104	41	63
Average	18	21	20	16
Max. val.	34	34	22	19
Min. val.	9	13	19	9
Range	25	21	3	10
Var.	36.77177	66.07778	3.971074	21.05575
Std dev.	6.063973	8.128824	1.992755	4.588654
Std error	1.620665	3.635321	1.409091	2.294327

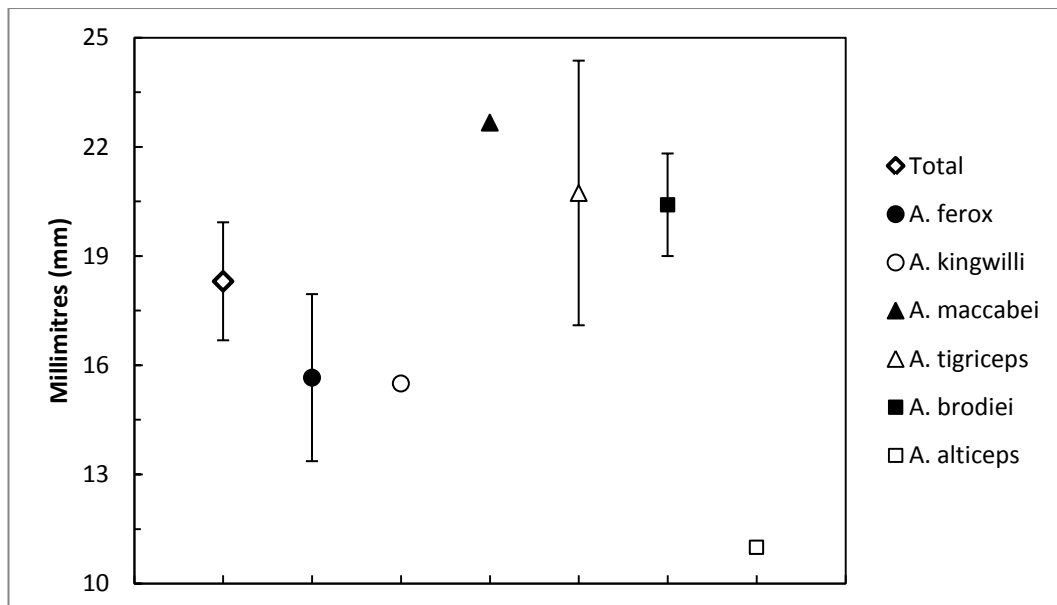


Figure 4.10 Average cell plot of the Diastema between last incisor and canine (Appendix B, Variable 55) Error bars represent \pm one standard error (Table 4.10).

4.2.2.10 Diastema between canine and first postcanine (Variable 57)

As mentioned in the previous chapter, the number and relative positions of the postcanines may vary within an individual. Coupling this with the variability of the canine position depending on an individual's developmental stage, the discontinuous range of measurements for the diastema between canine and first postcanine is considered to be caused due to the highly variable nature of the dentition.

Table 4.11 Summary statistics for Diastema between canine and first postcanine (Variable 57).

	Total	<i>A. tigriceps</i>	<i>A. ferox</i>
<i>n</i>	12	5	3
# Missing	4	0	2
Sum	219	91	54
Average	18	18	18
Max. val.	30	30	25
Min. val.	11	11	14
Range	19	19	11
Var.	36.18413	62.58889	34.7037
Std dev.	6.015325	7.911314	5.890985
Std error	1.736475	3.538047	3.401162

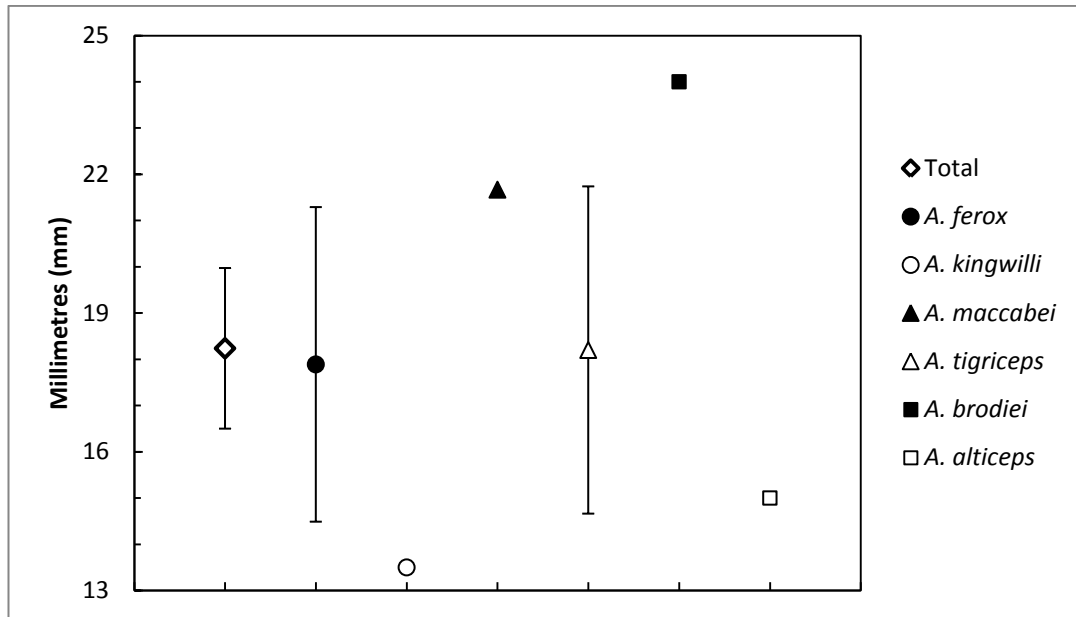


Figure 4.11 Average cell plot of the Diastema between canine and first postcanine (Appendix B, Variable 57) Error bars represent \pm one standard error (Table 4.11).

4.2.2.11 Maxillary postcanine series length (Variable 59)

The measurement of the length of the maxillary series length is strongly influenced by the number of postcanines present in the series. While the actual count of the number of postcanines may be of some importance, the actual length of the postcanine series is seen as less important.

In Figure 4.12 below, the two taxa with the lowest plots, *A. ferox* and *A. tigriceps* each contain examples of an individual with only one maxillary postcanine (Table 3.1). *A. maccabei*, *A. brodiei*, *A. kingwilli* and *A. alticeps* are each only

represented by a single specimen, thus no variability in the number of postcanines is recorded in the sample for these four taxa.

Table 4.12 Summary statistics for Maxillary postcanine series length (Variable 59).

	Total	<i>A. tigriceps</i>	<i>A. ferox</i>
<i>n</i>	13	5	4
# Missing	3	0	1
Sum	270	88	57
Average	21	18	14
Max. val.	34	29	20
Min. val.	8	8	10
Range	25	21	10
Var.	87.71546	77.11667	26.55556
Std dev.	9.365653	8.78161	5.153208
Std error	2.597565	3.927255	2.576604

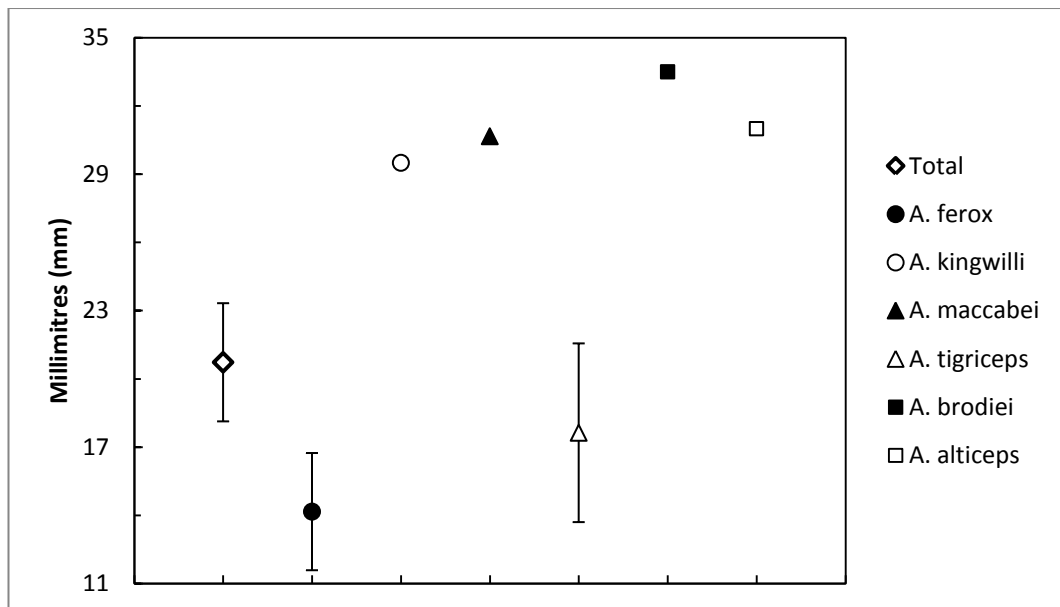


Figure 4.12 Average cell plot of the Maxillary postcanine series length (Appendix B, Variable 59) Error bars represent \pm one standard error (Table 4.12).

4.3 Results of Allometric Analyses

The first allometric analysis looked at 20 measurements and used the skull length measured from the tip of the snout to the foramen magnum (Variable 2) as the independent variable. Of these, 12 showed a significant [$p(\text{uncorr}) < 0.05$] correlation with the independent variable (Figure 4.13). For these 12 variables, the values of Pearson's product-moment correlation coefficient (r) ranged from 0.78-0.94. Coefficients of allometry (b_0) calculated using least squares (LS) regression differ considerably from those calculated using reduced major axis (RMA) and major axis (MA), the latter being larger (Niklas 1994).

Of the 16 variables showing significant relationships with total skull length, only two deviated from isometry (Table 4.13). The height of the orbit (Variable 27) shows significant ($p < 0.05$) negative allometry and the mesiodistal canine diameter (Variable 67) shows a marginally significant ($p < 0.054$) positive allometric relationship. While the value for the diastema between last maxillary incisor and canine (Variable 57) using RMA is significant for the value of $p(b_0=1)$.

Table 4.13 Results of regressions on the skull length (Variable 2.) Expected coefficient of allometry under isometry is 1.0 for all variables.

Var.	<i>n</i>	<i>r</i>	<i>t</i>	<i>p</i> (uncorr)	LEAST SQUARES			RMA			MA		
					Slope	Inter.	<i>p</i> (<i>b</i> ₀ =1)	Slope	Inter.	<i>p</i> (<i>b</i> ₀ =1)	Slope	Inter.	<i>p</i> (<i>b</i> ₀ =1)
3	8	0.9370	6.5709	0.0006	1.0368	-0.2999	0.8232	1.1065	-0.4677	0.5248	1.1141	-0.4858	0.4878
4	7	0.8967	4.5288	0.0062	1.4506	-1.3422	0.2185	1.6178	-1.7415	0.1117	1.7023	-1.9434	0.0905
6	8	0.9701	9.7920	0.0001	0.9428	0.0896	0.5740	0.9718	0.0197	0.7797	0.9710	0.0217	0.7608
12	8	0.9041	5.1831	0.0020	0.8082	-0.0832	0.2646	0.8939	-0.2895	0.5214	0.8833	-0.2642	0.4763
24	8	0.8518	3.9834	0.0073	0.9880	-0.3536	0.9630	1.1599	-0.7672	0.5431	1.1899	-0.8394	0.5001
25	8	0.6667	2.1909	0.0710	0.7151	0.2862	0.4162	1.0726	-0.5743	0.8314	1.1107	-0.6661	0.7963
26	8	0.8020	3.2888	0.0166	0.9469	-0.5843	0.8598	1.1807	-1.1469	0.5534	1.2295	-1.2643	0.5068
27	7	0.7472	2.5140	0.0536	0.4947	0.5016	0.0502	0.6621	0.1005	0.1466	0.5822	0.2919	0.0876
37	8	0.8546	4.0315	0.0069	1.1414	-0.8816	0.6352	1.3356	-1.3489	0.2807	1.4007	-1.5055	0.2426
40	7	0.6976	2.1768	0.0814	1.1704	-1.4135	0.7642	1.6778	-2.6298	0.2630	2.0409	-3.5000	0.2464
41	7	0.8655	3.8635	0.0118	1.4083	-1.8172	0.3135	1.6272	-2.3419	0.1459	1.7436	-2.6208	0.1219
49	8	0.8321	3.6751	0.0104	0.7038	-0.0151	0.1730	0.8459	-0.3569	0.4516	0.8181	-0.2901	0.3889
51	8	0.8432	3.8415	0.0085	1.1319	-1.5248	0.6702	1.3424	-2.0315	0.2894	1.4152	-2.2067	0.2508
52	7	0.8024	3.0064	0.0299	1.0684	-1.1930	0.8549	1.3316	-1.8237	0.3937	1.4252	-2.0482	0.3456
55	7	0.4327	1.0731	0.3323	1.0215	-1.1885	0.9829	2.3610	-4.3875	0.2722	4.6910	-9.9525	0.3610
57	7	0.0374	0.0836	0.9366	0.0605	1.0571	0.2507	1.6188	-2.6646	0.4314	26.8280	-62.872	0.9058
59	8	0.1784	0.4441	0.6726	0.4434	0.2395	0.5974	2.4859	-4.6762	0.1873	11.7660	-27.011	0.6455
61	8	0.6382	20.3070	0.0886	0.6481	0.4728	0.3124	1.0154	-0.4113	0.9630	1.0243	-0.4326	0.9535
65	7	0.4948	1.2731	0.2590	0.8502	-0.1899	0.8314	1.7184	-2.2634	0.3312	2.6713	-4.5392	0.3601
67	7	0.9116	4.9581	0.0043	1.2115	-1.5914	0.4264	1.3290	-1.8720	0.2360	1.3650	-1.9581	0.1975

Due to the small sample sizes ($6 < n \leq 9$) encountered in these analyses, an alternative measurement of the skull length was selected to use as the independent variable. Prepineal length of the skull (Variable 6), measured from the tip of the snout to the centre of the pineal opening, was chosen. Previous studies on ontogenetic growth in therapsids by Grine *et al.* (1978) and Tollman *et al.* (1979) have used a similar approach to increasing the size of the available sample. By doing so in this study the sample sizes were able to be increased ($6 < n \leq 13$) for several variables, and the number of variables able to be tested viably increased to 21 (Table 4.14).

In the analysis using prepineal skull length (Variable 6) as the independent variable, 19 of the regressions showed that the variable being tested had a significant relationship with the independent variable. The Pearson's product-moment correlation coefficient (r) for these 19 measurements ranged from 0.60-0.97. Six variables were shown to deviate from isometry. These measurements included antorbital skull length (Variable 3), minimum height of suborbital bar (Variable 41), dentary length (Variable 43), mandible length (Variable 45), maxillary bicanine breadth (Variable 65), and the mesiodistal diameter of the maxillary canine (Variable 67). All of these measurements showed positive allometry, with the exception of mandible length (Variable 45), which shows negative allometry.

Table 4.14 Results of regressions on the prepineal skull length (Variable 6.) Expected coefficient of allometry under isometry is 1.0 for all variables.

Var.	<i>n</i>	<i>r</i>	<i>t</i>	<i>p</i> (uncorr)	LEAST SQUARES			RMA			MA		
					Slope	Inter.	<i>p</i> (<i>b</i> ₀ =1)	Slope	Inter.	<i>p</i> (<i>b</i> ₀ =1)	Slope	Inter	<i>p</i> (<i>b</i> ₀ =1)
2	9	0.9703	10.612	1.44E-05	0.96606	0.12631	0.72034	0.99564	0.056268	0.9631	0.9955	0.056584	0.96025
3	13	0.93645	8.854	2.46E-06	1.2054	-0.64835	0.15947	1.2872	-0.84066	0.058597	1.309	-0.89176	0.048516
4	11	0.7345	3.2471	0.010044	0.90698	-0.00057	0.74675	1.2348	-0.76855	0.42228	1.3303	-0.99224	0.37674
7	10	0.14362	0.41047	0.69223	0.19186	1.0433	1.2207	1.3359	-1.6549	0.49284	4.3208	-8.6949	0.56065
12	11	0.84881	4.8165	0.000952	0.7348	0.13828	0.11614	0.86567	-0.17029	0.40149	0.8439	-0.11897	0.3516
24	10	0.88712	5.4366	0.000618	1.0685	-0.49071	0.73636	1.2045	-0.81052	0.32858	1.2329	-0.87746	0.29354
25	11	0.65475	2.5987	0.028798	0.80682	0.11488	0.54923	1.2323	-0.88488	0.47349	1.3717	-1.2124	0.41899
26	12	0.86721	5.5074	0.000259	1.0351	-0.74898	0.85558	1.1936	-1.1227	0.32725	1.226	-1.199	0.29465
27	11	0.61028	2.3111	0.04615	0.51667	0.46268	0.058877	0.84661	-0.31387	0.50992	0.76278	-0.11656	0.39469
37	13	0.68933	3.1559	0.009146	0.82971	-0.08012	0.53046	1.2036	-0.95926	0.45492	1.3064	-1.2007	0.40459
40	12	0.2962	0.98067	3.50E-01	0.63196	-0.08248	0.58053	2.1336	-3.6059	0.10907	5.7934	-12.193	0.35618
41	12	0.60086	2.377	0.038809	1.5841	-2.164	0.40132	2.6364	-4.6332	0.033936	4.0061	-7.8471	0.078435
49	12	81997	4.5299	0.001092	0.76273	-0.11092	0.18912	0.9302	-0.50581	0.68722	0.91557	-0.47132	0.6527
51	11	0.76458	3.5588	0.00613	1.0355	-1.2195	0.90564	1.3543	-1.9715	0.25431	1.4808	-2.27	0.22334
52	7	0.89801	4.5638	0.006036	1.1967	-1.4447	0.48695	1.3326	-1.7643	0.26047	1.3754	-1.865	0.2201
55	11	0.32957	1.0472	0.32231	0.73709	-0.46154	0.71741	2.2365	-3.977	0.11283	5.6079	-11.881	0.33793
57	10	0.18723	0.53911	0.60448	0.42417	0.21672	0.48513	2.2654	-4.1035	0.14642	9.8436	-21.884	0.57735
59	11	0.000221	0.000663	0.99949	0.000616	1.2706	0.31035	2.789	-5.3125	0.086453	10997	-25962	0.99941
61	11	0.4473	1.5004	0.16776	0.45218	0.96016	0.10247	1.0109	-0.35892	0.97195	1.0245	-0.39108	0.95849
65	10	0.58357	2.0326	0.076547	2.0984	-3.0881	0.31841	3.5957	-6.5744	0.036124	5.8557	-11.836	0.10387
67	12	0.91094	6.9828	3.79E-05	1.8548	-3.048	0.009206	2.0361	-3.4719	0.002958	2.1592	-3.7597	0.00256

CHAPTER FIVE - SPECIMEN LOCALITIES & BIOSTRATIGRAPHY

Localities of 14 of the 16 specimens which have been identified as *Aelurognathus* are known (Figure 5.1 & Table 5.1). Thirteen of these localities are in South Africa, with a single specimen of *Aelurognathus tigriceps* (SAM-PK-7847) from Malawi. Of the 13 South African specimens, ten were found in the region between the towns of Murraysburg, Richmond, Graaff-Reinet and Aberdeen in the Eastern Cape and Western Cape Provinces.

Table 5.1 Localities and Assemblage Zones for specimens belonging to *Aelurognathus*.

Taxon	Collection number	Locality Name	Assemblage Zone ^a
<i>A. tigriceps</i>	SAM-PK-2342	Dunedin, Beaufort West	<i>Cistecephalus</i>
	SAM-PK-2672	Dunedin, Beaufort West	<i>Cistecephalus</i>
	SAM-PK-4334	Unknown ^b	-
	SAM-PK-7847	Chiweta, Mt Walker Area, Malawi	- ^c
	SAM-PK-10071	Dunedin, Beaufort West	<i>Cistecephalus</i>
<i>A. kingwilli</i>	RC 60	Middelvlei, Murraysburg	<i>Cistecephalus</i>
	RC 62	Graaff-Reinet District	<i>Cistecephalus</i>
<i>A. ferox</i>	RC 81	Riversdale, Graaff-Reinet	<i>Cistecephalus</i>
	RC 82	Upper Dalham, Graaff-Reinet	<i>Cistecephalus</i>
	BP/1/2465	Oudeplaas, Richmond	<i>Cistecephalus</i>
	TMP 132	no locality recorded	-
<i>A. maccabei</i>	RC 34	St. Olives, Graaff-Reinet	<i>Dicynodon</i> ^d
<i>A. brodiei</i>	BP/1/2190	Poortjie, Graaff-Reinet	<i>Dicynodon</i> ^d
	TMP 1493	Houd Constant, Graaff-Reinet	<i>Dicynodon</i> ^d
<i>A. alticeps</i>	BP/1/813	Hoeksplaas, Murraysburg	<i>Dicynodon</i> ^d
	BP/1/1566	Ringsfontein, Murraysburg	<i>Dicynodon</i> ^d

a According to Smith & Keyser (1995b) and Kitching (1995)

b Possibly from Zuurplaats, Graaff-Reinet (*Cistecephalus* AZ), see detailed discussion in text.

c Deposits of the Upper Bone Bed correspond to the *Cistecephalus* AZ (Sigogneau 1970) and are Late Permian in age (Brink 1986)

d *Daptocephalus* Zone of Kitching (1970, 1977)

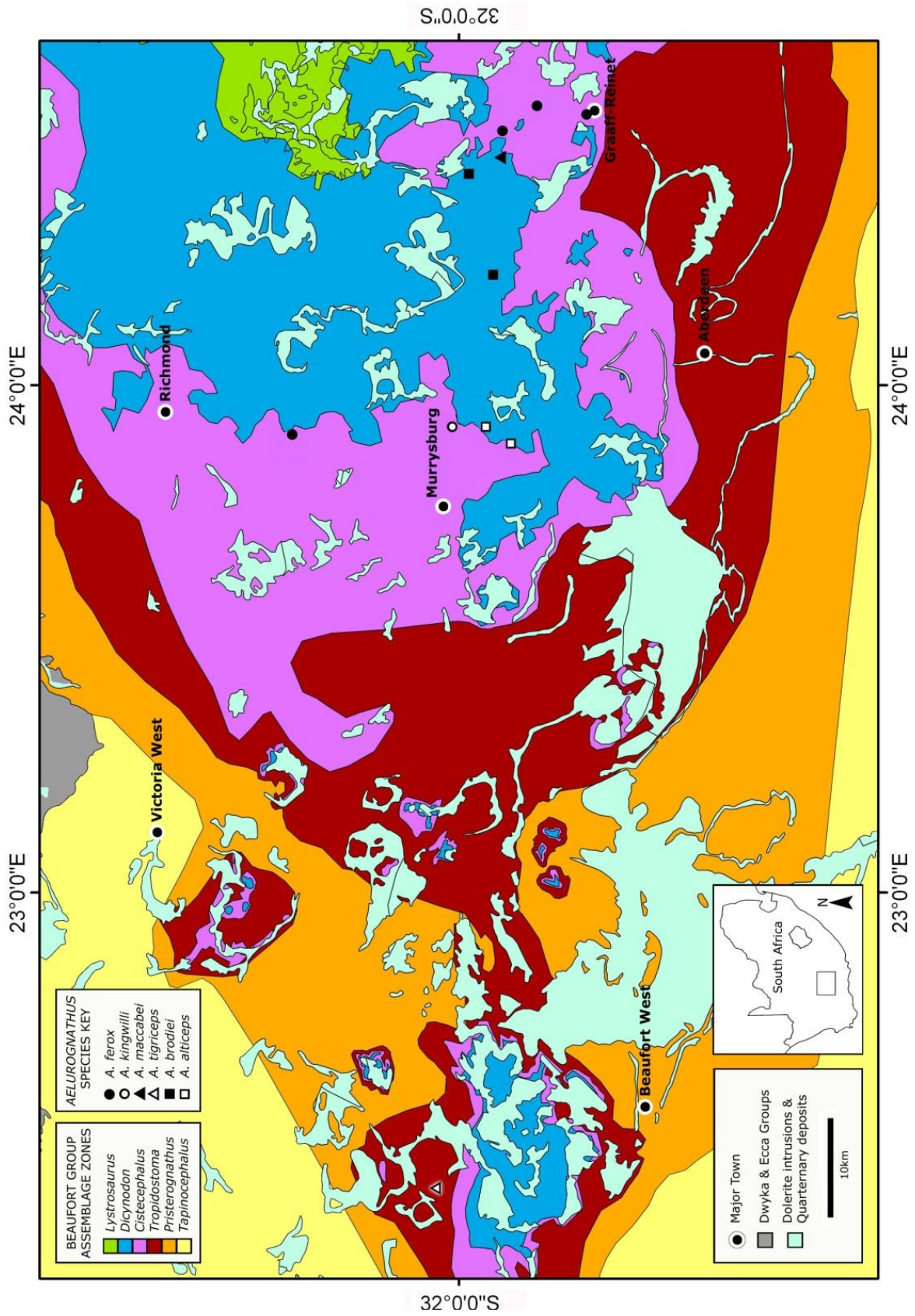


Figure 5.1 Biozonation map of the southern Karoo Basin showing the localities of the South African specimens of *Aelurognathus*.

5.1 Specimens from the *Cistecephalus* Assemblage Zone

Three specimens of *Aelurognathus tigriceps* were found on Dunedin, Beaufort West in the Western Cape Province. At least two of these specimens, SAM-PK-2342 and SAM-PK-2672, may come from the same outcrop, as Broom & Haughton (1913, p. 26) and Haughton (1915, p. 88) described the localities as “3 miles WSW. of the homestead on the farm.” This locality is considered to be in the *Cistecephalus* Assemblage Zone (AZ) (Kitching 1970, 1977; Sigogneau 1970, Sigogneau-Russell 1989). SAM-PK-10071 is also from *Cistecephalus* AZ deposits on Dunedin (Kitching 1970, 1977; Sigogneau 1970, Sigogneau-Russell 1989), less information was provided about its locality and it may not originate from the same outcrop as the two other specimens. According to the most recent Beaufort Group biozone distribution map of van der Walt *et al.* (2010), the locality of Dunedin is shown to be located within the *Tropidostoma* AZ. This is may be due to the fossil localities being plotted according to the farm centroid established by Nicolas *et al.* (2009), and not on the actual provenance of their discovery. In addition, smaller outcrops of *Cistecephalus* AZ deposits may not be visible on Figure 5.1 due to the small scale of the map.

The last specimen of *A. tigriceps*, SAM-PK-4334, has no recorded locality according to Sigogneau (1970), Sigogneau-Russell (1989) and Gebauer (2007), however, Haughton (1918) mentions a skull closely allied to *Scymnognathus* (= *Aelurognathus*) *tigriceps* as having been found on the farm Zuurplaats, Graaff-Reinet. In this paper, Haughton also names SAM-PK-4334 as *Aelurognathus*

tigriceps? in his Figure 55 (p. 206). If SAM-PK-4334 was found on Zuurplaats, then it represents the only specimen of *Aelurognathus tigriceps* found in close proximity to the localities of the other *Aelurognathus* specimens. Zuurplaats is a neighbouring farm to Houd Constant, the locality where the holotype of *Aelurognathus brodiei* was discovered, in the Murraysburg/ Graaff-Reinet District. In contrast Dunedin is approximately 110 km from the closest *Aelurognathus* locality, Ringsfontein.

RC 60, the only specimen of *Aelurognathus kingwilli*, was discovered on the farm Middelvlei in the Murraysburg District. Broom (1948, p. 599) wrote that the specimen is, “*probably from near the top of the Cistecephalus zone.*” The works of Kitching (1970, 1977), Sigogneau (1970) and Sigogneau-Russell (1989) agree with the biostratigraphic placement of Broom (1948). This locality is close to those where specimens of *Aelurognathus alticeps* were found.

Specimens belonging to *Aelurognathus ferox* all come from rocks of the *Cistecephalus* AZ (Kitching 1970, 1977; Sigogneau 1970, Sigogneau-Russell 1989). Three of these specimens, RC 62, RC 81 and RC 82, come from the Graaff-Reinet Commonage and the farms Riversdale and Upper Dalham respectively. The fourth specimen of *A. ferox* comes from the farm Oudeplaas in the more north-westerly Richmond District. Oudeplaas is the next most isolated *Aelurognathus* locality in South Africa after Dunedin.

5.2 Specimens from the *Dicynodon* Assemblage Zone

The single specimen assigned to *Aelurognathus maccabei* was recovered from the farm, St Olives, Graaff-Reinet. These deposits have been described as coming from the *Dicynodon* AZ (Kitching 1970, 1977; Sigogneau 1970, Sigogneau-Russell 1989), but there are portions of St Olives that extend down to the *Cistecephalus* AZ. The referred specimen of *Aelurognathus brodiei* (BP/1/2190) was found on the neighbouring farm, Poortjie, Graaff-Reinet. Brink & Kitching (1953, p. 14) describe the locality of BP/1/2190 as, “*about a mile or two from the locality [of A. maccabei] on the neighbouring farm...*” Brink & Kitching (1953, p. 14) also noted that the difference in stratigraphic height between the two localities is, “*about 300 feet,*” with Poortjie being the lower of the two. These beds were described as being from the middle *Cistecephalus* Zone by Brink & Kitching (1953), and are described as being of the *Daptocephalus* Zone in Kitching (1970, 1977), Sigogneau (1970) and Sigogneau-Russell (1989), which is equivalent to the *Dicynodon* AZ (Kitching 1995). The holotype of *A. brodiei* (TMP 1493) comes from the farm Houd Constant, Graaff-Reinet. Broom (1941) wrote that TMP 1493 was found “*about two miles to the north of the homestead*” (p. 198). These deposits have been described as forming part of the *Dicynodon* AZ (Kitching 1970, 1977; Sigogneau 1970, Sigogneau-Russell 1989).

5.3 Summary

Geographically 13 of the 14 South African specimen localities are within 50 km of one another. The most isolated locality, Dunedin, is approximately 110 km away from Ringsfontein, the nearest locality, and approximately 160 km from the furthest locality, Graaff-Reinet Commonage. Despite such close proximities, with several specimens occurring on the same or neighbouring farms, the beds from which the fossils were retrieved may differ from one another stratigraphically by several metres. What the plot of the localities relative to the boundaries of the various Assemblage Zones of the Beaufort Group shows, is that specimens assigned to *Aelurognathus* have been found only in the southern regions of the Karoo basin. This outcome has three implications; either *Aelurognathus* had not yet reached the north eastern regions of the Karoo Basin while these rocks were being deposited, the rocks of the southern and northern regions of the Karoo Basin were deposited at different times, or there was no sediment being deposited in the north of the Karoo Basin during the period that the *Cistecephalus* and lower *Dicynodon* AZs were being laid down.

As a specimen of *Aelurognathus* (SAM-PK-7847) is known from similarly aged Permian deposits of Malawi, the first inference is less likely. and suggests that the rocks of the *Dicynodon* AZ in the northern part of the basin represent only the upper part of the biozone.

CHAPTER SIX - DISCUSSION

Gorgonopsian taxonomy has been a difficult topic to address, largely due to the conservative cranial morphology of the group. This has led to the description of a large number of species and genera, often established on characters now considered to be rather trivial. The bold taxonomic reassessment of Gebauer (2007) greatly reduced the number of genera considered to be valid. Gebauer (2007) placed several additional species, considered by previous authors to belong in other genera, into *Aelurognathus*. The taxa remained as separate species, thus raising the species count of *Aelurognathus* to six, compared with only three recognised by Sigogneau-Russell (1989). Due to the number of newly assigned species to *Aelurognathus*, this project was undertaken in order to better understand the taxonomy of the genus as defined by Gebauer (2007).

Diagnostic features used by Gebauer (2007) to assign species to *Aelurognathus* include: a heavy skull, rounded snout with dorsal constrictions, large septomaxilla, small orbits, large maxillary ridge, robust cranial arches, high temporal opening, ventral extension of the posterior zygomatic arch and well developed palatal tuberosities.

All 16 specimens assigned to *Aelurognathus* were examined in the study, which incorporated both qualitative (morphological comparisons) and quantitative (univariate & allometric statistics) techniques.

6.1 Morphology

6.1.1 Introduction

In the past, a great deal of taxonomic importance has been placed on characters such as: overall skull size, numbers of postcanine teeth, presence and shape of the preparietal, and the participation of the frontal on the supraorbital margin (e.g. Broom 1932, Sigogneau 1970, Sigogneau-Russell 1989). The anatomical descriptions undertaken for this project indicate that all of these characters are variable amongst specimens assigned to *Aelurognathus* by Gebauer (2007).

When assessing the relationship between the presence or absence of a preparietal, as well as participation of the frontal in the orbital margin, there are two discernible morphotypes. The first includes all specimens assigned to *A. tigriceps*, *A. maccabei* and *A. alticeps* and a single specimen of *A. ferox* (RC 62), which have a preparietal present and a small contribution of the frontal to the supraorbital margin. The second morphotype, which includes the single specimen of *A. kingwilli* and specimens of *A. ferox* (RC 81 & BP/1/2465), also has a contribution of the frontal on the supraorbital margin, but lacks a preparietal. A third potential morphotype, represented by *A. brodiei* (TMP 1493), may not have a contribution of the frontal on the supraorbital margin, but because of the incomplete nature of the specimen it is difficult to establish the limit of the frontal and whether it contacts the orbital margin or not. Due to the skull roof having been reconstructed using plaster, it is also unknown whether a preparietal was present.

6.1.2 Size of individuals

Size is a particularly poor character to use for taxonomic determination, especially if the growth range of the taxon is only poorly known as is often the case in palaeontology. In many instances where a smaller individual has been described as a new taxon, after further study these specimens have later been redescribed as juveniles of another species. A number of papers (Dodson 1975, 1976) dealing with dinosaur taxonomy have highlighted this problem. The same doubtless applies to Gorgonopsian taxonomy and has been partly addressed by Sigogneau (1970), Sigogneau-Russell (1989) and Gebauer (2007).

Not only is there a noticeable size difference between juvenile and adult specimens of the same taxon, but the overall morphology and relative ratios between different dimensions of the skull also change (Simpson *et al.* 1960). This is especially true for the skull, where complex soft tissue structures, such as the brain and eyes develop comparatively faster than other structures (Reiss 1989). In turn these structures dictate the size of the surrounding bony structures, namely the braincase and orbital diameter. Thus juveniles tend to have relatively shorter snout compared to the overall length of the cranium, while the orbit diameter is comparatively larger.

Differences in the relationships between measurable parameters were addressed using univariate and allometric studies as outlined in a previous chapter and will be discussed further in a following section.

While using skull size and proportion to define palaeontological taxa can be easily discredited, using other morphological characters such as presence/ absence of cranial elements (e.g. preparietal in *Gorgonopsia*) or sutural limitation/ placement to distinguish taxa appears to hold more ground.

6.1.3 Characters of the skull roof

Work by Toerien (1953) on the Dicynodontia, one of the few therapsid groups that exhibit a preparietal bone, showed that there are several possible configurations of the sutures in the skull roof in the genus *Dicynodon*. In particular, the observed variation was related to the size and shape of the preparietal, whether or not the preparietal contacted the anterior margin of the pineal opening and whether the postorbitals meet each other posterior to the pineal opening. Due to the large sample size in his study ($n \approx 2000$), Toerien (1953) observed several intermediate stages between each of the conditions mentioned above and stated that it was not possible to attribute these intermediate conditions to age or sex of the individuals. Toerien (1953) went on to remark that, “*if only two specimens representing the extremes were known, they would certainly have been regarded as separate species*” (p. 56).

Recent work by Jasinowski (*pers. comm.* 2010), on the dicynodont, *Lystrosaurus*, has also shown high variability in the skull roof of the genus, to the extent that a supernumerary bone, an element between the frontals and nasals, may be present,

partially fused to the frontals or completely absent. Such variability in the configuration of the sutures of the skull is also known in populations of extant mammals e.g. *Pongo*, *Homo*, *Lemur*, *Ursus*, *Hippopotamus*, *Phascolomys* and *Procavia* (Cunningham 1866, 1896; Firbas 1968; Jalil & Janvier 2005; del Papa & Perez 2007).

This is likely the situation in *Aelurognathus*, which because it was a carnivore, has a much smaller sample size ($n = 16$), and thus there are not many specimens to compare. An additional complicating factor is the distortion and poor preservation of several of the specimens studied.

Based on current knowledge of cranial bone variability present in extant and extinct tetrapods, the presence or absence of the preparietal bone between the two morphotypes of *Aelurognathus* is insufficient to warrant that the two morphotypes represent separate species.

6.1.4 Dentition

All dentition in *Gorgonopsia* replaced at least once, therefore none of the teeth may be equated to ‘molars’ of modern mammals (Kermack 1956). Teeth of younger, smaller individuals, would most likely have been replaced more frequently and more quickly, possibly giving the impression that the canines of each side were both in a functional state. Larger individuals would have taken longer to replace a

canine tooth, due to the increased size of the tooth, and thus the amount of resources and time required for it to develop and erupt into a functional state. In medium-to-large Gorgonopsia the difference in development/ stage of eruption between the canine teeth of each side is more evident (Kermack 1950).

Staggering in the eruption times of teeth are not limited to the canines as in several specimens of *Aelurognathus*, a differing numbers of postcanine teeth have been observed on the left and right maxillae of the same individual. *A. maccabei* (RC 34) is one such individual, which also shows alveoli where a tooth has fallen out and has yet to be replaced. The case in this individual provides some evidence as to why classifying Gorgonopsia taxa based on the number of postcanine teeth is unreliable.

Due to convoluted taxonomic histories of many gorgonopsians, which include a plethora of now redundant names to the literature, it is not easy to discern whether small specimens represent juveniles of larger individuals or are indeed representatives of another taxon. In addition the poor and often incomplete preservation of specimens adds to this confusion.

Interestingly the number of incisors present on each premaxillae of an individual is not variable in the Gorgonopsia. This suggests the possibility of a different replacement mechanism involved during the replacement of incisors and may provide an insight into the mechanism present in members of modern placental mammals.

If true molars were present in the Gorgonopsia we would expect larger individuals to have a greater number of 'postcanine' teeth. However the situation in '*Aelurognathus*' does not agree with this, and in most cases medium to large specimens (e.g. SAM 7847, RC 62, RC 81 and RC 82) have fewer postcanines (1-3) than that observed in smaller specimens, e.g. BP/1/813, which has 4 to 5 postcanines. SAM-PK-4334, one of the smaller specimens in the sample, is an exception to this and only has 2 postcanines.

One way to account for such an observation is that some postcanines in the smaller specimens have yet to erupt, a claim that may be substantiated through the use of CT scanning to observe unerupted teeth (Rubidge & de Klerk 2007). Such technology may be used to determine if the observed increase in the number of postcanine teeth is due to ontogenetic growth, by determining if there are more unerupted postcanines present relative to the number of erupted postcanines.

While not in the scope of this study, additional experiments and observations to determine postcanine dental succession could add to further disprove the validity of using varying numbers of postcanine teeth in order to distinguish between taxa of the Gorgonopsia, and possibly other (theriodont) therapsids.

6.2. Statistical Analyses

6.2.1 Univariate analyses

The results from the univariate analyses show that the specimens measured cover a continuous range, for most of the measurements taken, and may span several growth stages. A brief discussion is provided in the results section for each of the measurements that did not have a continuous plot. In several of these examples, the inconsistency in the range of measurements may be attributed to small sample sizes and or the distortion of specimens.

The only exception was for orbital length (Variable 26). It had a relatively large sample size ($n = 14$). Both *A. tigriceps* and *A. alticeps* fall well outside of the lower most limits of the other taxa. These two taxa are also described as having a small orbit. As such Variable 26 was the only univariate statistic to provide support for prior morphological observations.

6.2.2. Allometry

The results of the allometric analyses with total skull length (Fm) as the independent variable, showed that all measurements, except for the height of the orbit (27), length of the maxillary canine-postcanine diastema (57) and mesiodistal diameter of the mandibular canine (67), had a tendency towards isometric growth (Tables 4.13 & 4.14).

In comparison, when prepineal skull length (Pin) was used as the independent variable six measurements deviated from isometry. These were antorbital skull length (3), height of the suborbital bar (41), total dentary length (43*), dentary length (RL) (45), maxillary bicanine breadth (65) and the mesiodistal diameter of the maxillary canine (67).

6.3 Systematic Palaeontology

Results of this project to determine the number of valid species of *Aelurognathus* through the use of both morphological and statistical analyses, suggests that there is only a single valid species of *Aelurognathus*, which is *Aelurognathus tigriceps*. The following section provides a summary of the previous taxonomic assignments pertinent to the genus and provides an updated diagnosis for *Aelurognathus*.

SYNAPSIDA Osborn 1903

THERAPSIDA Broom 1905

THERIODONTIA Owen 1876

GORGONOPSIA Seeley 1895

RUBIDGEINAE Sigogneau 1970

AELUROGNATHUS Haughton 1924

Type Species: *Aelurognathus tigriceps* Broom & Haughton 1913

Diagnosis: As for type species

AELUROGNATHUS TIGRICEPS Broom & Haughton 1913

Scymnognathus tigriceps (Broom & Haughton 1913, p. 26)

Scymnognathus serratidens (Haughton 1915, p. 88)

Scymnognathus tigriceps? (Haughton 1918, p. 205)

Aelurognathus nyasaensis (Haughton 1926, p.73)

Prorubidgea maccabei (Broom 1940, p. 169)

Prorubidgea pugnax (Broom 1940)

Sycosaurus brodiei (Broom 1941, p. 198)

Tigricephalus kingwilli (Broom 1948, p. 599)

Smilesaurus ferox (Broom 1948, p. 599)

Smilesaurus maccabei (Broom 1948, p.601)

Pardocephalus wallacei (Broom 1948, p. 603)

Prorubidgea robusta (Brink & Kitching 1953, p. 14)

Lycaenops alticeps (Brink & Kitching 1953, p. 22)

Prorubidgea brinki (Mantel 1958, p. 67)

Arctops? ferox (Sigogneau 1970, p. 148)

Aelurognathus cf. tigriceps (Sigogneau 1970, p. 166)

Aelurognathus serratidens (Sigogneau 1970, p. 167)

Lycaenops kingwilli (Sigogneau 1970, p. 198)

Prorubidgea alticeps (Sigogneau 1970, p. 269)

Prorubidgea alticeps? (Sigogneau 1970, p. 272)

Prorubidgea brodiei (Sigogneau 1970, p. 278)

Prorubidgea brodiei (Sigogneau Russell 1989, p. 107)

Aelurognathus nyassaensis (Sigogneau 1970, p. 166)

Aelurognathus kingwilli (Gebauer 2007, p. 186)

Aelurognathus ferox (Gebauer 2007, p. 186)

Aelurognathus maccabei (Gebauer 2007, p. 186)

Aelurognathus alticeps (Gebauer 2007, p. 187)

Aelurognathus broodiei (Gebauer 2007, p. 187)

Aelurognathus nyassicus (Gebauer 2007, p. 225)

6.3.1 Holotype

SAM-PK-2342. Skull with lower jaw, cervical vertebrae, pectoral girdle, humerus and radius, crushed cubitus and forefoot. Skull is crushed and somewhat incomplete. The locality is Dunedin, Beaufort West, South Africa. *Cistecephalus* Assemblage Zone, Late Permian.

6.3.2 Referred material

- I SAM-PK-4334 complete but crushed skull and lower jaw. Provenance unknown
- II SAM-PK-10071 laterally compressed and incomplete skull with attached lower jaw. Dunedin, Beaufort West, South Africa. *Cistecephalus* AZ.
- III SAM-PK-7847 (*Aelurognathus nyasaensis*) Distorted anterior half of skull and lower jaw. Chiweta, Mount Walker area, Malawi. Upper Bone Bed, equivalent to *Cistecephalus* AZ.
- IV SAM-PK-2672 (*Aelurognathus serratidens*) Anterior half of compressed skull. Dunedin, Beaufort West, South Africa. *Cistecephalus* Zone.

- V RC 34 (*Prorubidgea maccabei*) Complete, well preserved skull from St. Olives, Graaff-Reinet. *Cistecephalus* AZ.
- VI TMP 1493 (*Sycosaurus brodiei*) An incomplete skull with lower jaw. Houd Constant, Graaff-Reinet, South Africa.
- VII BP/1/2190 (*Prorubidgea robusta*) a well preserved skull with lower jaw, cervical vertebrae and a hand covering part of the skull. Poortjie, Graaff-Reinet, South Africa. *Dicynodon* AZ
- VIII RC 60. (*Tigricephalus kingwilli*) Well preserved skull from Middelvlei, Murraysburg Dist, South Africa, *Cistecephalus* AZ.
- IX RC 62 (*Smilesaurus ferox*) Compressed skull with lower jaw and postcranial elements attached. Graaff-Reinet Commonage, *Cistecephalus* AZ.
- X RC 81 (*Smilesaurus maccabei*) Fairly complete skull with lower jaw and vertebra attached from Riversdale, Graaff-Reinet, *Cistecephalus* AZ
- XI RC 82 (*Pardocephalus wallacei*) Incomplete skull from Upper Dalham, Graaff-Reinet, *Cistecephalus* AZ
- XII BP/1/2465 (*Arctops? ferox*) Complete, slightly distorted skull from Oudeplaas, Richmond *Cistecephalus* AZ.
- XIII TMP 132 (*Arctops? ferox*) Incomplete and compressed skull from an unrecorded locality.
- XIV BP/1/813 (*Prorubidgea alticeps*) an incomplete and altered skull with dentary. Hoeksplaas, Murraysburg, South Africa.
- XV BP/1/1566 (*Prorubidgea brinki*) a complete skull with lower jaw, somewhat laterally compressed. Ringsfontein, Murraysburg, South Africa.

6.3.3 Revised diagnosis

Skull is robust with well developed and broad cranial arcades. The posterior region of the zygomatic arch curves ventrally. The snout has a well defined convex profile. A depression occurs anterior to the small orbit. The frontal may contribute to the supraorbital margin. The maxilla has a prominent posterior projection that often bears a ridge. A large septomaxilla is present. A preparietal may be present or absent. If present, the preparietal tends to lie between the two temporal fenestrae, which are situated high on the skull. Palatal tuberosities are broad and well defined and may bear denticles.

CHAPTER SEVEN - CONCLUSION

Taxonomy of the Gorgonopsia has always been complex and difficult to unravel, largely because of the relatively conservative morphology displayed within the group. This morphological conservancy has led previous authors to place a lot of taxonomic weight on characters that are of little or no taxonomic importance. In many cases these morphological characters were used to diagnose and differentiate between a large number of species and even genera.

This project has demonstrated that the six species previously attributed to the genus *Aelurognathus* can be divided into three morphotaxa, based exclusively on the variation exhibited on the skull roof. While these may be sufficient to divide the genus into three species, on the basis of morphological differences, comparison of the various skulls attributed to *Aelurognathus* by Gebauer (2007) with other extant and extinct synapsid taxa has shown that these morphological differences observed between morphotypes may in fact be due to variation at the individual level and are of no taxonomic importance.

This single species hypothesis was tested using several statistical techniques. Due to poor preservation and taphonomic distortion of many of the specimens, as well as the limit to the number of specimens assigned to the genus, sample sizes used in the analyses were quite small ($8 > n < 14$). These statistical tests provided support that all specimens of *Aelurognathus*, most of which have been considered to belong

to separate species, do in fact belong to a single species that exhibits some morphological variation.

This study suggests that many of the morphological characters currently used to differentiate between different gorgonopsian species, and even genera in some instances, may in fact be variable morphological features of a single species. It is proposed that all six species of *Aelurognathus* described by Gebauer (2007) be synonymised with *Aelurognathus tigriceps*.

8 REFERENCES

ABDALA, F. & GIANNINI, N.P. (2000) Gomphodont cynodonts of the Chañares Formation: The analysis of an ontogenetic sequence. *Journal of Vertebrate Paleontology*. 20(3): 501-506.

ABDALA, F. & GIANNINI, N.P. (2002) Chiniquodontid cynodonts: Systematic and morphometric considerations. *Palaeontology*. 45(6): 1151-1170.

ALEXANDER, R. McN. (1895) Body support, scaling and allometry. In: HILDEBRAND, M. & WAKE, D.B. (Eds) *Functional vertebrate morphology*. The Belknap Press of Harvard University Press, Cambridge, Massachusetts. pp. 27-37.

BOWRING, S.A., ERWIN, D.H., JIN, Y.G., MARTIN, M.W. DAVIDEK, K. & WANG, G. (1998) U/Pb zircon geochronology and tempo of the End-Permian mass Extinction. *Science* 280: 1039-1045.

BRINK, A.S. (1977) A model of tooth replacement in the “mammal-like reptile” *Diademodon*. *South African Journal of Science*. 73: 138-143.

BRINK, A.S. (1986) *Illustrated bibliographical catalogue of the Synapsida*. Geological Survey of South Africa, Handbook 10, Volume 1.

BRINK, A.S. (1988) *Illustrated bibliographical catalogue of the Synapsida*. Geological Survey of South Africa, Handbook 10, Volume 2.

BRINK, A.S. & KITCHING, J.W. (1953) Studies on new specimens of the Gorgonopsia *Palaeontologia africana* 1: 1-28.

BROOM, R. (1905) On the use of the term Anomodontia. *Records of the Albany Museum*. 1(4): 266-269.

BROOM, R. (1910a) Observations on some specimens of South African fossil reptiles preserved in the British Museum. *Transactions of the Royal Society of South Africa*. 2: 19-25.

BROOM, R. (1910b) A comparison of the Permian reptiles of North America with those of South Africa. *Bulletin of the American Museum of Natural History*. 28: 197-234.

BROOM, R. (1912) On some new fossil Reptiles from the Permian and Triassic beds of South Africa. *Proceedings of the Royal Society of London*. p. 859-876.

BROOM, R. (1913a) A revision of the reptiles from the Karroo. *Annals of the South African Museum*. 12: 361-366.

BROOM, R. (1913b) On the Gorgonopsia, a suborder of the mammal-like reptiles. *Proceedings of the Zoological Society of London*. 1: 225-230.

BROOM, R. (1915) Croonian Lecture: On the origin of mammals. *Philosophical Transactions of the Royal Society of London, Series B*. 206: 1-48.

BROOM, R. (1932) *The mammal-like reptiles of South Africa and the origins of mammals*. H. F. & G. Witherby, London. 367 pp.

BROOM, R. (1936) On some new genera and species of Karroo fossil reptiles, with notes on some others. *Annals of the Transvaal Museum*. 18(4): 349-386.

BROOM, R. (1938) On a new family of carnivorous therapsids from the Karroo beds of South Africa. *Proceedings of the Royal Society of London, series B*. 108(3): 527-533.

BROOM, R. (1940) On some new genera and species of fossil reptiles from the Karroo beds of Graaff-Reinet. *Annals of the Transvaal Museum*. 20: 157-192.

BROOM, R. (1941) Some new Karroo reptiles, with notes on a few others. *Annals of the Transvaal Museum*. 20(3); 193-213.

BROOM, R. (1948) A contribution to our knowledge of the vertebrates of the Karroo beds of South Africa. *Transactions of the Royal Society of Edinburgh*. 61(2): 577-629.

BROOM, R. & HAUGHTON, S.H. (1913) On a new species of *Scymnognathus* (*S. tigriiceps*). *Annals of the South African Museum*. 12(1): 26-35.

BROOM, R. & GEORGE, M. (1950) Two new gorgonopsian genera from the Bernard Price Collection. *South African Journal of Science*. 46(6): 188-190

CROMPTON, A.W. (1963) Tooth replacement in the cynodont *Thrinaxodon liorhinus* Seeley. *Annals of the South African Museum*. 46(20): 479-521.

CUNNINGHAM, R.O. (1866) On the occurrence of a pair of supernumerary bones in the skull of a lemur and on a peculiarity in the skull of a young orang. *Proceedings of the Zoological Society of London*. 64(4): 996-999.

CUNNINGHAM, R.O. (1896) Note on the presence of supernumerary bones occupying the place of prefrontals in the skulls of certain mammals. *Proceedings of the Zoological Society of London*. 67(1): 76-77.

DEL PAPA, M.C., & PEREZ, S.I (2007) The Influence of Artificial Cranial Vault Deformation on the Expression of Cranial Nonmetric Traits: Its Importance in the Study of Evolutionary Relationships. *American Journal of Physical Anthropology*. 134(2): 251-262.

DODSON, P. (1975) Taxonomic implications of relative growth in lambeosaurine dinosaurs. *Systematic Zoology*. 24(1): 37-54.

DODSON, P. (1976) Quantitative Aspects of Relative Growth and Sexual Dimorphism in *Protoceratops*. *Journal of Paleontology*. 50(5): 929-940.

EMERSON, S.B. & BRAMBLE, D.M. (1993) Scaling, allometry and skull design. In: HANKEN, J. & HALL, B.K. (Eds) *The skull*. University of Chicago Press, Chicago, Illinois. Pp 384-416.

FIRBAS, W. 1968. Supernumerary bone in a skull of a brown bear from the Kamchatka Peninsula. *Journal of Mammalogy*. 49:775.

FLORES, D.A., GIANNINI, N. & ABDALA, F. (2006) Comparative postnatal ontogeny of the skull in the australidelphian metatherian *Dasyurus albopunctatus* (Marsupialia: Dasyuromorpha: Dasyuridae). *Journal of Morphology*. 267: 426-440.

GEBAUER, E.V.I. (2007) *Phylogeny and evolution of the Gorgonopsia with a special reference to the skull and skeleton of GPIT/RE/7113 ('Aelurognathus?' parringtoni)*. Unpublished Dr. rer. nat. dissertation. Eberhard-Karls Universität Tübingen. 316 pp.

GIANNINI, N.P., ABDALA, F. & FLORES, D.A. (2004) Comparative postnatal ontogeny of the skull in *Dromiciops gliroides* (Marsupialia: Microbiotheriidae). *American Museum Novitates*. 3460: 1-17.

GRINE, F.E., HAHN, B.D. & GOW, C.E. (1978) Aspects of relative growth and variability in *Diademodon* (Reptilia: Therapsida). *South African Journal of Science*. 78: 50-58.

HAMMER, Ø., HARPER, D.A.T. & RYAN, P.D. (2001) PAST: Palaeontological Statistics software package for education and data analysis. *Palaeontologia Electronica*. 4(1): 9.

HAUGHTON, S.H. (1915) Investigations in South African fossil reptiles and Amphibia, 7. On some new gorgonopsians. *Annals of the South African Museum*. 12: 82-90.

HAUGHTON, S.H. (1918) Investigations in South African fossil reptiles and Amphibia, 11. Some new carnivorous therapsids, with notes upon the braincase in certain species. *Annals of the South African Museum*. 12(6): 175-216.

HAUGHTON, S.H. (1924) Investigations in South African fossil reptiles and Amphibia. 12. On some new gorgonopsian skulls in the collections of the South African Museum. *Annals of the South African Museum*. 12: 499-518.

HAUGHTON, S.H. (1926) On Karroo vertebrates from Nyasaland. *Transactions of the Geological Society of Southern Africa*. 29: 69-83.

HOPSON, J.A. & BARGHUSEN, H. (1986) An analysis of therapsid relationships. In: HOTTON, N., MACLEAN, P.D., ROTH, J.J. & ROTH, E.C. (Eds) *The ecology and biology of mammal-like reptiles*. Smithsonian institution Press, Washington. pp. 83-106.

HUXLEY, J.S. (1932) *Problems of relative growth*. Dial Press, New York. 276 pp.

IVAKHNENKO, M.F., GOLUBEV, V.K., GUBIN, Y.M., KALANDADZE, N.N., NOVIKOV, I.V., SENNIKOV, A.G. & RAUTIAN, A.S. (1997) [Пермские и триасовые тетраподы Восточной Европы/ Permian and Triassic Tetrapods of Eastern Europe]. *GEOS*, Moscow, 215 pp. [in Russian]

JALIL, N.-E., & JANVIER, P. 2005. Les pareiasaures (Amniota, Parareptilia) du Permien supérieur du Bassin d'Argana, Maroc. *Geodiversitas* 27:35-132.

KEMP, T.S. (1969) On the Functional Morphology of the Gorgonopsid Skull. *Philosophical Transactions of the Royal Society of London. Series B.* 256(801): 1-83.

KEMP, T.S. (1982) *Mammal-like reptiles and the origin of mammals.* Academic Press, London. 363 pp.

KEMP, T.S. (2005) *The origin and evolution of mammals.* Oxford University Press, Oxford. 331 pp.

KEMP, T.S. (2011) The Origin and radiation of Therapsids. In: CHINSAMY-TURAN, A. *Forerunners of mammals: Radiation, histology, biology.* Indiana University Press, Bloomington, Indiana. pp. 1-28.

KERMACK, K.A. (1956) Tooth replacement in mammal-like reptiles of the suborders Gorgonopsia and Therocephalia. *Philosophical Transactions of the Royal Society of London, Series B.* 240: 95-133.

KERMACK, K.A. & HALDANE, J.B.S. (1950) Organic correlation and allometry. *Biometrika.*37: 30-41.

KEYSER, A.W. (1975) A re-evaluation of the cranial morphology and systematics of some tuskless Anomodontia. *Memoirs of the Geological Survey of South Africa.* 67: 1-110.

KITCHING, J.W. (1970) A short review of the Beaufort zoning in South Africa. In: HAUGHTON, S.H. (Ed.) *Second Symposium on Gondwana Stratigraphy and Palaeontology*, I.U.G.S., Cape Town and Johannesburg pp. 309-312/3

KITCHING, J.W. (1977) The distribution of the Karroo vertebrate fauna. *Memoirs of the Bernard Price Institute for Palaeontological Research*. 1: 1-131.

KITCHING, J.W. (1995) Biostratigraphy of the *Dicynodon* Assemblage Zone. In: RUBIDGE, B.S. (Ed.) *Biostratigraphy of the Beaufort Group (Karoo Supergroup)*. South African Committee for Stratigraphy, Biostratigraphic Series No. 1. Council for Geosciences, Pretoria. pp. 29-34.

LYDEKKER, R. (1890) *Catalogue of the fossil Reptilia and Amphibia in the British Museum (Natural History) Part IV, containing the orders Anomodontia, Ecaudata, Caudata and Labyrinthodontia; and supplement*. London. 295 pp.

MAISCH, M.W. (2002) Observations on Karroo and Gondwana vertebrates. Part 3: Notes on the gorgonopsians from the Upper Permian of Tanzania. *Neues Jahrbuch für Geologie und Paläontologie Monatshefte*. 2002(4): 237-251.

MANTON, A.A. (1958) Two Gorgonopsian skulls. *Palaeontologia africana*. 6: 51-76.

NICOLAS, M.V.M. (2007) *Tetrapod biodiversity through the Permo-Triassic Beaufort Group (Karoo Supergroup) of South Africa*. Unpublished Ph.D thesis, University of the Witwatersrand, Johannesburg.

NICOLAS, M., KEMP, C. & RUBIDGE, B. (2009) Beaufort Group GIS initiative: creating and maintaining an interactive fossil database for palaeontological research. *Palaeontologia Africana*. 44: 171-172.

NIKLAS, K.J. (1994) *Plant allometry. The scaling of form and process*. University of Chicago Press. 395 pp.

OSBORN, (1903) On the primary division of the Reptilia, into two sub-classes, Synapsida and Diapsida. *Science* 17: 275-276.

OWEN, R. (1876) *Descriptive and illustrated catalogue of the fossil Reptilia of South Africa in the collection of the British Museum*. London. xii + 88 pp.

PRAVOSLAVLEV, P.A. (1927) [The skull cap of *Inostrancevia* sp.] *Ezheg russ. Pal. Obshch.* 6: 51-56. [in Russian]

RADINSKY, L.B (1981a) Evolution of the skull shape in carnivores 1. Representative modern carnivores. *Biological Journal of the Linnaean Society*. 15: 369-388.

RADINSKY, L.B (1981b) Evolution of the skull shape in carnivores 2. Additional modern carnivores. *Biological Journal of the Linnaean Society*. 16: 337-355.

REISS, M.J. (1989) *The allometry of growth and reproduction*. Cambridge University Press, Cambridge. 182 pp.

RUBIDGE, B.S. (1988) *A palaeontological and palaeoenvironmental synthesis of the Permian Ecca-Beaufort contact in the southern Karoo between Prince Albert and Rietbron, Cape Province, South Africa*. Unpublished Ph.D. thesis. University of Port Elizabeth. 347 pp.

RUBIDGE, B.S. (1993) New South African fossil links with the earliest mammal-like reptile (therapsid) faunas from Russia. *South African Journal of Science*. 89: 460-461.

RUBIDGE, B.S. (1995) Biostratigraphy of the *Eodicynodon* Assemblage Zone. In: RUBIDGE, B.S. (Ed.) *Biostratigraphy of the Beaufort Group (Karoo Supergroup)*. South African Committee for Stratigraphy, Biostratigraphic Series No. 1. Council for Geosciences, Pretoria. pp. 3-7.

RUBIDGE, B.S. & DE KLERK, W.J. (2007) Only Albany dinocephalian reveals new toothy information. *Palaeontologia africana*. 42: 130.

RUBIDGE, B.S & SIDOR, C.A. (2001) Evolutionary patterns among Permian-Triassic therapsids. *Annual Review of Ecology and Systematics*. 32:449-480

SEELEY, H.G. (1894) Researches on the structure, organisation, and classification of the fossil Reptilia. Part IX., Section 1. On the Therapsuchia. *Philosophical Transactions of the Royal Society of London. Series B*. 185: 987-1018.

SIDOR, C.A., HOPSON, J.A. & KEYSER, A.W. (2004) A new burnetiamorph therapsid from the Teekloof Formation, Permian, of South Africa. *Journal of Vertebrate Paleontology* 24(4):938–950.

SIGOGNEAU, D. (1970) *Révision systématique des Gorgonopsians Sud-Africains*. Cahiers de Paléontologie, Paris. 414 pp.

SIGOGNEAU-RUSSELL, D. (1989) Theriodontia I. In: WELLNHOFER, P. (Ed.) *Encyclopedia of Paleoherpetology, Part 17B/ I*. Gustav Fischer Verlag, Stuttgart. 127 pp.

SIMPSON, G.G., ROE, A. & LEWONTIN, R.C. (1960) *Quantitative Zoology* (Revised Edition). Harcourt, Brace & Company, New York. 440 pp.

SMILEY, T.M., SIDOR, C.A., MAGA, A. & IDE, O. (2008) the vertebrate fauna of the Upper Permian of Niger. VI. First evidence of a gorgonopsian therapsid. *Journal of Vertebrate Paleontology*. 28(2): 543-547.

SMITH, R.M.H. & KEYSER, A.W. (1995a) Biostratigraphy of the *Tapinocephalus* Assemblage Zone. In: RUBIDGE, B.S. (Ed.) *Biostratigraphy of the Beaufort Group (Karoo Supergroup)*. South African Committee for Stratigraphy, Biostratigraphic Series No. 1. Council for Geosciences, Pretoria. pp. 8-12.

SMITH, R.M.H. & KEYSER, A.W. (1995b) Biostratigraphy of the *Cistecephalus* Assemblage Zone. In: RUBIDGE, B.S. (Ed.) *Biostratigraphy of the Beaufort Group (Karoo Supergroup)*. South African Committee for Stratigraphy, Biostratigraphic Series No. 1. Council for Geosciences, Pretoria. pp. 23-28.

SWOFFORD, D.L. (1998) *Phylogenetic Analysis Using Parsimony (and other methods)*. Version 4.0b10, Sinauer Associates, Sunderland, Massachusetts.

TOERIEN, M.J. (1953) The evolution of the palate in South African Anomodontia and its classificatory significance. *Palaeontologia africana*. 1: 49-117.

TOLLMAN, S.M., GRINE, F.E. & HAHN, B.D. (1979) Ontogeny and sexual dimorphism in *Aulacephalodon* (Reptilia, Anomodontia). *Annals of the South African Museum*. 81(4): 159-186.

VAN DER WALT, M., DAY, M., RUBIDGE, B., COOPER, A.K. & NETTERBERG, I. (2010) A new GIS-based biozone map of the Beaufort Group (Karoo Supergroup), South Africa. *Palaeontologia africana*. 45: 1-5.

VON HUENE, F. (1950) Die Theriodontier der ostafrikanischen Ruhuhu-Gebietes in der Tübinger Sammlung. *Neus Jahrb. Geol. Pal. Abh.* 92: 47-136.

WATSON, D.M.S. (1914) Notes on some carnivorous therapsids. *Proceedings of the Zoological Society of London.* 1914: 1021-1038.

WATSON, D.M.S. & ROMER, A.S. (1956) A classification of therapsid reptiles. *Bull. Mus. Comp. Zool. Harvard.* 114(2): 35-89.

9 APPENDIX A:

Table A1 List of African taxa recognised in previous taxonomic revisions of the Gorgonopsia. (For detailed information of the synonymisations that have occurred, refer to original texts).

Gorgonopsinae		
Sigogneau 1970	Sigogneau-Russell 1989	Gebauer 2007
	<i>Aelurognathus nyasaensis</i>	
<i>Aelurognathus quadrata</i>	<i>Aelurognathus quadrata</i>	
<i>Aelurognathus serratidens</i>	<i>Aelurognathus serratidens</i>	
<i>Aelurognathus</i> cf. <i>serratidens</i>	<i>Aelurognathus</i> cf. <i>serratidens</i>	
<i>Aelurognathus sollasi</i>	<i>Aelurognathus sollasi</i>	See entry under Rubidgeinae
<i>Aelurognathus tigriceps</i>	<i>Aelurognathus tigriceps</i>	
<i>Aelurognathus</i> cf. <i>tigriceps</i>		
<i>Aelurognathus</i> sp.		
<i>Aelurognathus?</i> <i>parringtoni</i>	<i>Aelurognathus?</i> <i>parringtoni</i>	
<i>Aelurosaurus breviceps</i>		
<i>Aelurosaurus felinus</i>	<i>Aelurosaurus felinus</i>	<i>Aelurosaurus felinus</i>
<i>Aelurosaurus</i> cf. <i>felinus</i>	<i>Aelurosaurus</i> cf. <i>felinus</i>	
<i>Aelurosaurus polyodon</i>	<i>Aelurosaurus polyodon</i>	
<i>Aelurosaurus whaitsi</i>	<i>Aelurosaurus whaitsi</i>	
<i>Aelurosaurus wilmanae</i>	<i>Aelurosaurus wilmanae</i>	<i>Aelurosaurus wilmanae</i>
<i>Aelurosaurus</i> sp.	<i>Aelurosaurus</i> sp.	
<i>Aelurosaurus?</i> <i>watermeyeri</i>	<i>Aelurosaurus?</i> <i>watermeyeri</i>	
cf. <i>Aelurosaurus?</i> <i>watermeyeri</i>		
	? <i>Aelurosaurus</i>	
<i>Aloposaurus gracilis</i>	<i>Aloposaurus gracilis</i>	<i>Aloposaurus gracilis</i> <i>Aloposaurus tenuis</i> <i>Aloposaurus watermeyeri</i> <i>Aloposaurus</i> sp.
	<i>Aloposaurus</i> sp.	
<i>Aloposaurus?</i> <i>tenuis</i>	<i>Aloposaurus?</i> <i>tenuis</i>	cf. <i>Aloposaurus tenuis</i>
cf. <i>Aloposaurus?</i> <i>tenuis</i>	cf. <i>Aloposaurus?</i> <i>tenuis</i>	
<i>Arctognathus breviceps</i>	<i>Arctognathus breviceps</i>	<i>Arctognathus breviceps</i>
<i>Arctognathus curvimola</i>	<i>Arctognathus curvimola</i>	<i>Arctognathus curvimola</i>
<i>Arctognathus</i> cf. <i>curvimola</i>	<i>Arctognathus</i> cf. <i>curvimola</i>	<i>Arctognathus</i> cf. <i>curvimola</i>
<i>Arctognathus?</i> <i>cookei</i>		
<i>Arctognathus?</i> <i>nasuta</i>	<i>Arctognathus?</i> <i>nasuta</i>	
cf. <i>Arctognathus?</i> <i>nasuta</i>	cf. <i>Arctognathus?</i> <i>nasuta</i>	
<i>Arctops kitchingi</i>		
<i>Arctops watsoni</i>	<i>Arctops watsoni</i>	
<i>Arctops</i> cf. <i>watsoni</i>	<i>Arctops</i> cf. <i>watsoni</i>	
<i>Arctops willistoni</i>	<i>Arctops willistoni</i>	
<i>Arctops?</i> <i>ferox</i>	<i>Arctops?</i> <i>ferox</i> <i>Arctops?</i> <i>kitchingi</i>	
<i>Arctops?</i> <i>minor</i>	<i>Arctops?</i> <i>minor</i>	
<i>Broomisaurus planiceps</i>	<i>Broomisaurus planiceps</i>	

Gorgonopsinae continued		
Sigogneau 1970	Sigogneau-Russell 1989	Gebauer 2007
	<i>Cephalicustriodus kingoriensis</i>	
<i>Cerdorhinus parvidens</i> <i>Cerdorhinus? rubidgei</i>	<i>Cerdorhinus parvidens</i> <i>Cerdorhinus? rubidgei</i>	
<i>Cyonosaurus kitchingi</i> <i>Cyonosaurus cf. kitchingi</i> <i>Cyonosaurus longiceps</i> <i>Cyonosaurus cf. longiceps</i> <i>Cyonosaurus rubidgei</i> <i>Cyonosaurus cf. rubidgei</i>	<i>Cyonosaurus kitchingi</i> <i>Cyonosaurus longiceps</i> <i>Cyonosaurus cf. longiceps</i> <i>Cyonosaurus rubidgei</i> <i>Cyonosaurus cf. rubidgei</i>	<i>Cyonosaurus broomianus</i> <i>Cyonosaurus kitchingi</i> <i>Cyonosaurus longiceps</i> <i>Cyonosaurus rubidgei</i> <i>Cyonosaurus tenuirostris</i> <i>Cyonosaurus sp.</i>
<i>Eoartctops vanderbyli</i>	<i>Eoartctops vanderbyli</i> <i>Eoartctops sp.</i>	<i>Eoartctops vanderbyli</i>
<i>Galesuchus gracilis</i>	<i>Galesuchus gracilis</i> <i>Galesuchus sp.</i>	
<i>Gorgonops dixeyi</i> <i>Gorgonops eupachygnathus</i> <i>Gorgonops kaiseri</i> <i>Gorgonops longifrons</i> <i>Gorgonops torvus</i> <i>Gorgonops whaitsi</i> <i>Gorgonops cf. whaitsi</i>	<i>Gorgonops eupachygnathus</i> <i>Gorgonops longifrons</i> <i>Gorgonops torvus</i> <i>Gorgonops whaitsi</i> <i>Gorgonops cf. whaitsi</i> <i>Gorgonops? dixeyi</i> <i>Gorgonops? kaiseri</i>	<i>Gorgonops capensis</i> <i>Gorgonops dixeyi</i> <i>Gorgonops torvus</i> <i>Gorgonops? eupachygnathus</i> <i>Gorgonops? kaiseri</i> <i>Gorgonops? whaitsi</i>
<i>Leontocephalus cadlei</i> <i>Leontocephalus haughtoni</i>	<i>Leontocephalus cadlei</i> <i>Leontocephalus haughtoni</i> <i>Leontocephalus? intactus</i>	
<i>Leontocephalus? rubidgei</i>	<i>Leontocephalus? rubidgei</i>	
<i>Lycaenops angusticeps</i> <i>Lycaenops cf. angusticeps</i>	<i>Lycaenops angusticeps</i> <i>Lycaenops cf. angusticeps</i>	<i>Lycaenops angusticeps</i> <i>Lycaenops attenuates</i>
<i>Lycaenops kingwilli</i> <i>Lycaenops ornatus</i> <i>Lycaenops? microdon</i> <i>Lycaenops? minor</i> <i>Lycaenops? tenuirostris</i>	<i>Lycaenops kingwilli</i> <i>Lycaenops ornatus</i> <i>Lycaenops? microdon</i> <i>Lycaenops? minor</i> <i>Lycaenops? tenuirostris</i>	<i>Lycaenops ornatus</i> <i>Lycaenops quadrata</i> <i>Lycaenops sollasi</i> <i>Lycaenops sp.</i>
		<i>Njalila insigna</i> <i>Njalila nasuta</i>
<i>Paragalerhinus rubidgei</i>	<i>Paragalerhinus rubidgei</i>	
<i>Scylacognathus grimbeeki</i>	<i>Scylacognathus grimbeeki</i>	
<i>Scylacognathus parvus</i> <i>Scylacognathus robustus</i>	<i>Scylacognathus parvus</i> <i>Scylacognathus robustus</i>	<i>Scylacognathus kitchingi</i> <i>Scylacognathus parvus</i> <i>Scylacognathus robustus</i>
<i>Scylacops bigendens</i> <i>Scylacops capensis</i> <i>?Scylacops</i>	<i>Scylacops bigendens</i> <i>Scylacops capensis</i> <i>?Scylacops</i>	

Rubidgeinae		
Sigogneau 1970	Sigogneau-Russell 1989	Gebauer 2007
see entry under Gorgonopsinae	see entry under Gorgonopsinae	<i>Aelurognathus alticeps</i> <i>Aelurognathus broodiei</i> ³ <i>Aelurognathus ferox</i> <i>Aelurognathus kingwilli</i> <i>Aelurognathus maccabei</i> <i>Aelurognathus tigriceps</i>
<i>Broomicephalus laticeps</i>	<i>Broomicephalus laticeps</i>	
<i>Clelandina rubidgei</i> <i>Clelandina scheepersi</i>	<i>Clelandina rubidgei</i> <i>Clelandina scheepersi</i>	<i>Clelandina laticeps</i> <i>Clelandina rubidgei</i> <i>Clelandina scheepersi</i>
<i>Dinogorgon pricei</i> <i>Dinogorgon quinquemolaris</i> <i>Dinogorgon rubidgei</i>	<i>Dinogorgon pricei</i> <i>Dinogorgon quinquemolaris</i> <i>Dinogorgon rubidgei</i> <i>Dinogorgon sp.</i>	
“ <i>Gorgognathus maximus</i> ”		
<i>Prorubidgea alticeps</i> <i>Prorubidgea alticeps?</i>	<i>Prorubidgea alticeps</i>	
<i>Prorubidgea brodiei</i> <i>Prorubidgea maccabei</i> <i>Prorubidgea robusta</i> <i>Prorubidgea sp.</i>	<i>Prorubidgea brinki</i> <i>Prorubidgea broodiei</i> ⁴ <i>Prorubidgea maccabei</i> <i>Prorubidgea robusta</i> <i>Prorubidgea sp.</i>	
<i>Rubidgea atrox</i> <i>Rubidgea majora</i> <i>Rubidgea platyrhina</i> <i>Rubidgea cf. platyrhina</i>	<i>Rubidgea atrox</i> <i>Rubidgea majora</i> <i>Rubidgea platyrhina</i> <i>Rubidgea cf. platyrhina</i>	<i>Rubidgea atrox</i>
<i>Rubidgea sp.</i>	<i>Rubidgea sp.</i>	<i>Rubidgea pricei</i> <i>Rubidgea quinquemolaris</i> <i>Rubidgea sp.</i>
<i>Sycosaurus laticeps</i>	<i>Sycosaurus laticeps</i>	<i>Sycosaurus laticeps</i> <i>Sycosaurus kingoriensis</i> <i>Sycosaurus terror</i>
<i>Sycosaurus vanderhorsti</i>	<i>Sycosaurus vanderhorsti</i> <i>Sycosaurus? kingoriensis</i>	<i>Sycosaurus? intactus</i> <i>Sycosaurus sp.</i>
<i>?Sycosaurus kingoriensis</i>		

³ Incorrect spelling of *Aelurognathus* (= *Prorubidgea*) *brodiei* on p. 158, 183 & 187, probably inherited from Sigogneau-Russell (1989), see Footnote 2. Correctly spelt *P. brodiei* on p. 176.

⁴ *Lapsus clavis* in Sigogneau-Russell (1989), p. 107 that should read *Prorubidgea brodiei*.

10 APPENDIX B

Description of cranial & lower jaw measurements

Citations are in the form (author: measurement number/ abbreviation). When an asterisk (*) follows the citation, it denotes that the measurement has been modified.

Abbreviations for authors are as follows: S, Sigogneau (1970); GHG, Grine *et al.* (1978); TGH, Tollman *et al.* (1979); AG1, Abdala & Giannini (2000); AG2, Abdala & Giannini (2002); GAF, Giannini *et al.* (2004); FGA, Flores *et al.* (2006)

1. Anterior most point of snout to posterior most point of squamosal (S:lg.mx.; GHG:2; TGH:3)
2. Anterior most point of snout to foramen magnum (GHG:1; TGH:1; AG1:TL*; AG2:TL*; FGA:TL*)
3. Anterior most point of snout to anterior margin of orbit (S:lg.mu; GHG:3; TGH:3; AG1:MUL; AG2:MUL)
4. Anterior margin of orbit to posterior most point of squamosal (GHG:5; TGH:7*)
5. Anterior margin of orbit to foramen magnum (GHG:4; TGH:2*)
6. Anterior most point of snout to pineal foramen (S:pin.; TGH:23)
7. Pineal foramen to foramen magnum (S:pin.cr.*; TGH:22)
8. Anterior most point of snout to ventral most point Jugal flange (GHG:10)
9. Internarial width
10. Least snout width (S:4*; GHG:21; TGH:26*)

11. Greatest snout width (S:la.mu.*; GHG:22; TGH:26*)
12. Least interorbital width (S:io.*; GHG:20; TGH:24*; AG1:IO*; AG2:IO*)
13. Cranial width across jugal flanges (S:la.mx.*; GHG:19; AG1:SW*; AG2:SW*; GAF:BZ*; FGA:BZ*)
14. Intertemporal breadth across pineal foramen (GHG:23; TGH:29)
15. Minimum distance between the squamosals (GHG:26*; TGH:17)
16. Intermediate temporal breadth (TGH:18*)
17. Maximum cranial width (GHG:18*; TGH:19*; AG1:SW*; AG2:SW*; GAF:BZ*; FGA:BZ*)
18. Anterior-posterior length of temporal foramen (GHG:9; TGH:12)
19. Dorsal-ventral height of temporal fenestra (GHG:24*; TGH13⁵)
20. Width of occipital condyle (GHG:25*; TGH:20; AG1:OW*; AG2:OW*)
21. Width between post temporal foramina (GHG:27; TGH:21*)
22. Ventral point of occipital condyle to dorsal most point of skull roof (GHG:36; AG2:OH*; GAF:HO*; FGA:HO*)
23. Maximum height of mid skull roof above maxillary (GHG:37*; TGH:30*)
24. Maximum height of post orbital above maxillary base (GHG:38; TGH:30)
25. Maximum height of maxilla (S:ht.mu.*; 15*; GHG:39; TGH:30*; GAF:HM*; FGA:HM*)
26. Anterior-posterior length of orbit (S:ob.*; GHG:42; AG1:OL; AG2:OL; GAF:LO; FGA:LO)
27. Dorsal-ventral length of orbit (S:ob.*; GHG:43; TGH:27; AG1:OD*)

⁵ Shown in TGH Figure 1b, but not labelled.

28. Length of nasal aperture (GHG:44⁶)
29. Dorsal-ventral length of foramen magnum (GHG:45)
30. Foramen magnum width (GHG:46)
31. Maximum dorsal-ventral height of jugal (GHG:51; AG1:ZH*; AG2:ZH*)
32. Transverse process of the Pterygoid width (GHG:52; AG1:TP)
33. Palatal length (GHG:8*; TGH:4; AG1:PAL; AG2:PAL; GAF:PAL; FGA:PAL)
34. Pterygoid fossa length (TGH:5)
35. Least presphenoid breadth (TGH:9)
36. Interquadrate distance (TGH:10)
37. Canine-snout distance (TGH:11)
38. Width between premaxillary ridges (TGH:16)
39. Greatest snout depth (TGH:30)
40. Minimum width of postorbital bar (S:pob.)
41. Minimum height of suborbital bar (S:ss.ob.)
42. Minimum height of zygomatic arch (GHG 51*; AG1:ZH*; AG2:ZH*)
43. Total dentary length (GHG:12; AG2:DL⁷; GAF:LD*; FGA:LD*)
44. Anterior most point of dentary to last postcanine (GHG:13)
45. Anterior most point of dentary to the reflected lamina of the angular (GHG:14*)
46. Mandibular tooth row length (GHG:15)
47. Mandibular postcanine tooth row length (GHG:16)

⁶ Labelled as 49 in GHG Figure 1c.

⁷ Labelled 'ML' in AG2 Text-Figure 4.

48. Length of symphysis on lower jaw (GHG:17)
49. Maximum height of dentary corpus (S:de; GHG:40; GAF:HD*; FGA:HD*)
50. Projected rameal breadth (GHG:41)
51. Dentary thickness (GHG:31)
52. Minimum intercorporal breadth (GHG:32)
53. Minimum symphyseal breadth (GHG:33)
54. Maximum symphyseal breadth (GHG:34)
55. Length of diastema between last maxillary incisor and maxillary canine (S:I5-C)
56. Length of diastema between last mandibular incisor and mandibular canine (S: I5-C*)
57. Length of diastema between maxillary canine and first maxillary postcanine (S:C-Pc)
58. Length of diastema between mandibular canine and first mandibular postcanine (S:C-Pc*)
59. Total length of maxillary postcanine series (S:Pc; GHG:7*; AG1:UP; AG2:UP; GAF:UP; FGA:UP)
60. Total length of mandibular postcanine series (S:Pc*; GHG:16*; GAF:LP; FGA:LP)
61. First incisor on premaxilla-Last postcanine on maxilla(GHG:6)
62. First postcanine on maxilla-Last postcanine on maxilla (GHG:7)
63. Greatest length between maxillary tooth rows (GHG:28; AG1:PD*; AG2:PD*)

64. Least length between maxillary tooth rows (GHG:29; AG1:AD*; AG2:PD*)
65. Maxillary bicanine breadth (GHG:30; TGH:8; AG1:BW; AG2:BW)
66. Mandibular bicanine breadth (GHG:35)
67. Mesiodistal diameter of maxillary canine, or socket (S:C*; GHG:47; TGH:15*)
68. Buccolingual diameter of maxillary canine, or socket (S:C*; GHG:48; TGH:14⁸)
69. Mesiodistal diameter of mandibular canine, or socket (GHG:49)
70. Buccolingual diameter of mandibular canine, or socket (GHG:50)

⁸ Not shown in TGH Figure 1.

11 APPENDIX C

Table C1 List of measurements used in the univariate and bivariate allometric analyses described in Chapter 2 and reported in Chapter 4. Variables that could not be measured are denoted by a dash (-). A table of the raw data is included as a spreadsheet on the accompanying CD (Appendix E).

Collection Number	Variable									
	1	2	3	4	5	6	7	12	14	18
SAM-PK-2342	293	264	172	151	98	241	24	79	111	71
SAM-PK-2672	-	-	125	-	-	195	-	69	-	-
SAM-PK-4334	187	195	128	103	80	184	41	53	65	35
SAM-PK-7847	295	-	188	110	-	230	-	-	-	-
SAM-PK-10071	227	203	123	110	88	188	20	67	76	44
RC 34	308	260	167	153	98	234	29	79	105	65
RC 60	331	272	164	160	100	235	38	76		78
TMP 1493	-	-	-	150	-	-	-	87	97	71
BP/1/2190	291	-	151	140	-	212	-	81	106	49
BP/1/2465	337	300	189	151	126	280	37	86	107	73
RC 62	333	299	179	154	132	255	42	82	-	-
RC 81	-	343	222	-	119	321	28	89	-	-
RC 82	-	-	-	-	-	-	-	-	-	177
TMP 132	231	-	129	110	-	-	-	76	114	38
BP/1/813	214	-	105	107	-	185	26	-	-	57
BP/1/1566	262	237	125	144	105	198	37	64	82	86

Table C1 Continued Variables 19-45.

Collection Number	Variable									
	19	24	25	26	27	37	40	41	42	45
SAM-PK-2342	63	119	109	47	48	91	29	46	22	235
SAM-PK-2672	-	90	92	40	44	64	13	11	-	-
SAM-PK-4334	44	75	69	43	41	54	15	24	23	-
SAM-PK-7847	-	120	137	46	37	87	33	53	-	244
SAM-PK- 10071	60	104	118	40	45	50	25	33	-	-
RC 34	79	97	99	57	55	80	36	38	29	245
RC 60	74	108	105	58	58	90	22	34	33	230
TMP 1493	78	106	-	54	49	-	35	47	31	215
BP/1/2190	64	-	91	49	47	71	35	42	-	216
BP/1/2465	59	-	-	61	58	79	19	48	31	197
RC 62	-	120	110	59	-	94	-	-	39	230
RC 81	-	154	133	66	53	84	35	62	-	-
RC 82	-	-	-	-	-	26	55	54	-	231
TMP 132	51	-	-	30	47	32	18	24	33	156
BP/1/813	63	-	-	-	-	78	39	45	16	-
BP/1/1566	58	87	85	35	44	61	19	28	22	-

Table C1 Continued Variables 49-67.

Collection Number	Variable									
	49	51	52	55	57	59	61	65	67	
SAM-PK-2342	57	19	25	34	17	29	135	68	20	
SAM-PK-2672	40	-	-	22	11	24	94	64	15	
SAM-PK-4334	39	13	18	13	11	15	82	64	17	
SAM-PK-7847	56	19	-	17	30	8	124	90	25	
SAM-PK- 10071	43	12	23	18	22	12	85	57	15	
RC 34	43	15	26	23	22	31	131	76	22	
RC 60	48	15	23	16	14	30	127	50	24	
TMP 1493	49	-	-	19	24	34	-	-	19	
BP/1/2190	51	-	-	22	-	-	-	-	15	
BP/1/2465	57	21	-	17	15	17	94	-	31	
RC 62	57	16	-	19	14	10	110	117	28	
RC 81	58	27	37	-	-	20	108	-	-	
RC 82	56	16	25	18	25	10	89	85	23	
TMP 132	43	-	-	9	-	-	-	-	30	
BP/1/813	-	19	-	-	-	-	-	21	13	
BP/1/1566	42	13	17	11	15	31	99	71	17	

12 APPENDIX D

12.1 Supporting Figures & Tables for measurements with a continuous range in the univariate analyses.

Table D1 Summary statistics for skull length (Appendix B, Variable 2).

	Total	<i>A. tigriceps</i>	<i>A. ferox</i>
<i>n</i>	9	3	3
# Missing	7	2	2
Sum	2373	662	942
Average	264	221	314
Max. val.	343	264	343
Min. val.	195	195	299
Range	149	70	45
Var.	2260.478	1451.787	638.5833
Std dev.	47.54448	38.10232	25.27021
Std error	15.84816	21.99839	14.58976

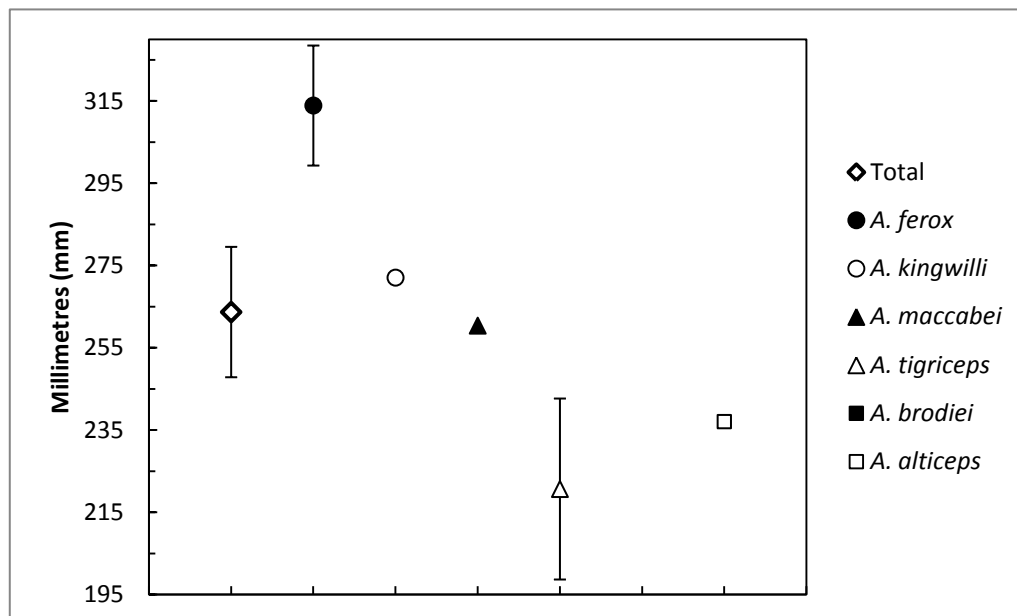


Figure D1 Average cell plot of the skull length (Appendix B, Variable 2) Error bars represent \pm one standard error (Table D1).

Table D2 Summary statistics for prepineal skull length (Appendix B, Variable 6).

	Total	<i>A. tigriceps</i>	<i>A. ferox</i>	<i>A. alticeps</i>
<i>n</i>	13	5	3	2
# Missing	3	0	2	0
Sum	2957	1038	855	383
Average	227	208	285	192
Max. val.	321	241	321	198
Min. val.	184	184	255	185
Range	137	57	66	13
Var.	1652.785	671	1107.75	84.5
Std dev.	40.65446	25.90367	33.28288	9.192388
Std error	11.27552	11.58447	19.21588	6.5

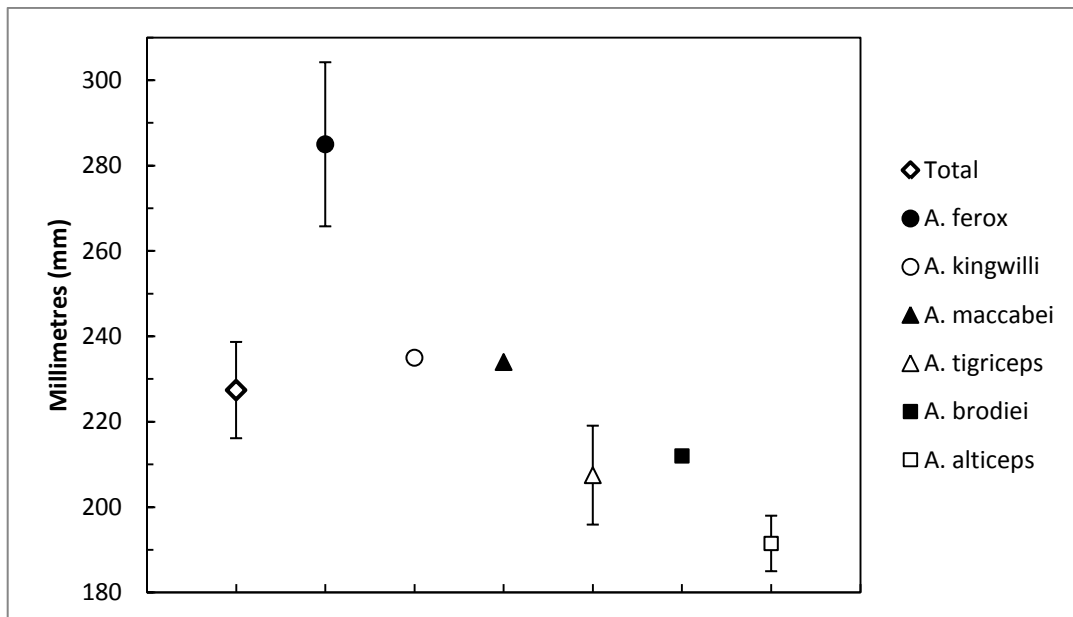


Figure D2 Average cell plot for prepineal skull length (Appendix B, Variable 6)

Error bars represent \pm one standard error (Table D2).

Table D3 Summary statistics for postpineal skull length (Appendix B, Variable 7).

	Total	<i>A. tigriceps</i>	<i>A. ferox</i>	<i>A. alticeps</i>
<i>n</i>	10	3	3	2
# Missing	6	2	2	0
Sum	320	85	107	63
Average	32	28	36	31
Max. val.	42	41	42	37
Min. val.	20	20	28	26
Range	23	22	15	12
Var.	61.4444	128.5833	54.25	66.125
Std dev.	7.8387	11.3395	7.36556	8.1317
Std error	2.4788	6.5468	4.25255	5.75

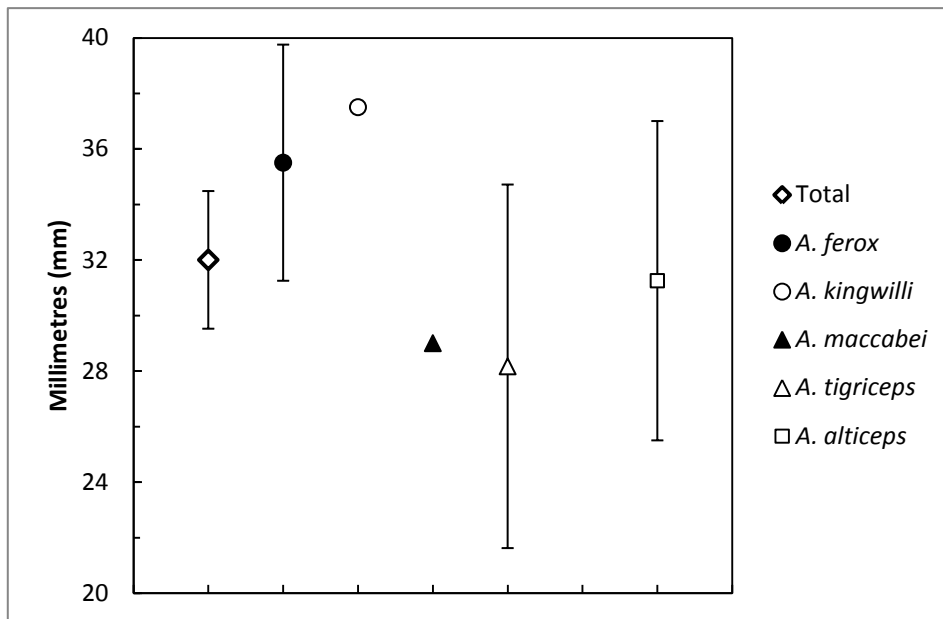


Figure D3 Average cell plot of the postpineal skull length (Appendix B, Variable

7) Error bars represent \pm one standard error (Table D3).

Table D4 Summary statistics for intertemporal width (Appendix B, Variable 14).

	Total	<i>A. tigriceps</i>	<i>A. brodiei</i>	<i>A. ferox</i>
<i>n</i>	9	3	2	2
# Missing	7	2	0	3
Sum	862	252	203	221
Average	96	84	101	111
Max. val.	114	111	106	114
Min. val.	65	65	97	107
Range	50	47	10	7
Var.	304.1258	586.5833	45.125	24.5
Std dev.	17.4392	24.2195	6.7175	4.9497
Std error	5.8131	13.9831	4.75	3.5

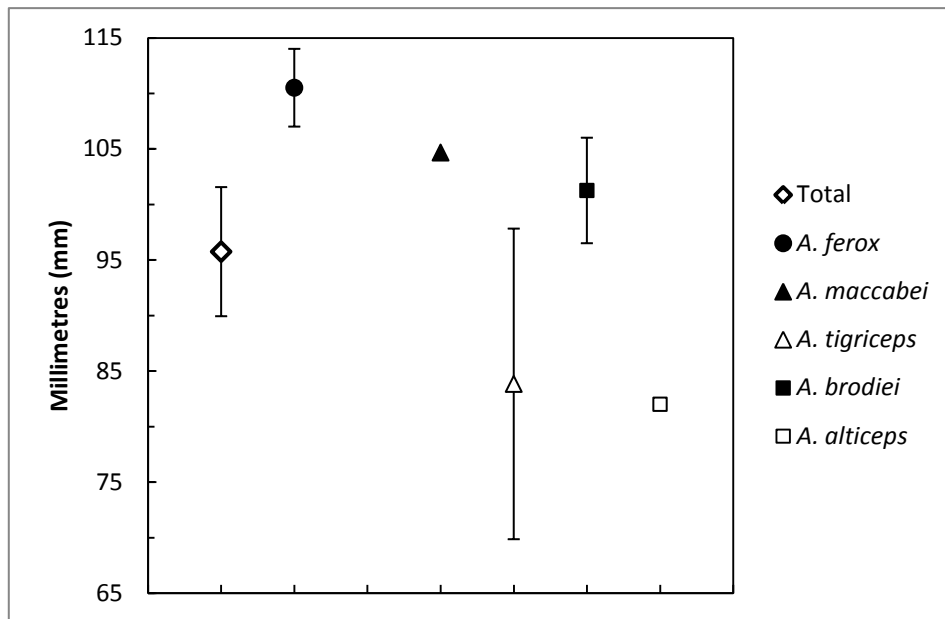


Figure D4 Average cell plot of the intertemporal width (Appendix B, Variable 14)

Error bars represent \pm one standard error (Table D4).

Table D5 Summary statistics for temporal opening length (Appendix B, Variable 18).

	Total	<i>A. tigriceps</i>	<i>A. brodiei</i>	<i>A. ferox</i>	<i>A. alticeps</i>
<i>n</i>	12	3	2	3	2
# Missing	4	2	0	2	0
Sum	743	150	120	188	143
Average	62	50	60	63	72
Max. val.	86	71	71	77	86
Min. val.	35	35	49	38	57
Range	51	36	21	39	29
Var.	284.4753	351	229.1746	452.1481	420.5
Std dev.	16.8664	18.735	15.1385	21.2638	20.5061
Std error	4.8689	10.8167	10.7046	12.2767	14.5

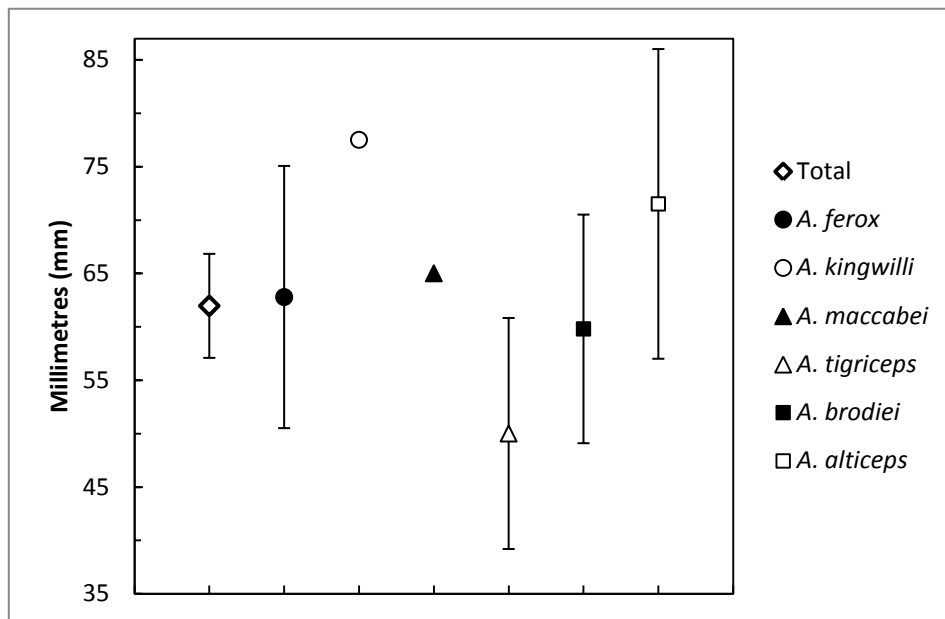


Figure D5 Average cell plot of the temporal opening length (Appendix B, Variable 18) Error bars represent \pm one standard error (Table D5).

Table D6 Summary statistics for temporal opening height (Appendix B, Variable 19).

	Total	<i>A. tigriceps</i>	<i>A. brodiei</i>	<i>A. ferox</i>	<i>A. alticeps</i>
<i>n</i>	11	3	2	2	2
# Missing	5	2	0	3	0
Sum	691	167	142	110	121
Average	63	56	71	55	61
Max. val.	79	63	78	59	63
Min. val.	44	44	64	51	58
Range	35	19	14	8	5
Var.	114.6719	104.3333	103.157	35.6543	12.5
Std dev.	10.7085	10.2144	10.15662	5.9711	3.5355
Std error	3.2287	5.8973	7.181818	4.2222	2.5

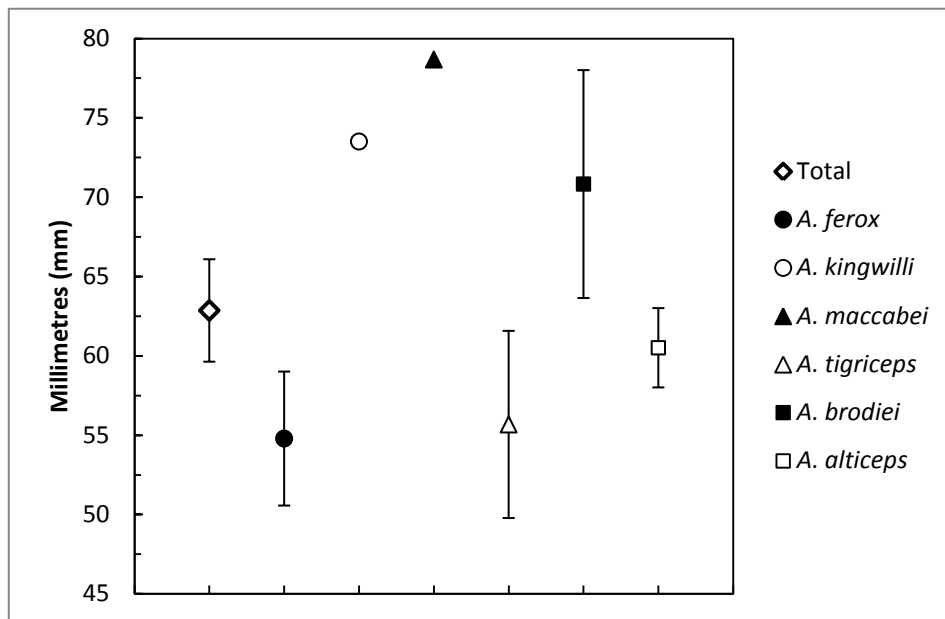


Figure D6 Average cell plot of the temporal opening height (Appendix B, Variable 19) Error bars represent \pm one standard error (Table D6).

Table D7 Summary statistics for maxilla height (Appendix B, Variable 25).

	Total	<i>A. tigriceps</i>	<i>A. ferox</i>
<i>n</i>	11	5	2
# Missing	5	0	3
Sum	1147	526	242
Average	104	105	121
Max. val.	137	137	133
Min. val.	69	69	110
Range	68	68	23
Var.	407.0399	667.0333	264.5
Std dev.	20.1752	25.827	16.2635
Std error	6.0831	11.5502	11.5

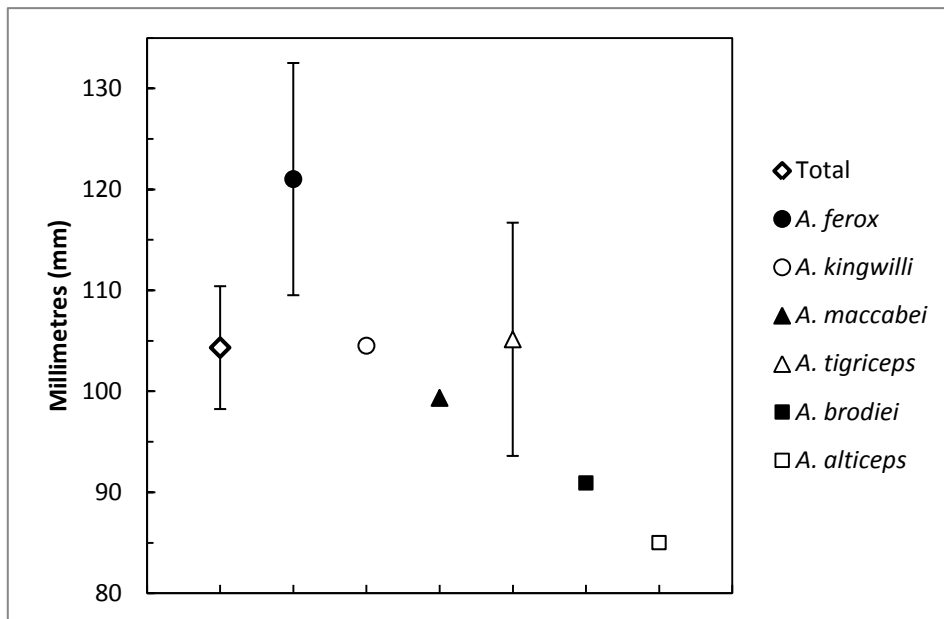


Figure D7 Average cell plot of the maxilla height (Appendix B, Variable 25) Error bars represent \pm one standard error (Table D7).

Table D8 Summary statistics for orbit length (Appendix B, Variable 27).

	Total	<i>A. tigriceps</i>	<i>A. brodiei</i>	<i>A. ferox</i>
<i>n</i>	13	5	2	3
# Missing	3	0	0	2
Sum	625	215	96	157
Average	48	43	48	52
Max. val.	58	48	49	58
Min. val.	37	37	47	47
Range	21	11	1	11
Var.	40.0371	18.0556	0.7531	32.1204
Std dev.	6.3275	4.2492	0.8678	5.6675
Std error	1.7549	1.9003	0.6136	3.2721

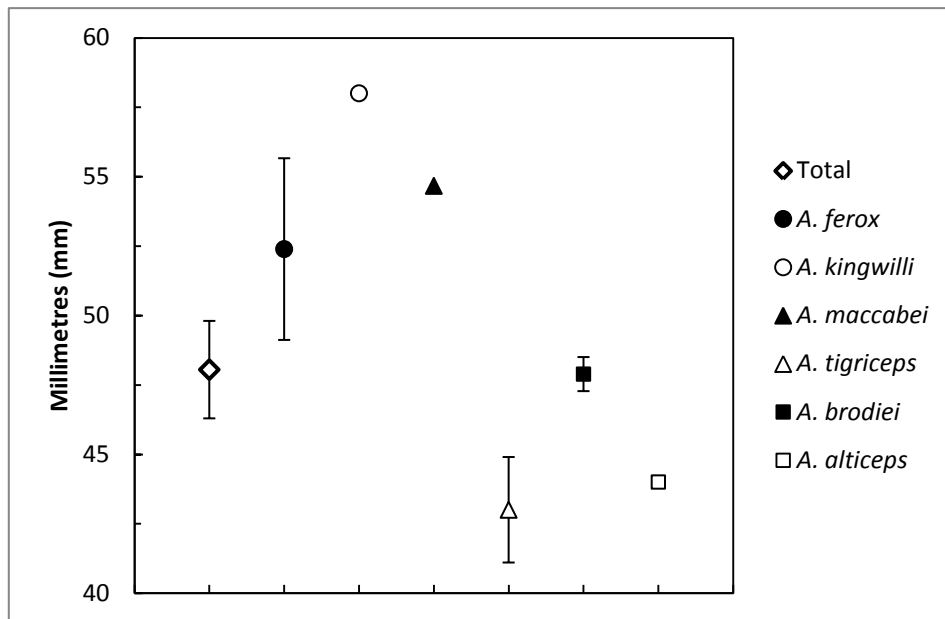


Figure D8 Average cell plot of the orbit length (Appendix B, Variable 27) Error bars represent \pm one standard error (Table D8).

Table D9 Summary statistics for minimum postorbital bar width (Appendix B, Variable 40).

	Total	<i>A. tigriceps</i>	<i>A. brodiei</i>	<i>A. ferox</i>	<i>A. alticeps</i>
<i>n</i>	15	5	2	4	2
# Missing	1	0	0	1	0
Sum	427	115	70	127	58
Average	28	23	35	32	29
Max. val.	55	33	35	55	39
Min. val.	13	13	35	18	19
Range	42	20	0	37	20
Var.	127.048	75.0222	0.1033	298.3399	200
Std dev.	11.2716	8.6615	0.3214	17.2725	14.1421
Std error	2.9103	3.8736	0.2273	8.6363	10

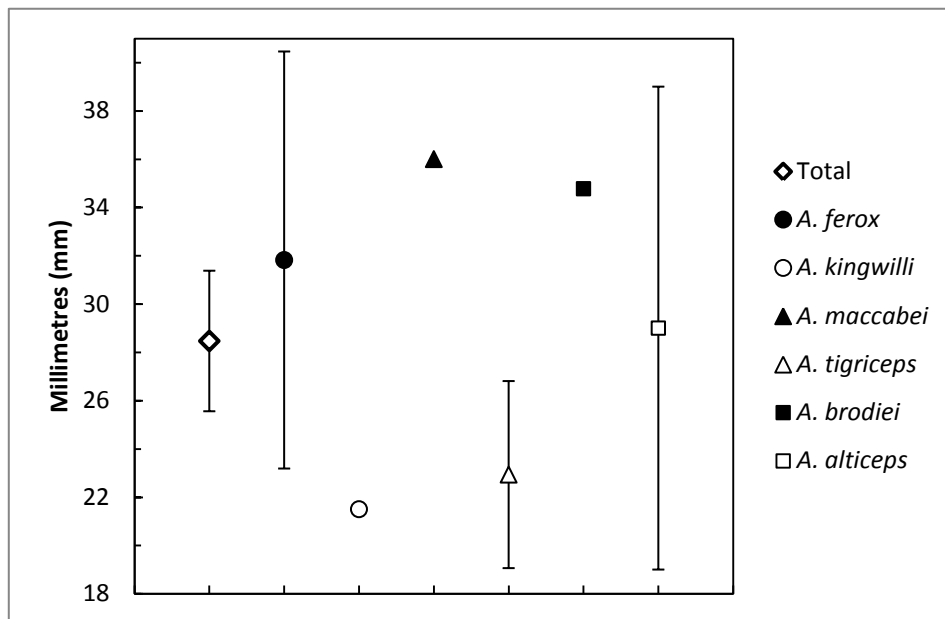


Figure D9 Average cell plot of the minimum postorbital bar width (Appendix B, Variable 40) Error bars represent \pm one standard error (Table D9).

Table D10 Summary statistics for minimum suborbital bar height (Appendix B, Variable 41).

	Total	<i>A. tigriceps</i>	<i>A. brodiei</i>	<i>A. ferox</i>	<i>A. alticeps</i>
<i>n</i>	15	5	2	4	2
# Missing	1	0	0	1	0
Sum	587	167	88	188	73
Average	39	33	44	47	36
Max. val.	62	53	47	62	45
Min. val.	11	11	42	24	28
Range	51	43	5	37	17
Var.	183.5989	290.3111	10.9597	254.8032	136.125
Std dev.	13.5499	17.0385	3.3105	15.9626	11.66736
Std error	3.4986	7.6199	2.3409	7.9813	8.25

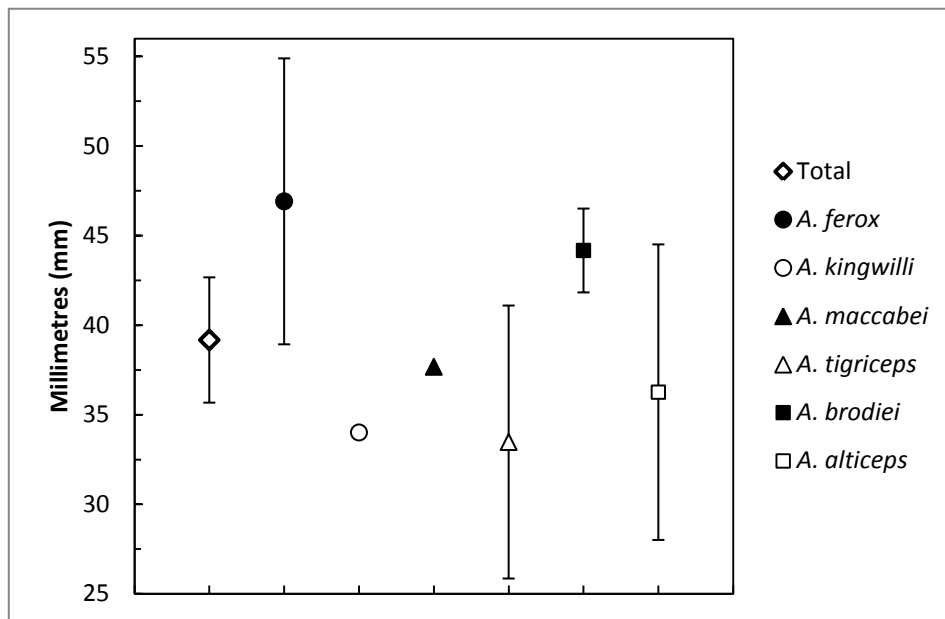


Figure D10 Average cell plot of minimum suborbital bar height (Appendix B, Variable 41) Error bars represent \pm one standard error (Table D10).

Table D11 Summary statistics for mandible length (Appendix B, Variable 45).

	Total	<i>A. tigriceps</i>	<i>A. brodiei</i>	<i>A. ferox</i>
<i>n</i>	10	2	2	4
# Missing	6	3	0	1
Sum	2198	479	431	813
Average	220	239	216	203
Max. val.	245	244	216	231
Min. val.	156	235	215	156
Range	89	8	1	75
Var.	714.1036	33.3472	0.9298	1257.649
Std dev.	26.7227	5.7747	0.9643	35.4634
Std error	8.4505	4.0833	0.6818	17.7317

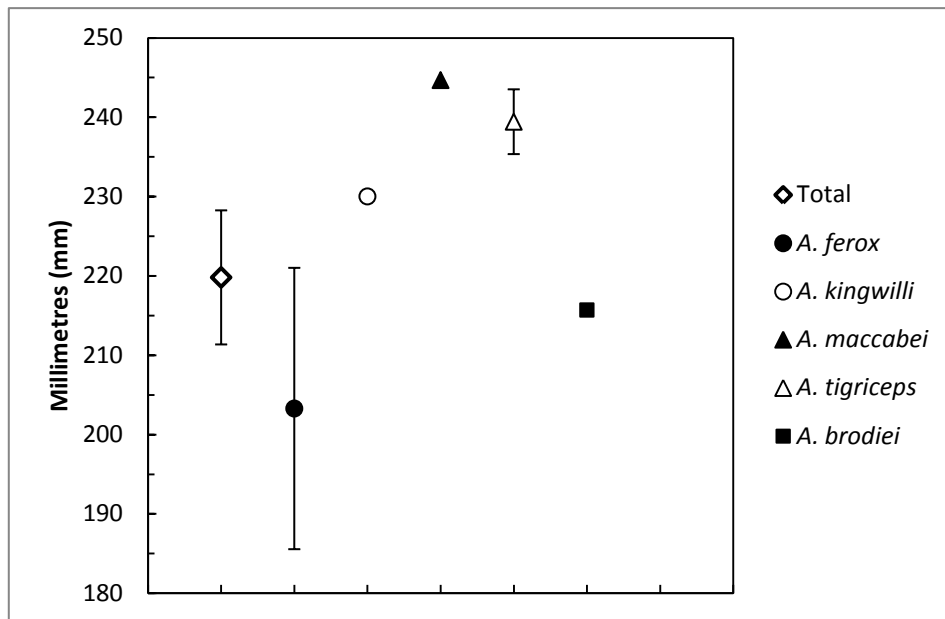


Figure D11 Average cell plot of the mandible length (Appendix B, Variable 45)

Error bars represent \pm one standard error (Table D11).

Table D12 Summary statistics for dentary corpus height (Appendix B, Variable 49).

	Total	<i>A. tigriceps</i>	<i>A. brodiei</i>	<i>A. ferox</i>
<i>n</i>	15	5	2	5
# Missing	1	0	0	0
Sum	737	235	100	270
Average	49	47	50	54
Max. val.	58	57	51	58
Min. val.	39	39	49	43
Range	19	18	2	15
Var.	50.2418	76.0222	1.8223	39.8127
Std dev.	7.0881	8.7191	1.3499	6.3097
Std error	1.8302	3.8993	0.9545	2.8218

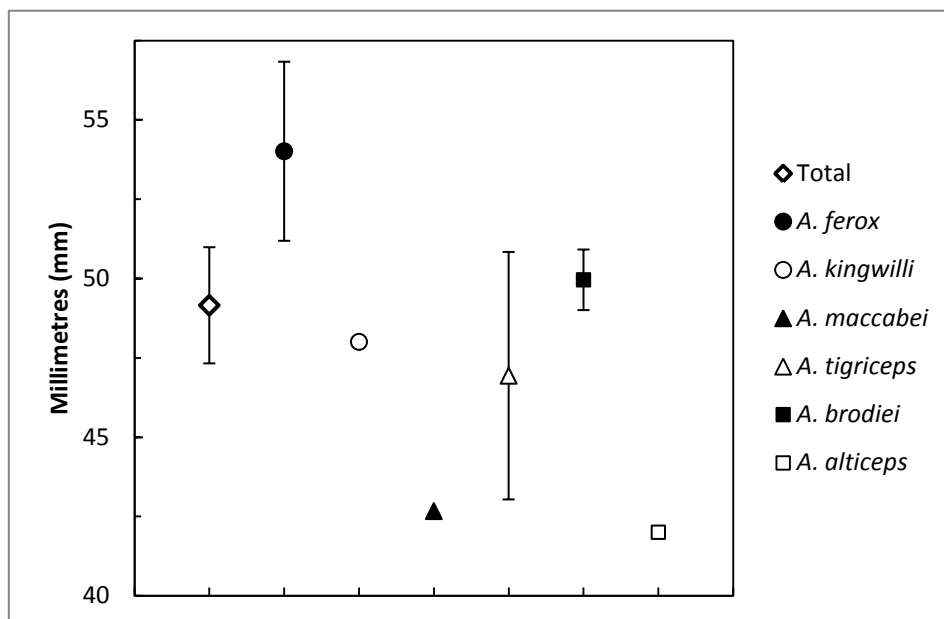


Figure D12 Average cell plot of the dentary corpus height (Appendix B, Variable 49) Error bars represent \pm one standard error (Table D12).

Table D13 Summary statistics for dentary thickness (Appendix B, Variable 51).

	Total	<i>A. tigriceps</i>	<i>A. ferox</i>	<i>A. alticeps</i>
<i>n</i>	12	4	4	2
# Missing	4	1	1	0
Sum	205	64	79	32
Average	17	16	20	16
Max. val.	27	19	27	19
Min. val.	12	12	16	13
Range	14	7	11	6
Var.	16.6075	14.1759	25.724	18
Std dev.	4.0752	3.7651	5.0719	4.2426
Std error	1.1764	1.8825	2.5359	3

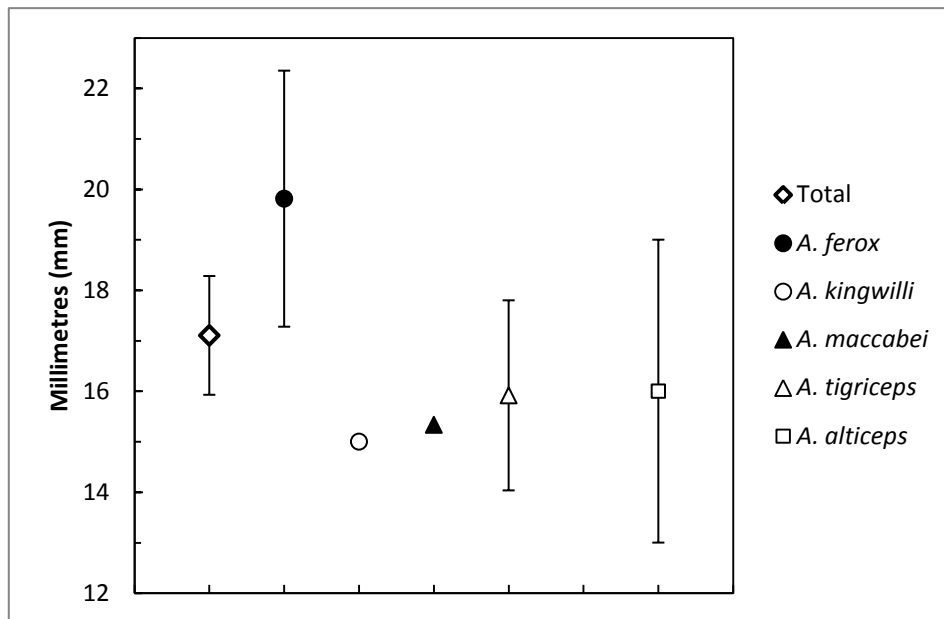


Figure D13 Average cell plot of the dentary thickness (Appendix B, Variable 51)

Error bars represent \pm one standard error (Table D13).

Table D14 Summary statistics for maxillary bicanine breadth (Appendix B, Variable 65).

	Total	<i>A. tigriceps</i>	<i>A. ferox</i>	<i>A. alticeps</i>
<i>n</i>	11	5	2	2
# Missing	5	0	3	0
Sum	762	342	202	92
Average	69	68	101	46
Max. val.	117	90	117	71
Min. val.	21	57	85	21
Range	96	33	31	50
Var.	591.2742	161.6333	485.6806	1250
Std dev.	24.3161	12.7135	22.0382	35.3553
Std error	7.3316	5.6857	15.5833	25

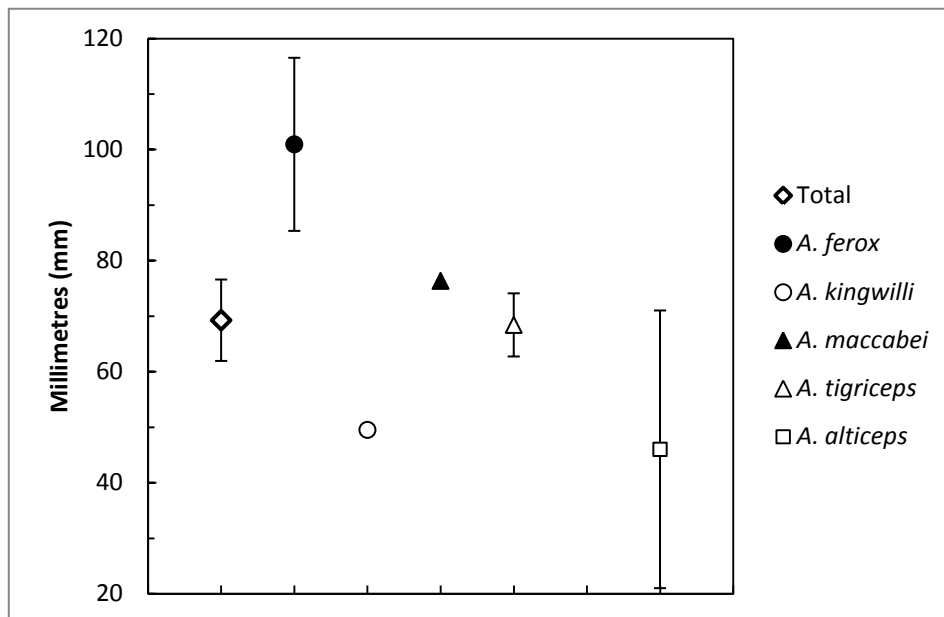


Figure D14 Average cell plot of the maxillary bicanine breadth (Appendix B, Variable 65) Error bars represent \pm one standard error (Table D14).

Table D15 Summary statistics for mesiodistal diameter of maxillary canine
(Appendix B, Variable 67).

	Total	<i>A. tigriceps</i>	<i>A. brodiei</i>	<i>A. ferox</i>	<i>A. alticeps</i>
<i>n</i>	15	5	2	4	2
# Missing	1	0	0	1	0
Sum	314	93	34	112	30
Average	21	19	17	28	15
Max. val.	31	25	19	31	17
Min. val.	13	15	15	23	13
Range	19	10	4	8	5
Var.	33.4659	18.0556	9.9215	12.7292	10.125
Std dev.	5.785	4.2492	3.1498	3.5678	3.182
Std error	1.4937	1.9003	2.2273	1.7839	2.25

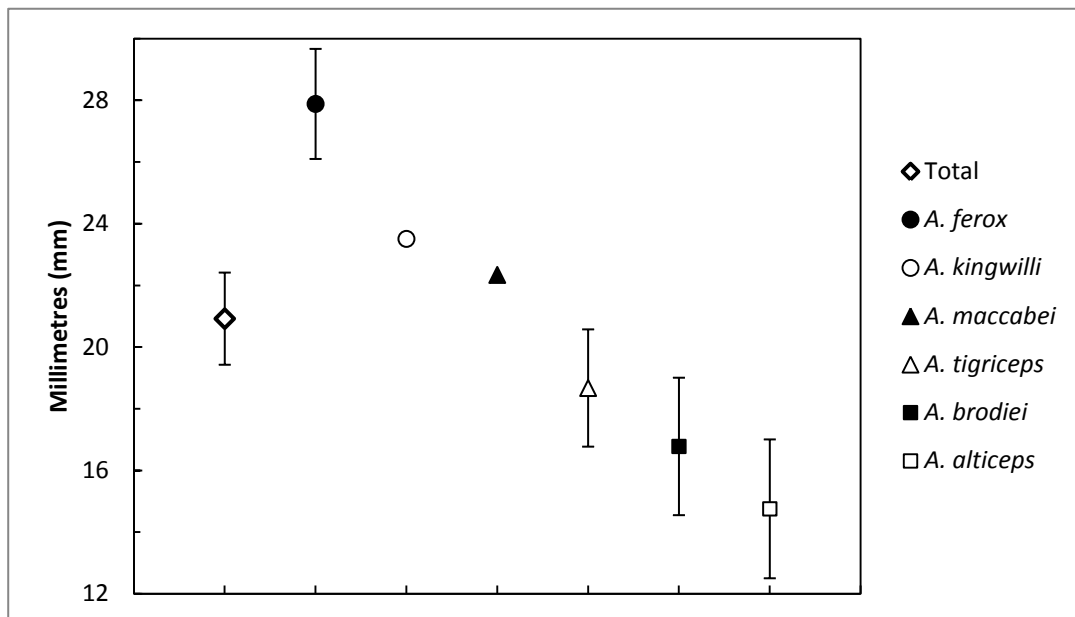


Figure D15 Average cell plot of the mesiodistal diameter of maxillary canine
(Appendix B, Variable 67) Error bars represent \pm one standard error (Table D15).

13.2 Supporting figures for the regression analyses using skull length (2) as the independent variable.

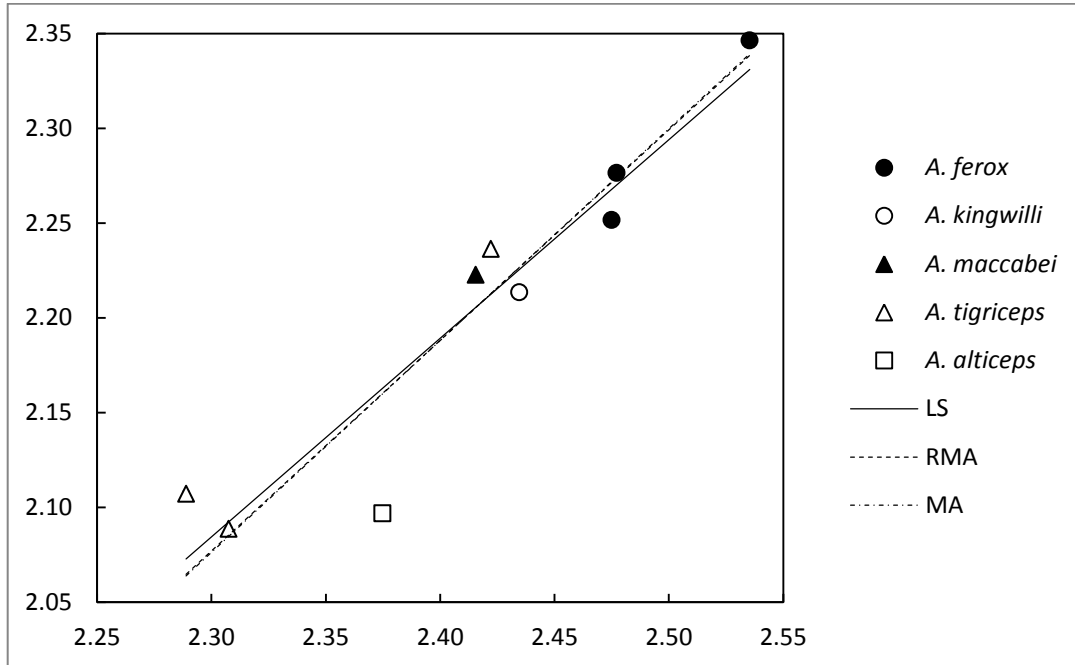


Figure D16 Bivariate plot of the antorbital skull length (Variable 3) against the skull length (Variable 2).

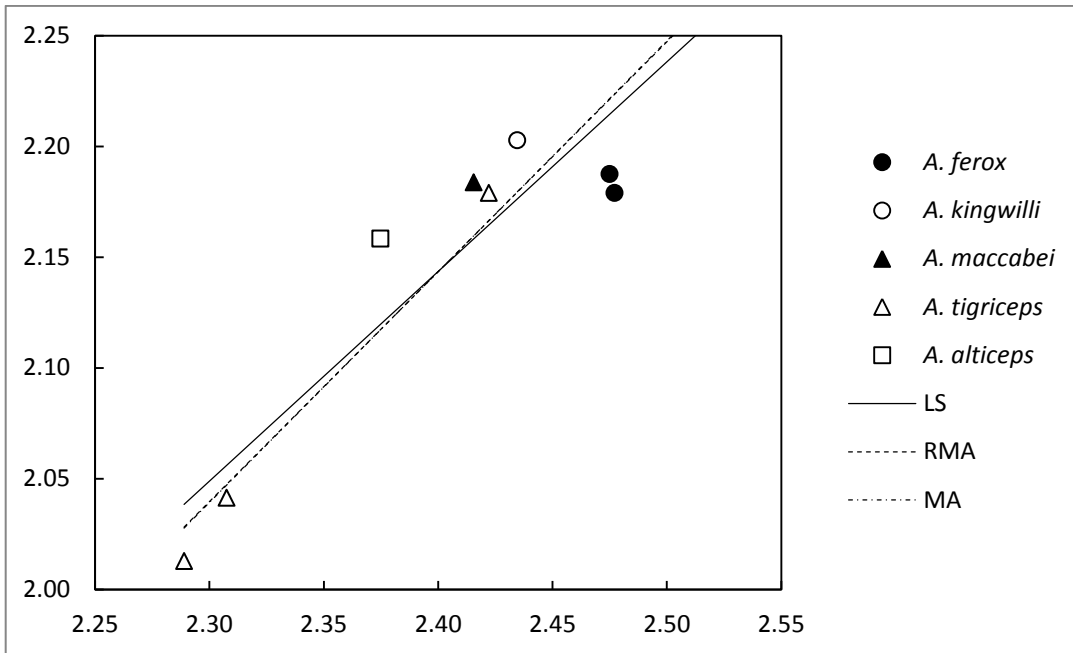


Figure D17 Bivariate plot of the postorbital skull length (Variable 4) against the skull length (Variable 2).

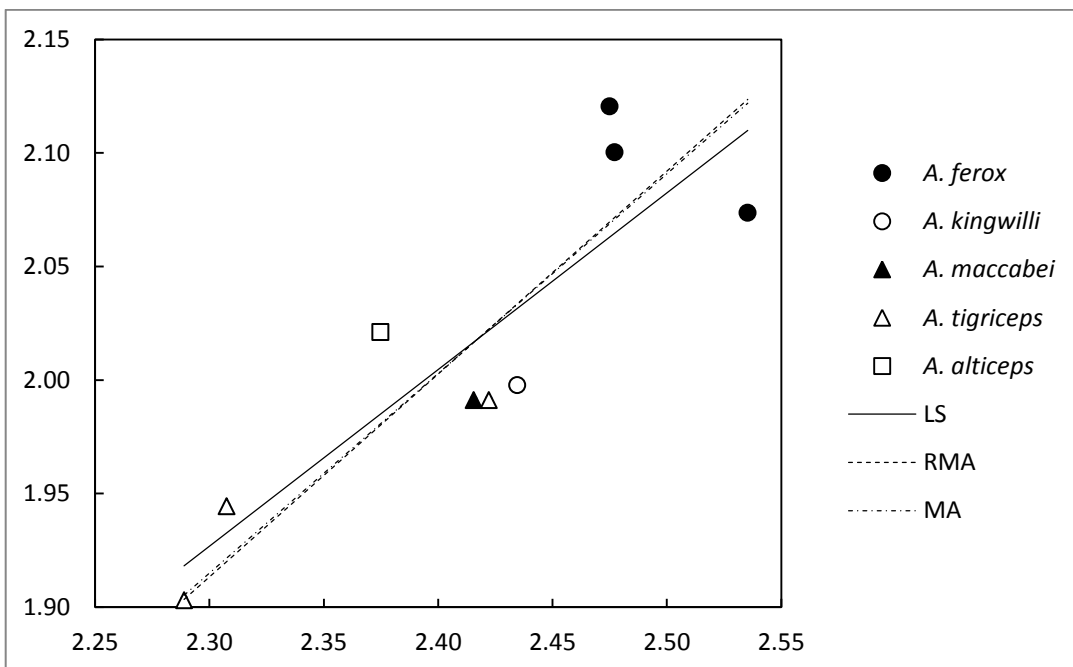


Figure D18 Bivariate plot of the total postorbital length (Variable 5) against the skull length (Variable 2).

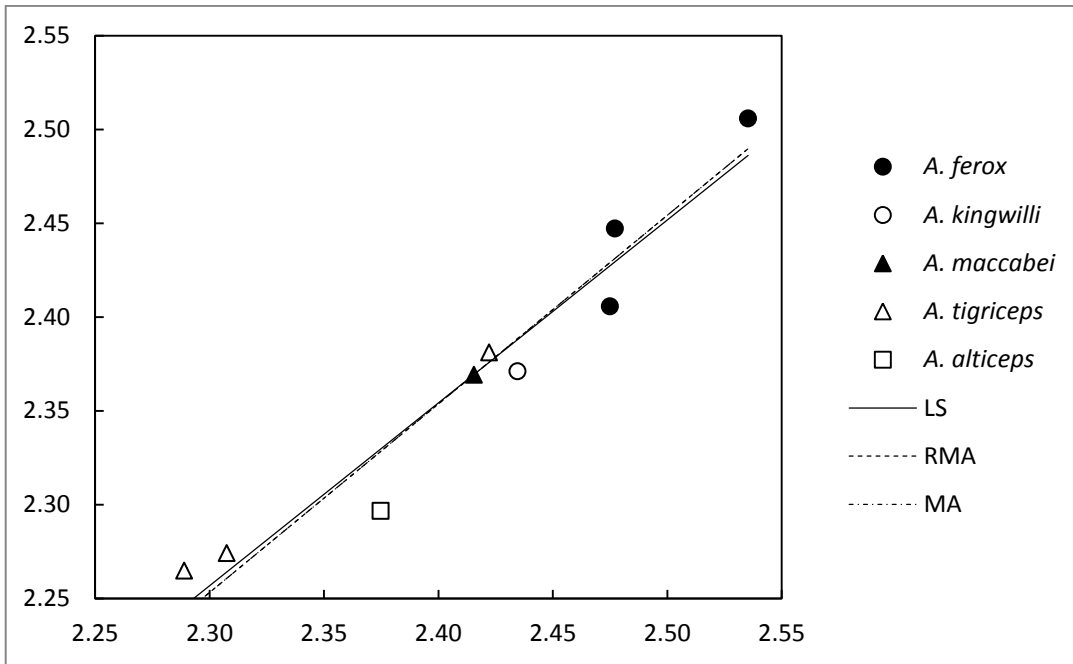


Figure D19 Bivariate plot of the prepineal skull length (Variable 6) against the skull length (Variable 2).

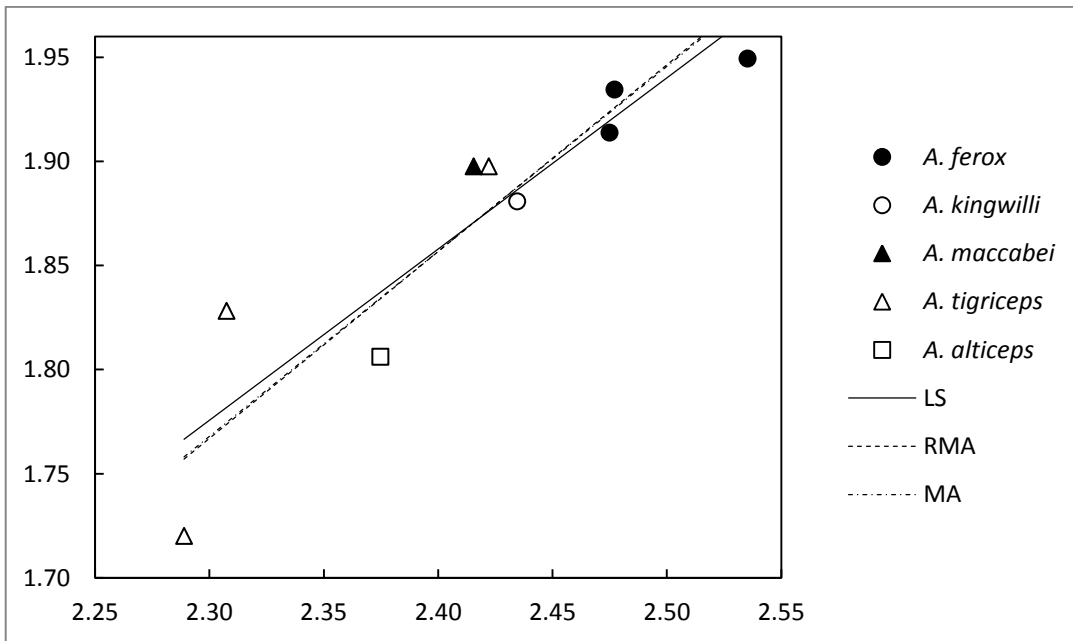


Figure D20 Bivariate plot of the interorbital width (Variable 12) against the skull length (Variable 2).

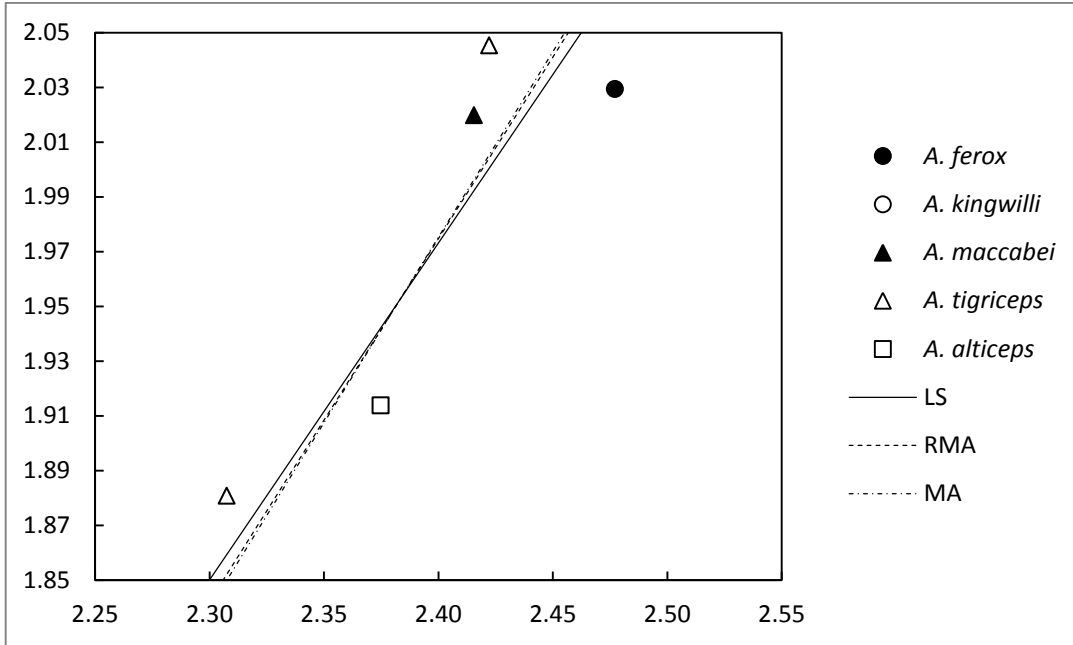


Figure D21 Bivariate plot of the intertemporal width (Variable 14) against the skull length (Variable 2).

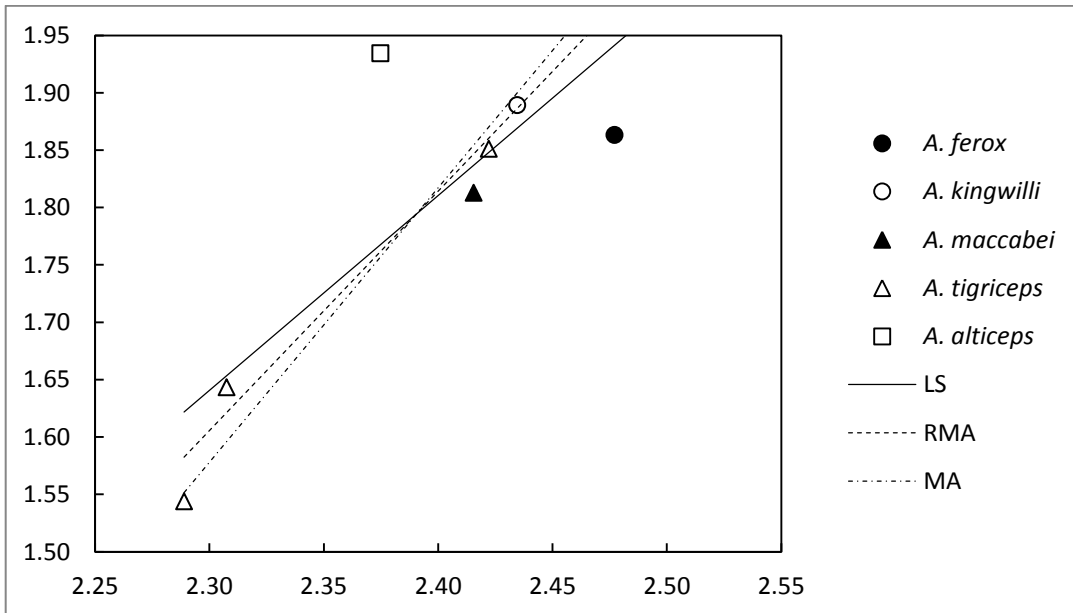


Figure D22 Bivariate plot of the temporal opening length (Variable 18) against the skull length (Variable 2).

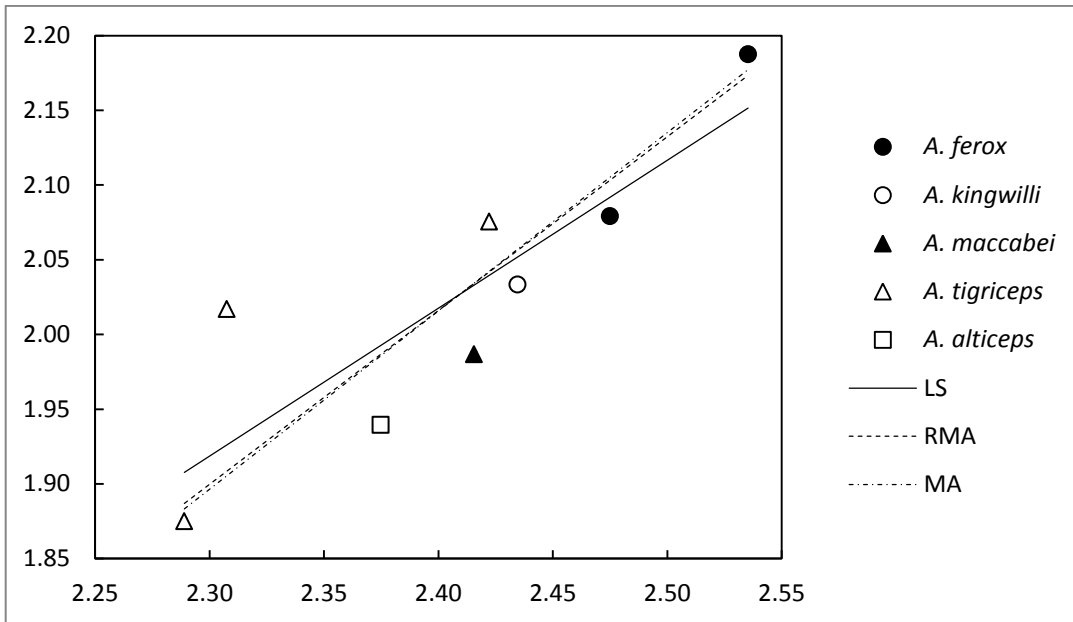


Figure D23 Bivariate plot of the lateral skull height (Variable 24) against the skull length (Variable 2).

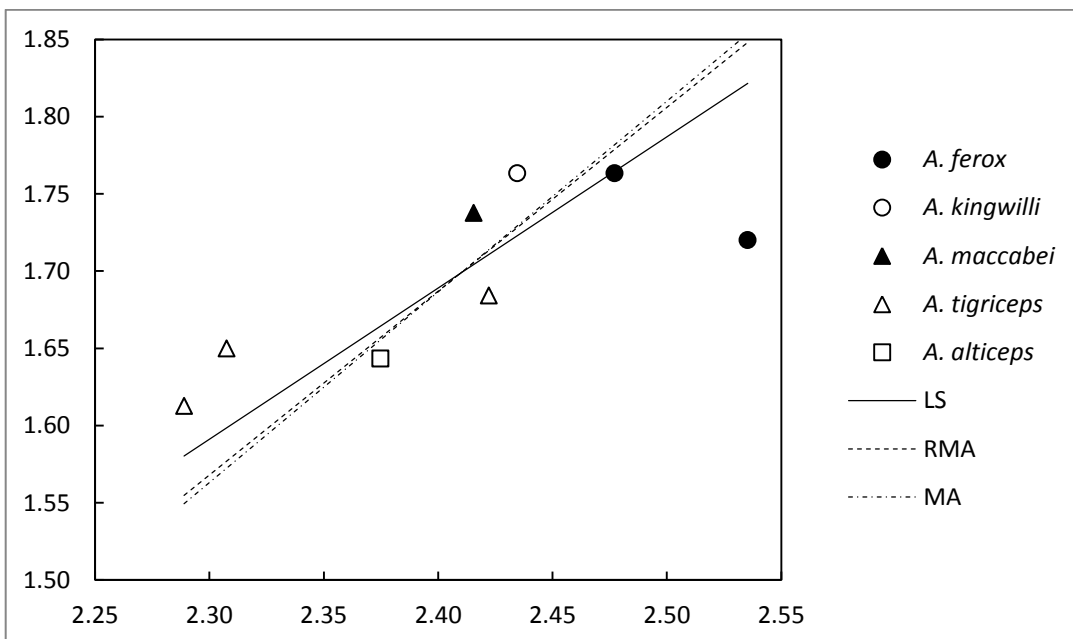


Figure D24 Bivariate plot of the orbit length (Variable 26) against the skull length (Variable 2).

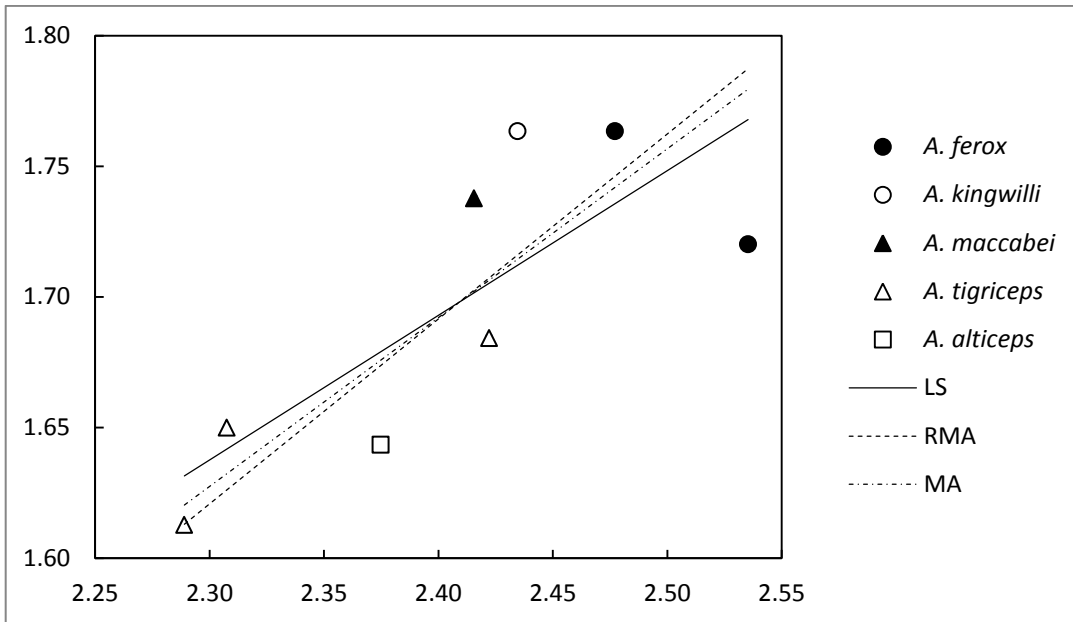


Figure D25 Bivariate plot of the orbit length (Variable 27) against the skull length (Variable 2).

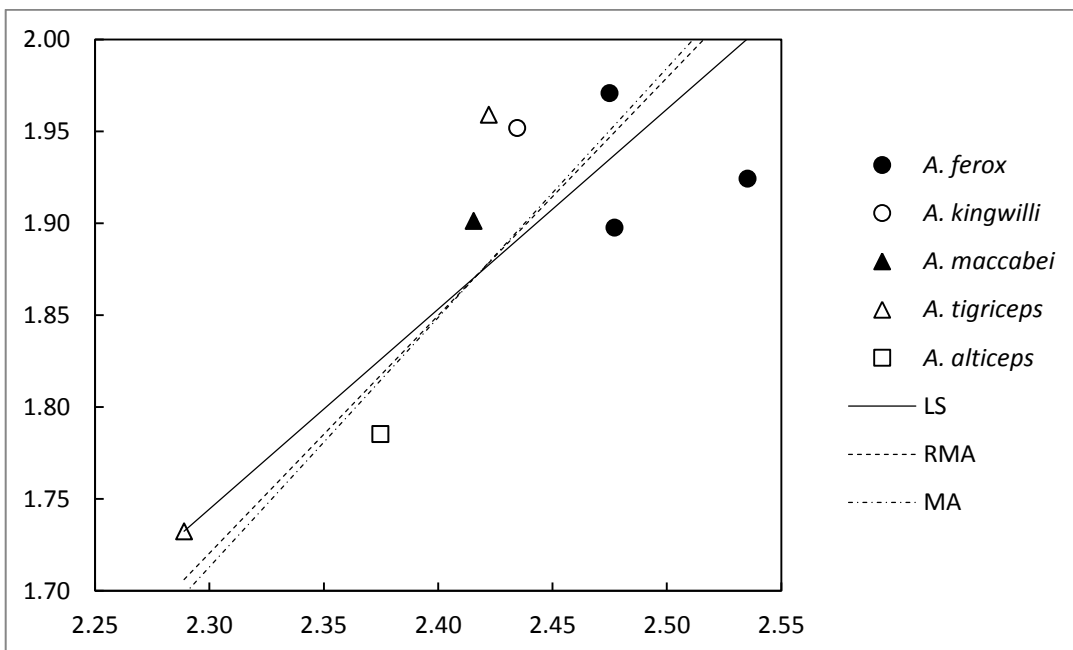


Figure D26 Bivariate plot of the snout-maxillary canine length (Variable 37) against the skull length (Variable 2).

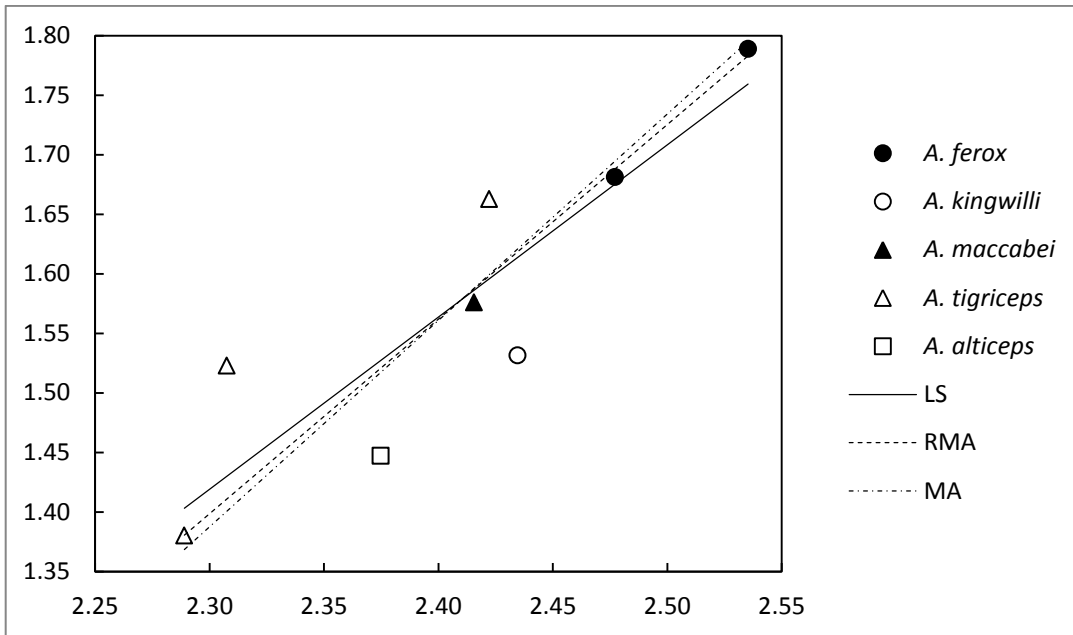


Figure D27 Bivariate plot of the minimum suborbital bar height (Variable 41) against the skull length (Variable 2).

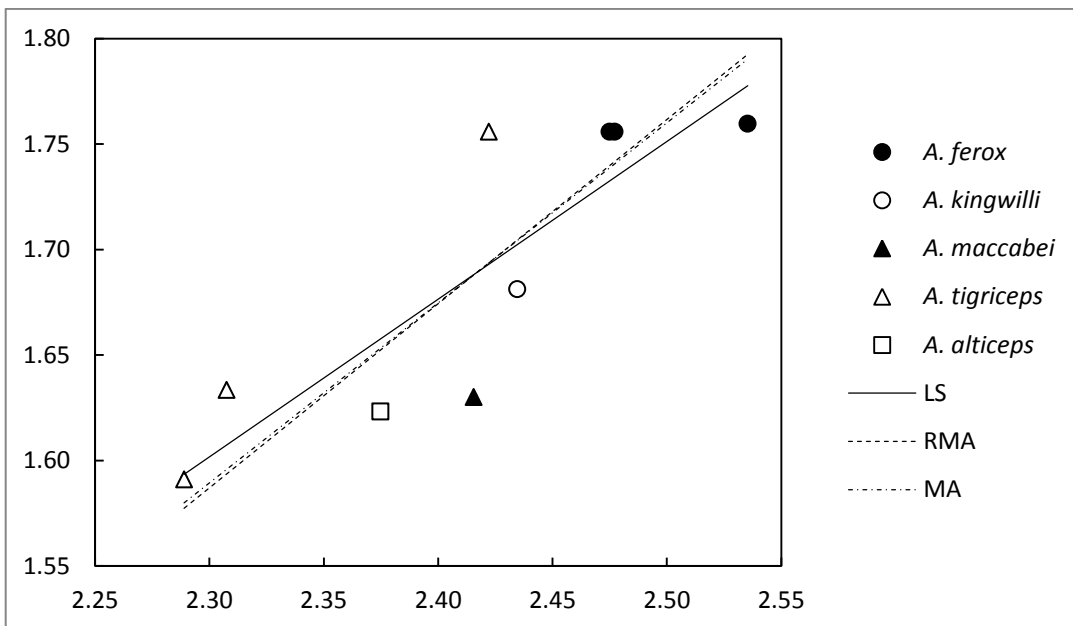


Figure D28 Bivariate plot of the dentary corpus height (Variable 49) against the skull length (Variable 2).

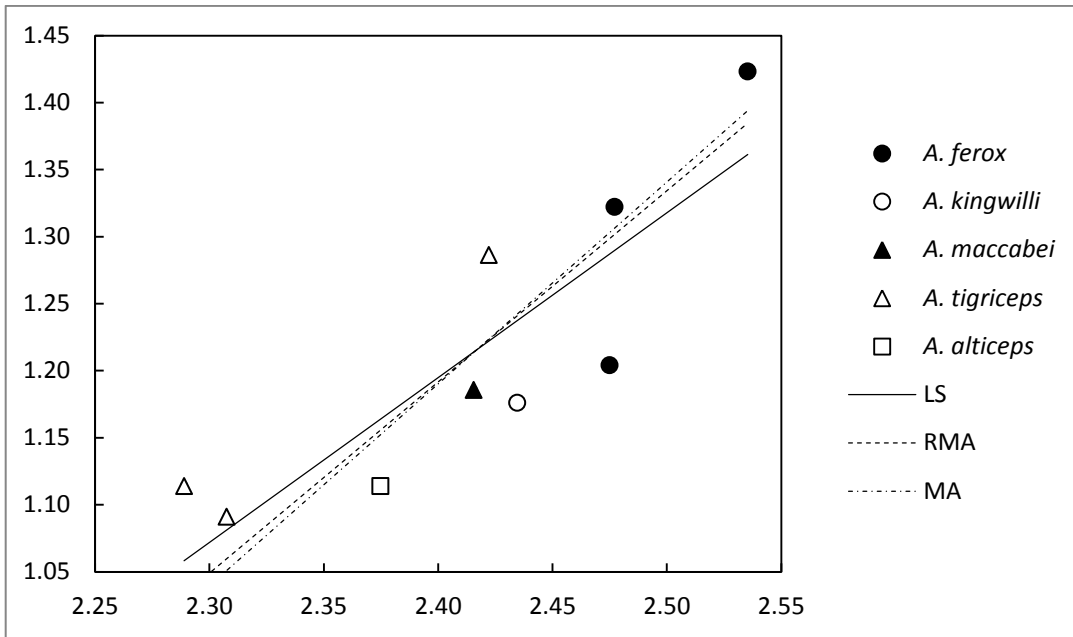


Figure D29 Bivariate plot of the dentary thickness (Variable 51) against the skull length (Variable 2).

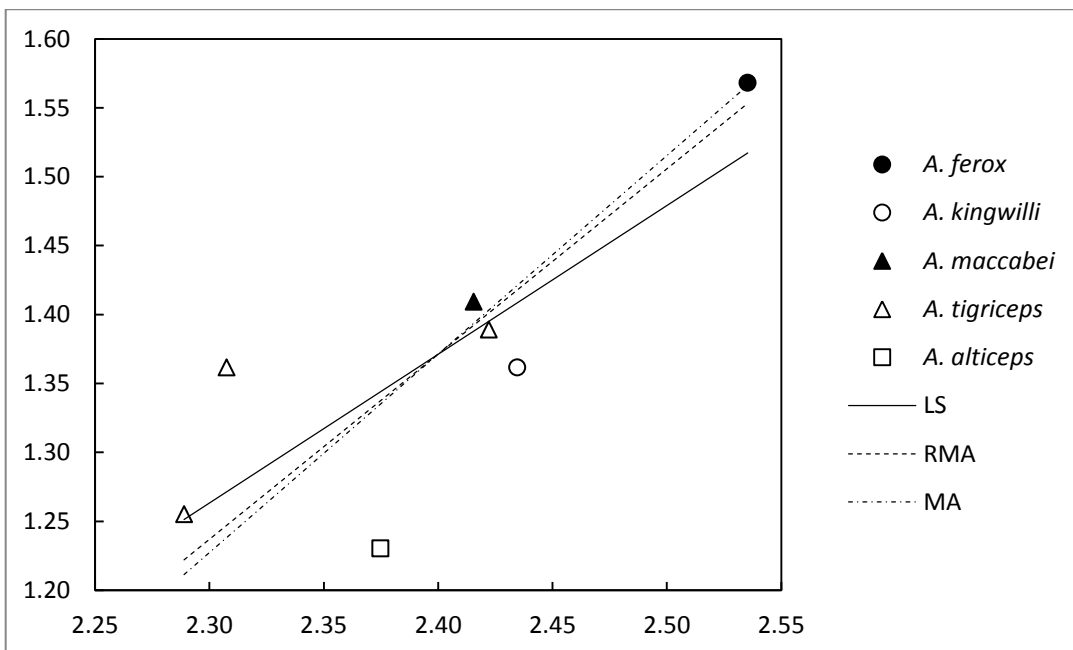


Figure D30 Bivariate plot of the minimum intercorporal breadth (Variable 52) against the skull length (Variable 2).

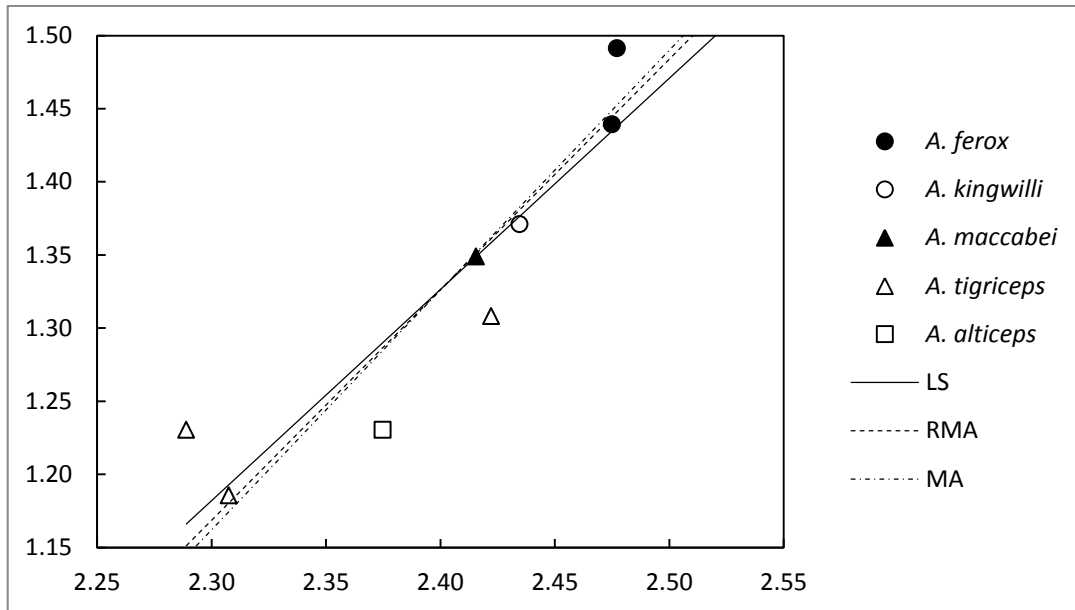


Figure D31 Bivariate plot of the mesiodistal diameter of maxillary canine (Variable 67) against the skull length (Variable 2).

13.4 Supporting figures for the regression analyses using prepineal skull length (6) as the independent variable.

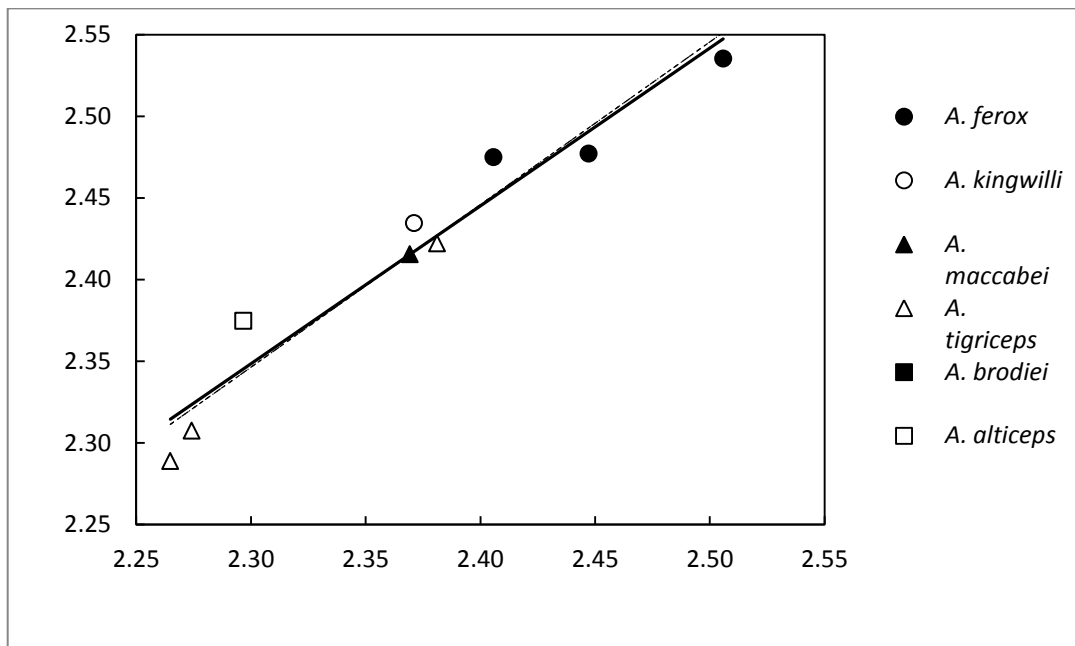


Figure D32 Bivariate plot of the skull length (Variable 2) against the prepineal skull length (Variable 6).

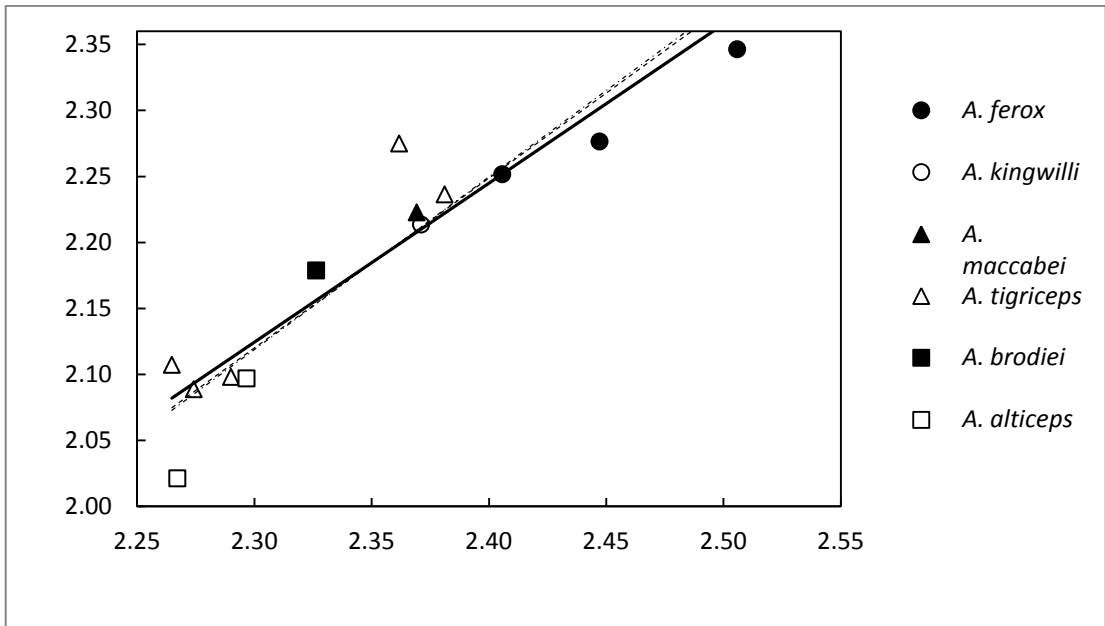


Figure D33 Bivariate plot of the antorbital skull length (Variable 3) against the prepineal skull length (Variable 6).

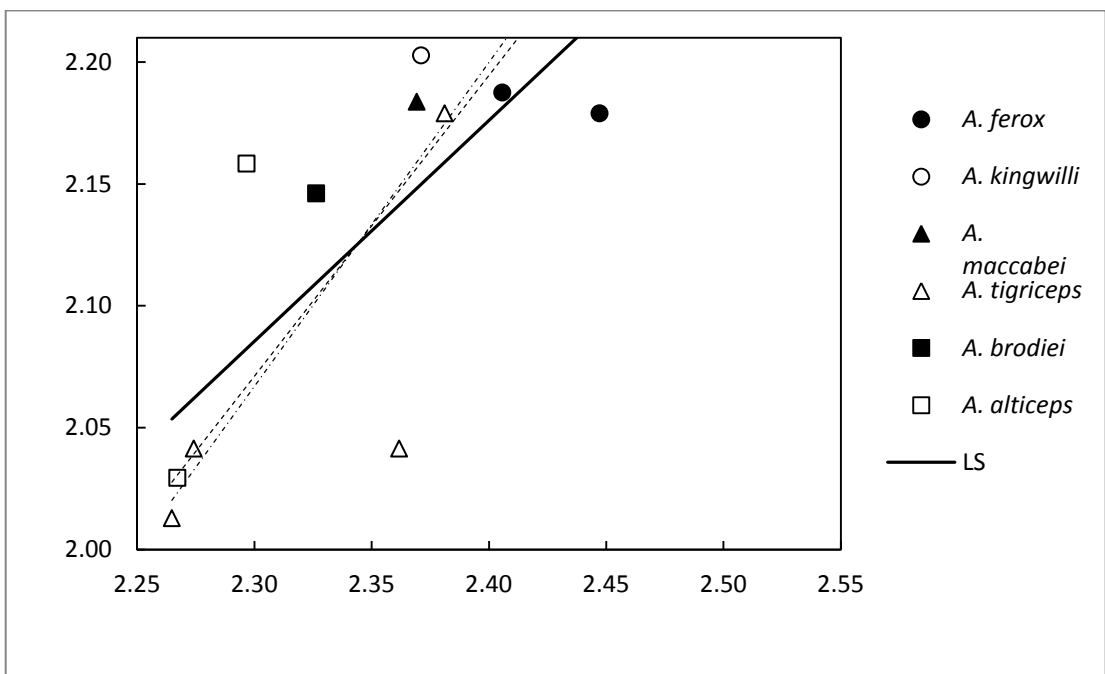


Figure D34 Bivariate plot of the postorbital skull length (Variable 4) against the prepineal skull length (Variable 6).

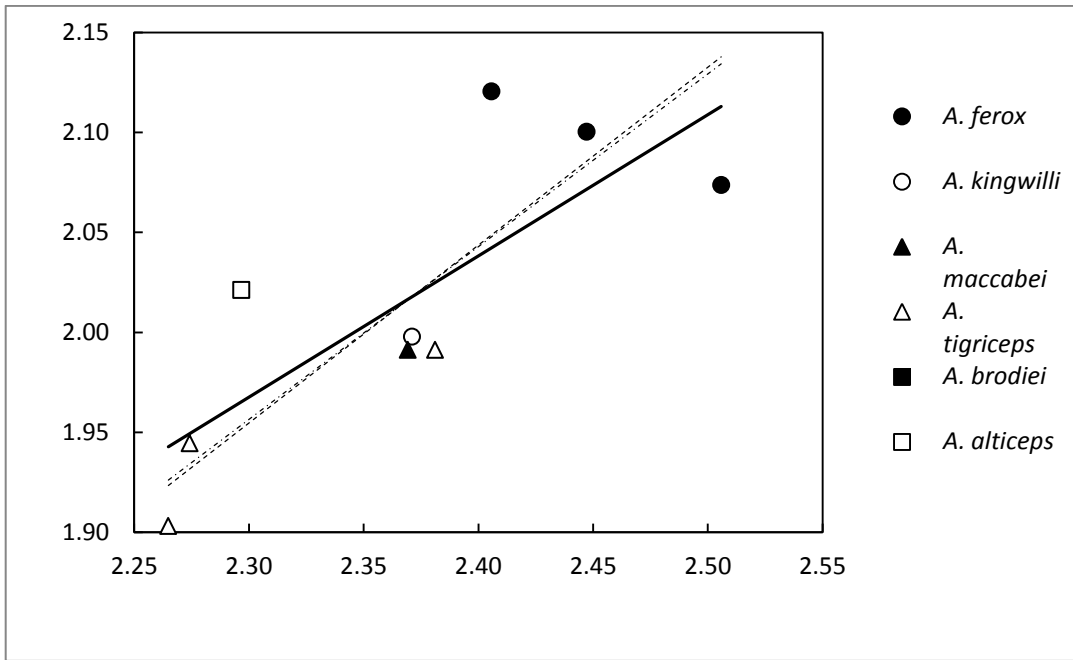


Figure D35 Bivariate plot of the total postorbital length (Variable 5) against the prepineal skull length (Variable 6).

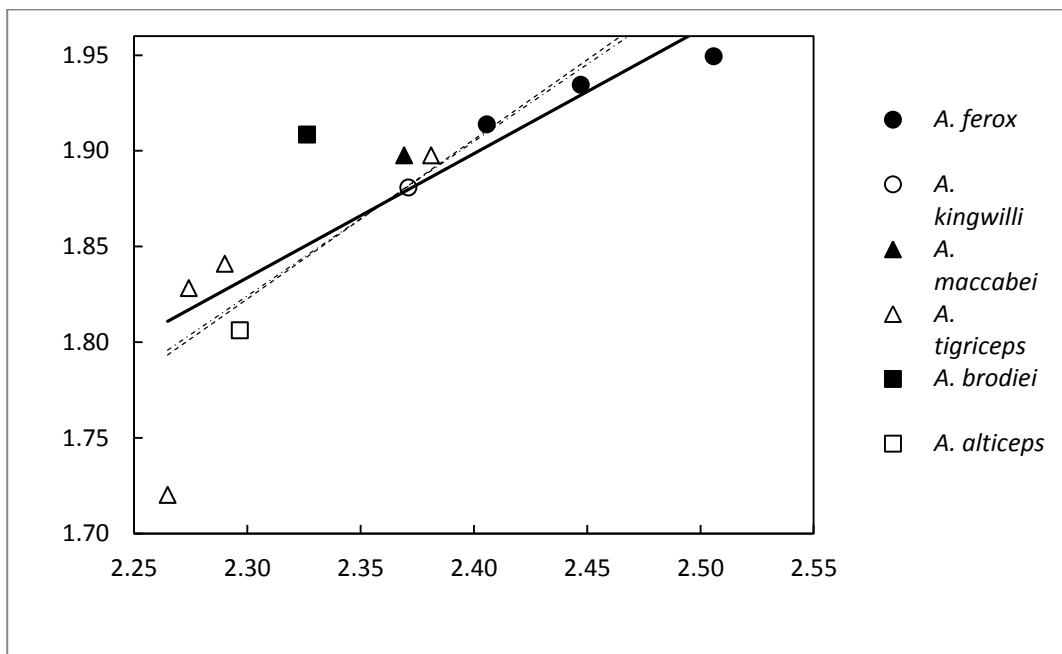


Figure D36 Bivariate plot of the interorbital width (Variable 12) against the prepineal skull length (Variable 6).

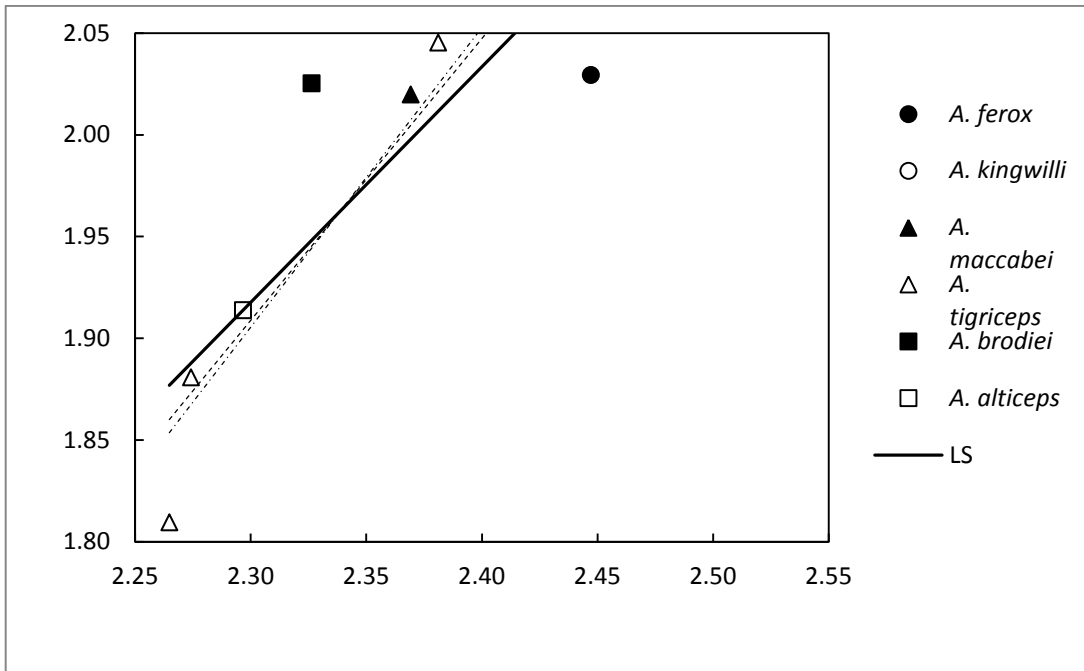


Figure D37 Bivariate plot of the intertemporal width (Variable 14) against the prepineal skull length (Variable 6).

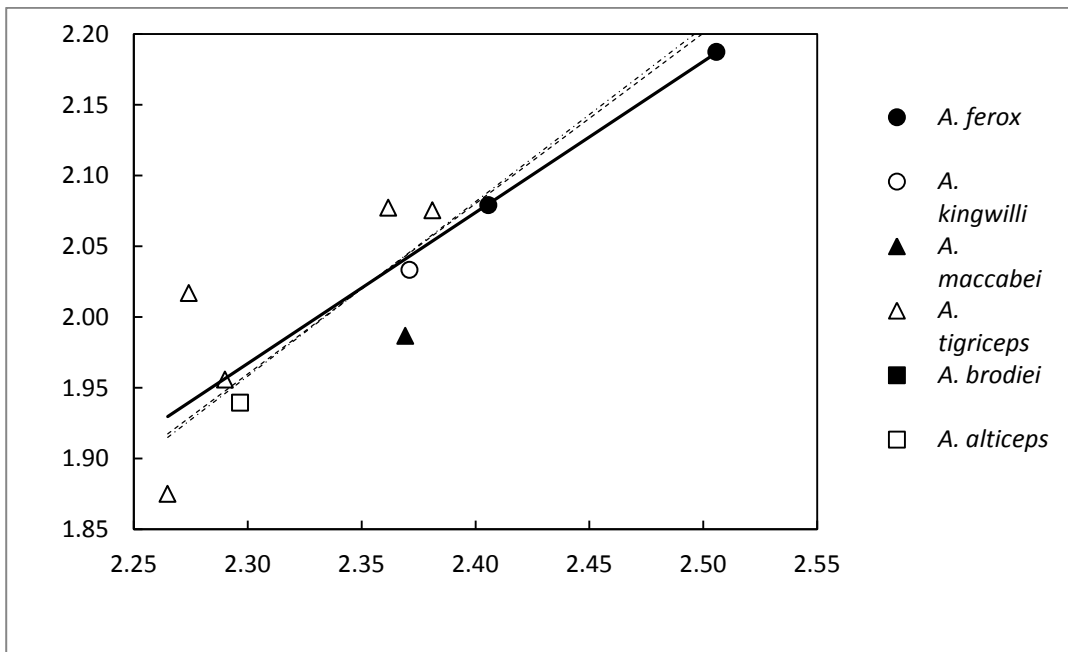


Figure D38 Bivariate plot of the lateral skull height (Variable 24) against the prepineal skull length (Variable 6).

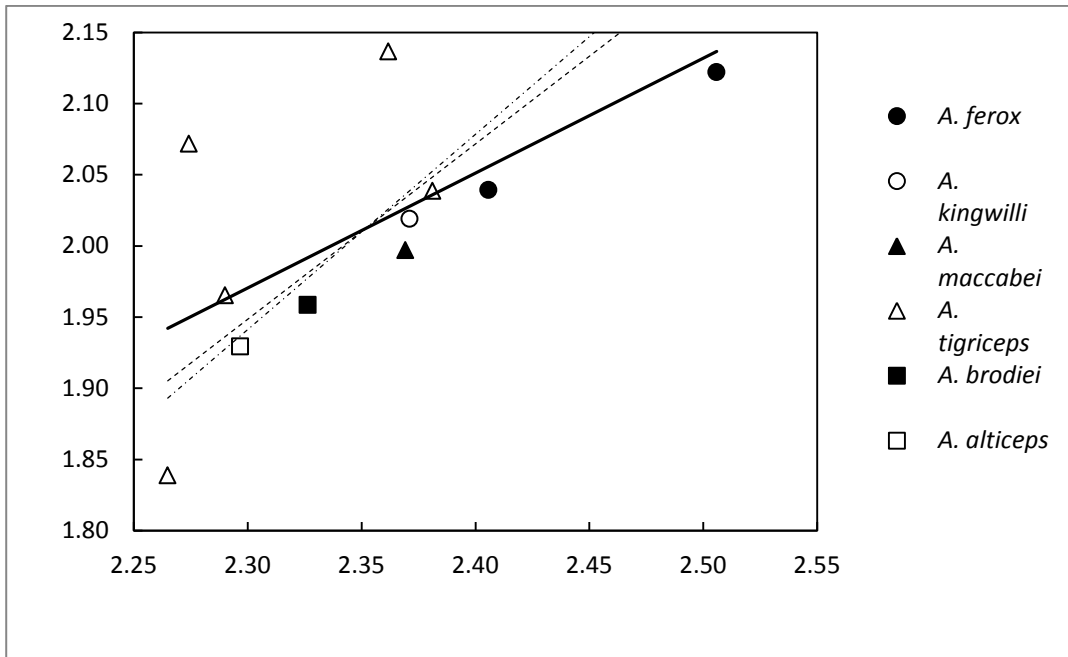


Figure D39 Bivariate plot of the Maxilla height (Variable 25) against the prepineal skull length (Variable 6).

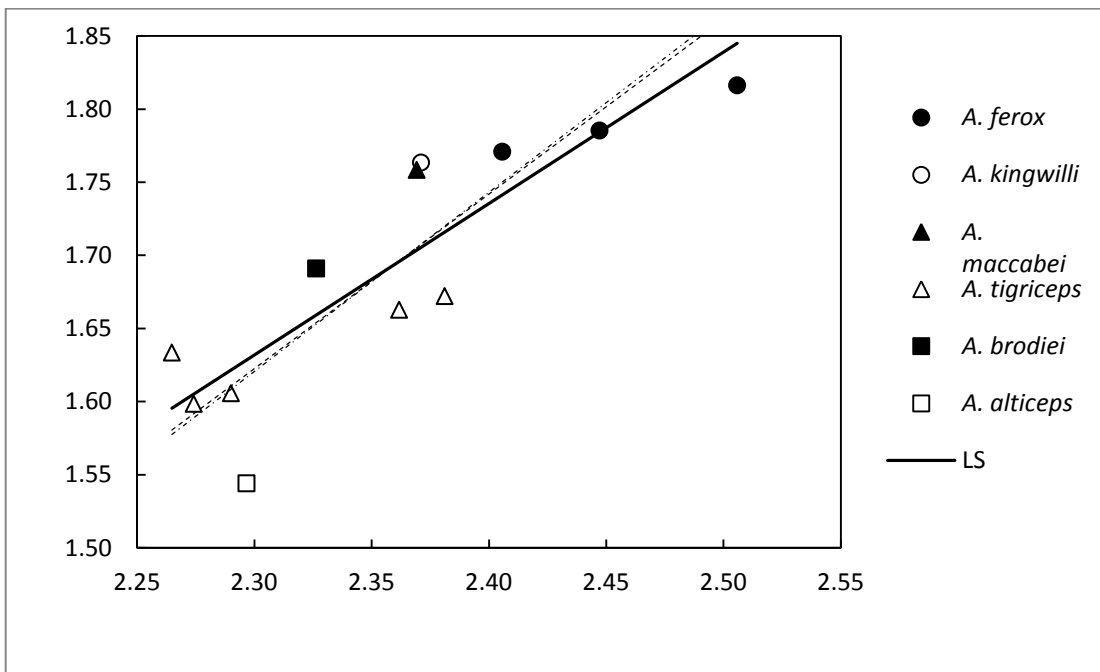


Figure D40 Bivariate plot of the orbit length (Variable 26) against the prepineal skull length (Variable 6).

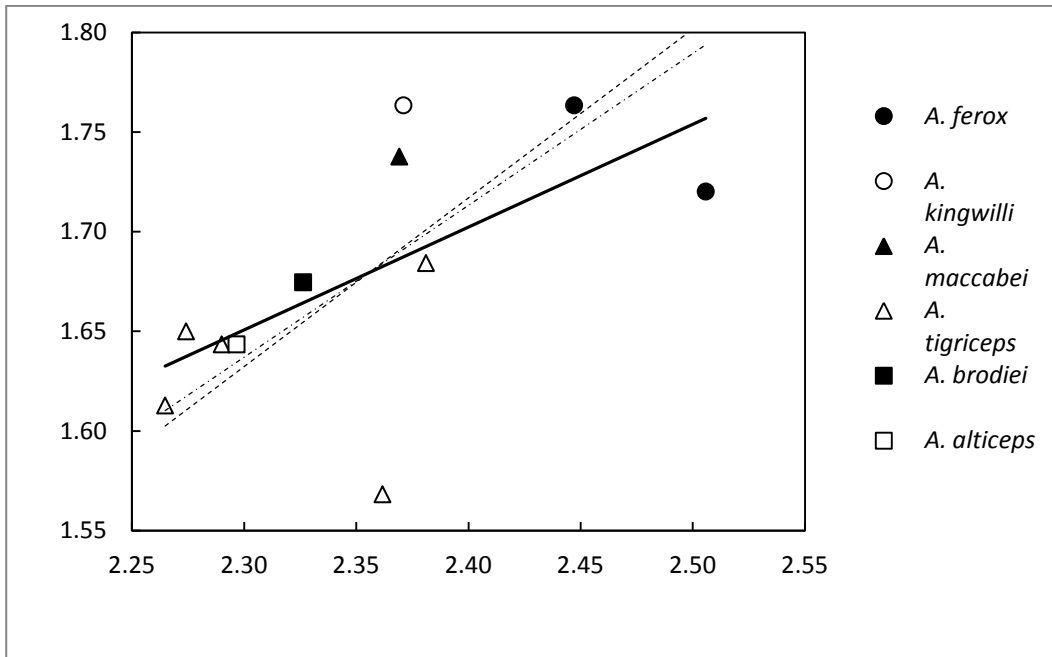


Figure D41 Bivariate plot of the orbit length (Variable 27) against the prepineal skull length (Variable 6).

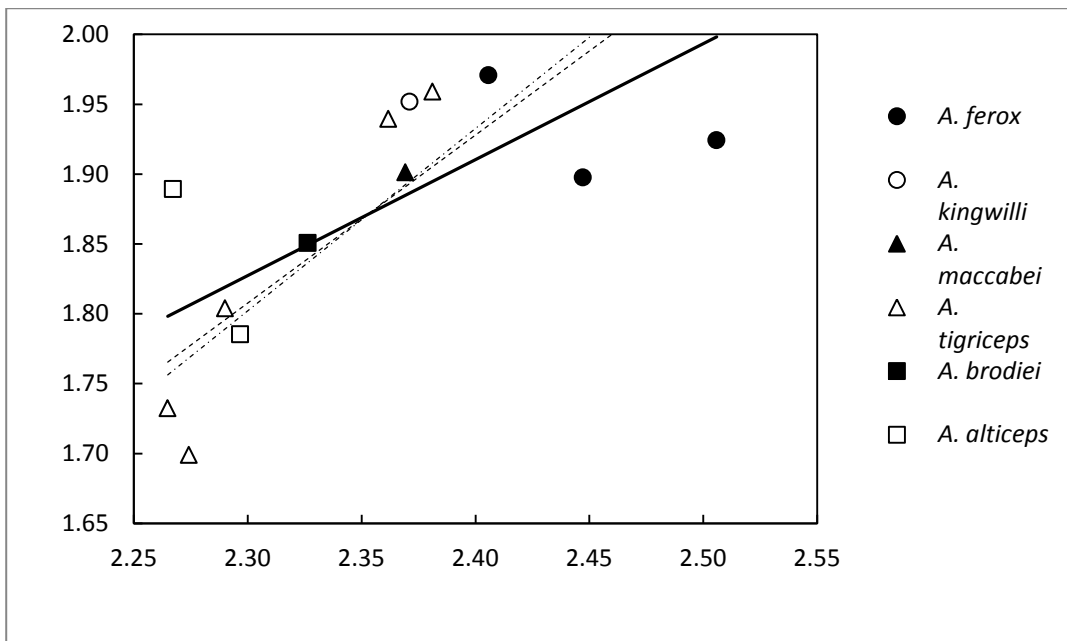


Figure D42 Bivariate plot of the snout-maxillary canine length (Variable 37) against the prepineal skull length (Variable 6).

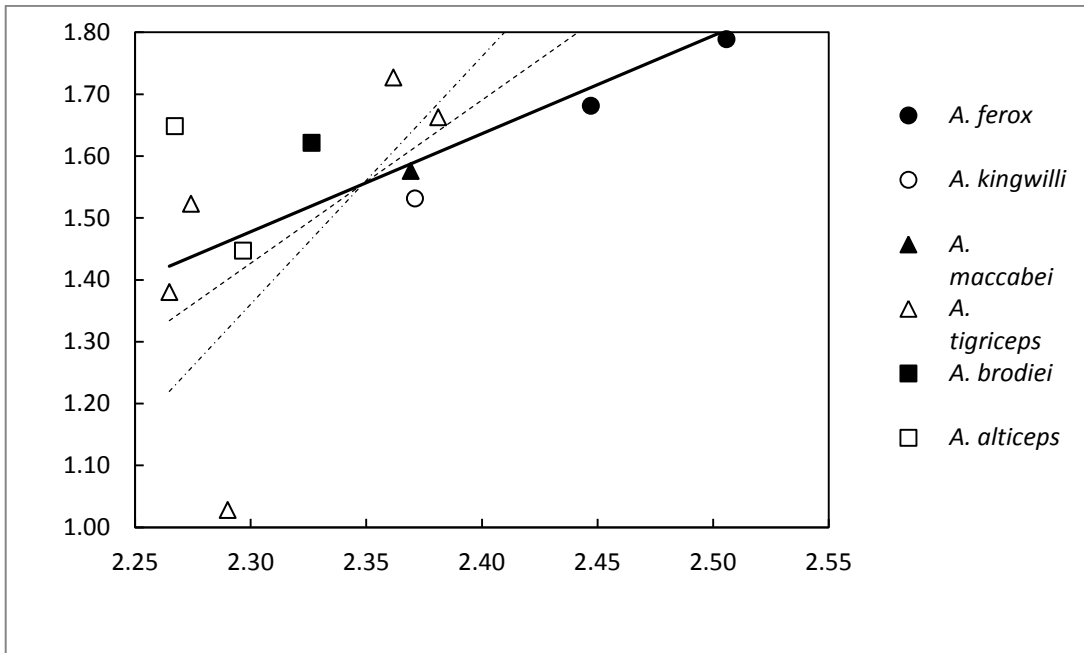


Figure D43 Bivariate plot of the minimum suborbital bar height (Variable 41) against the prepineal skull length (Variable 6).

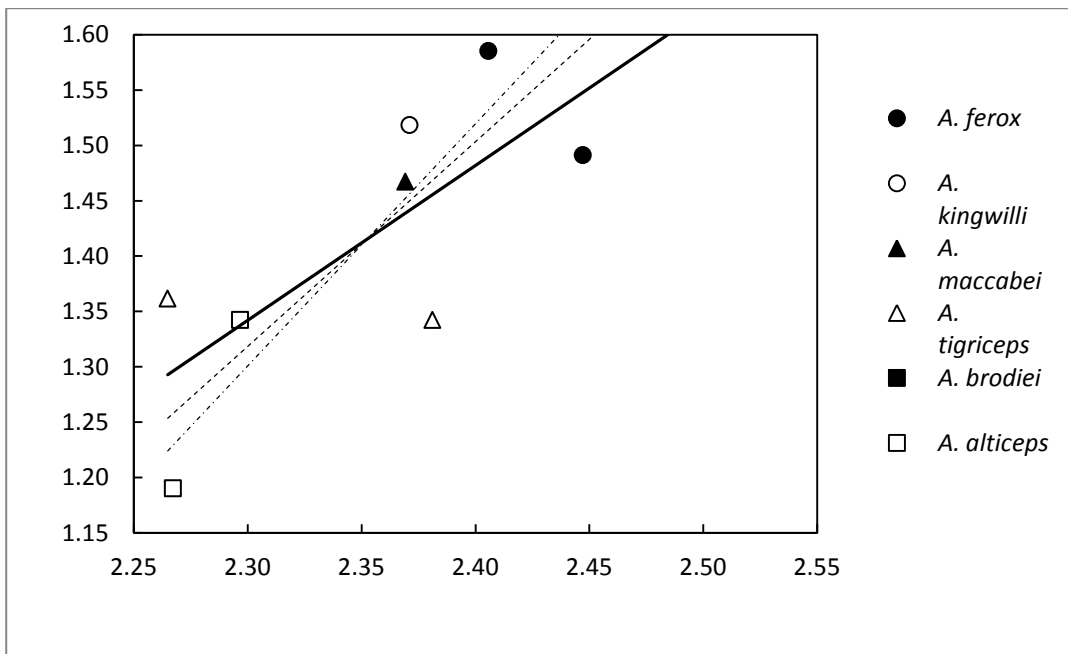


Figure D44 Bivariate plot of the minimum height of the zygomatic arch (Variable 42) against the prepineal skull length (Variable 6).

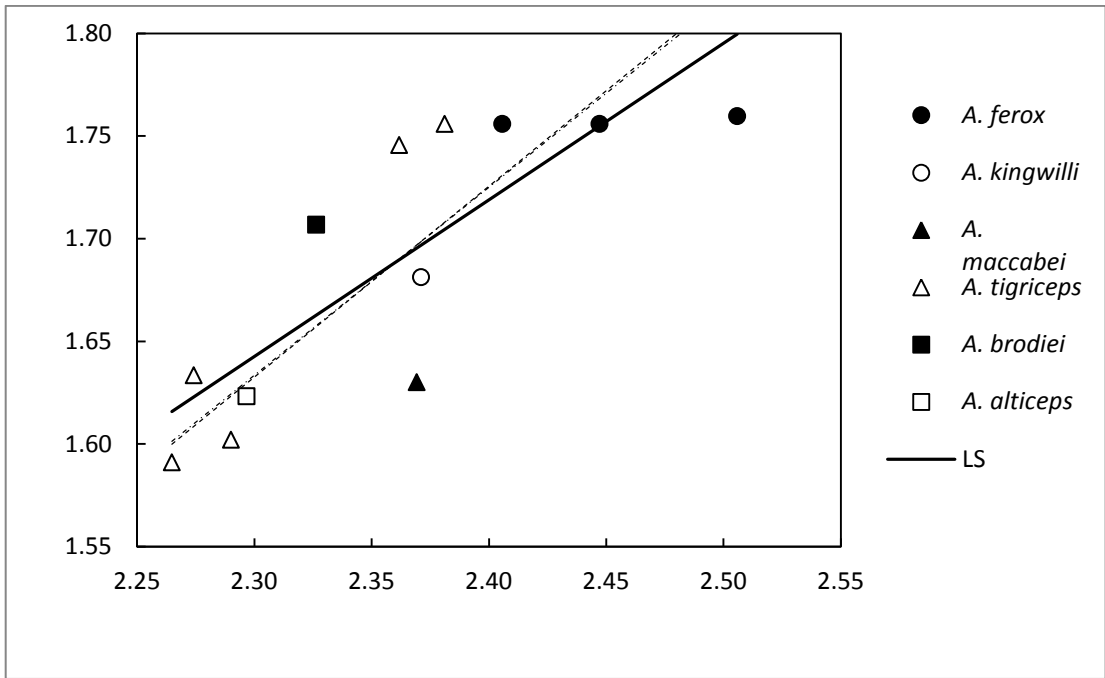


Figure D45 Bivariate plot of the dentary corpus height (Variable 49) against the prepineal skull length (Variable 6).

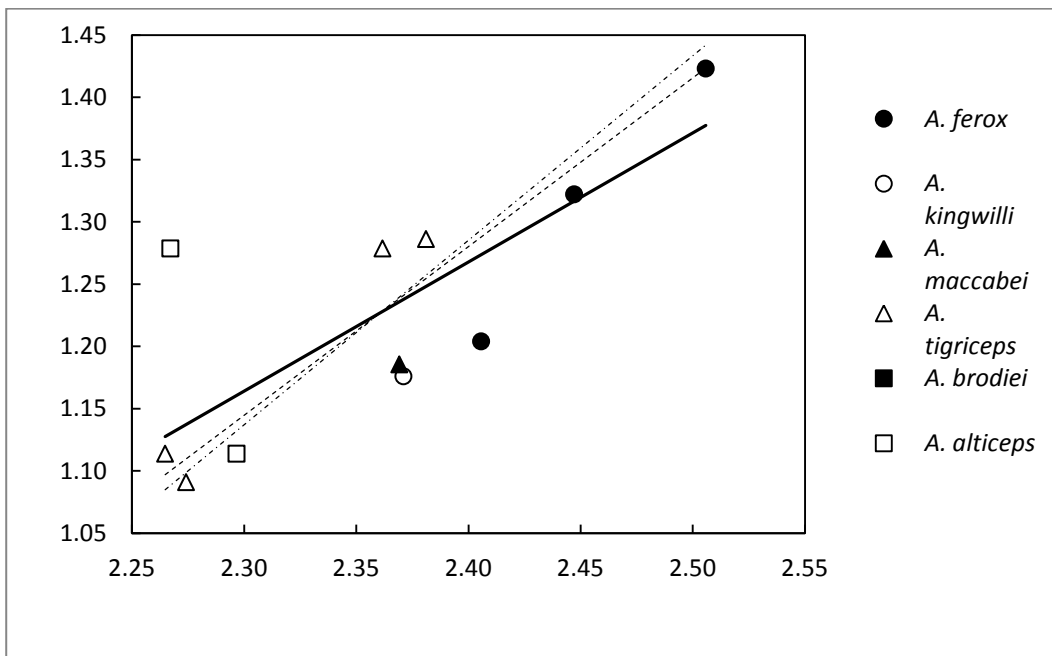


Figure D46 Bivariate plot of the dentary thickness (Variable 51) against the prepineal skull length (Variable 6).

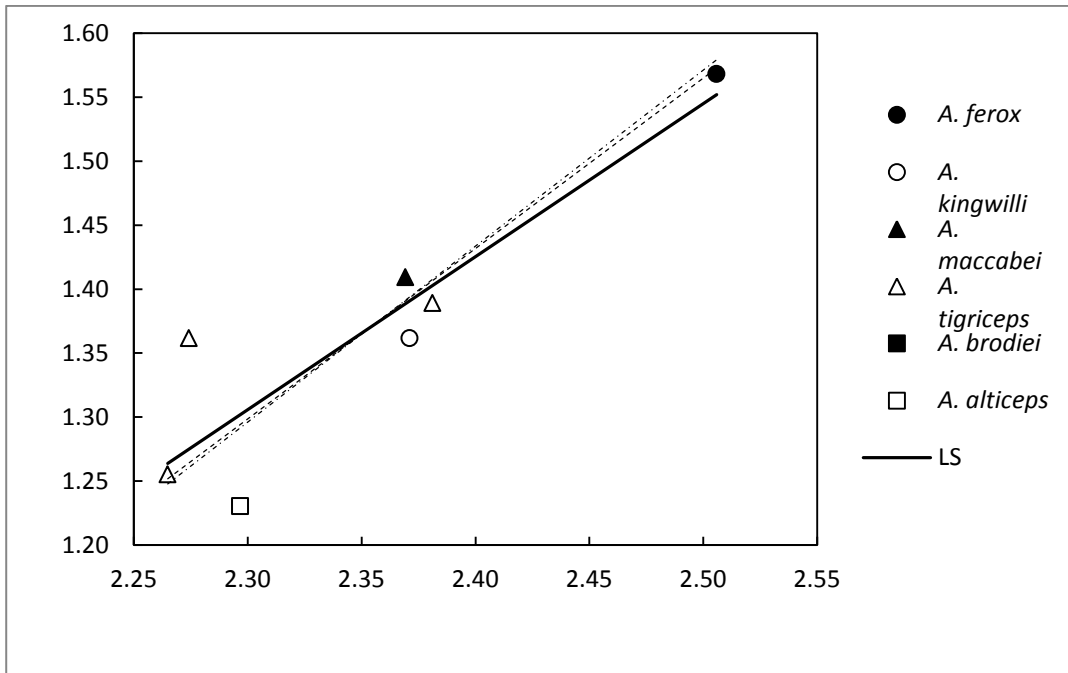


Figure D47 Bivariate plot of the minimum intercorporal breadth (Variable 52) against the prepineal skull length (Variable 6).

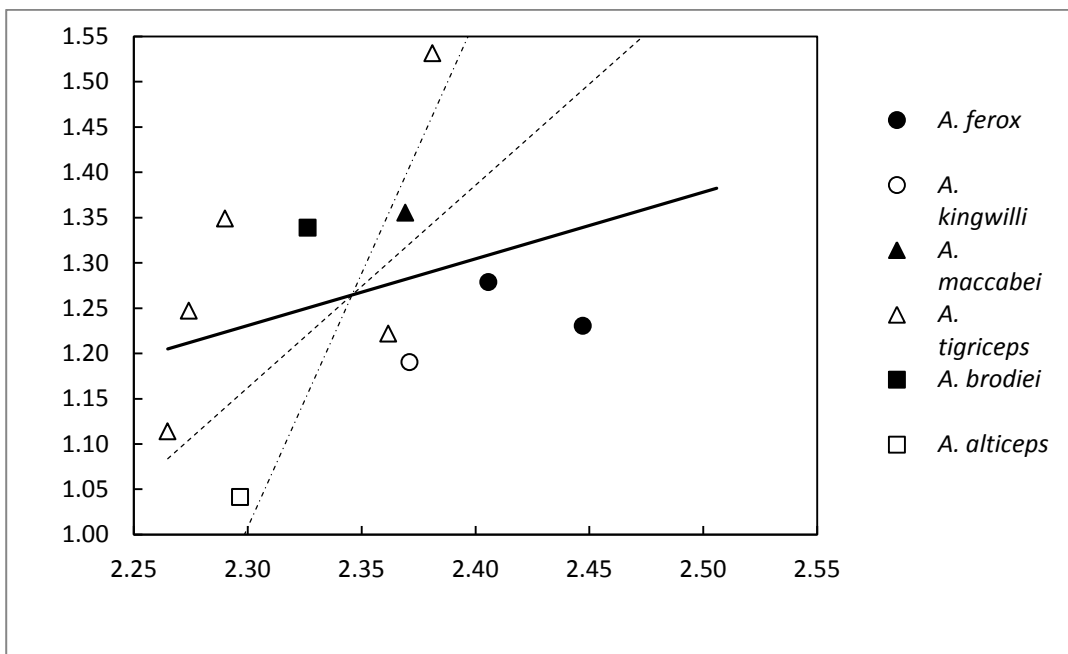


Figure D48 Bivariate plot of the Diastema between last incisor and canine (Variable 55) against the prepineal skull length (Variable 6).

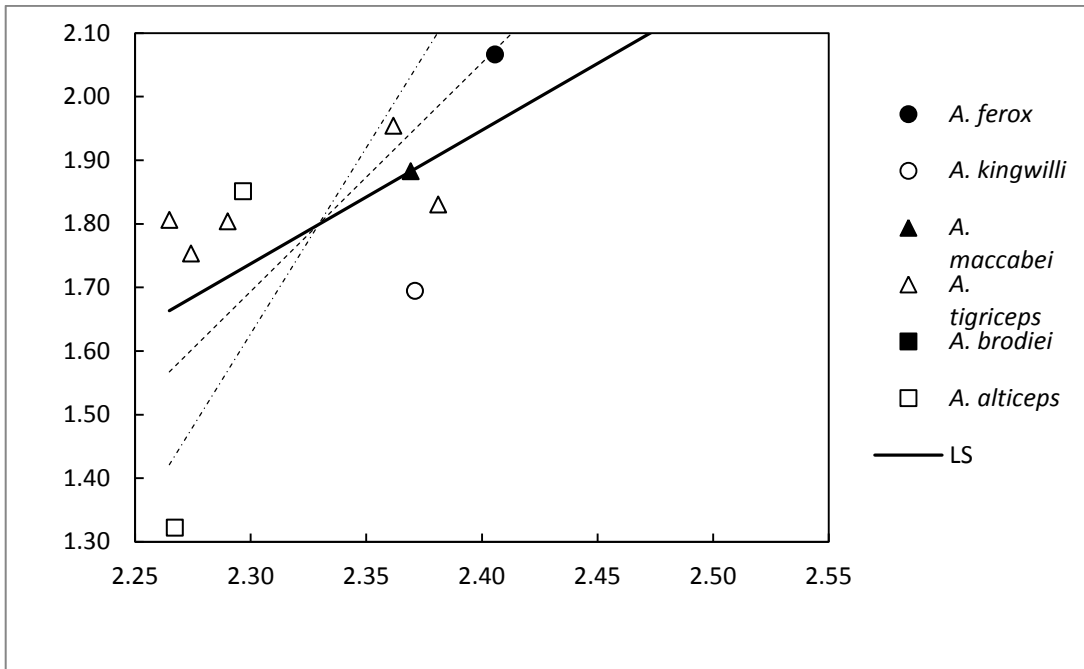


Figure D49 Bivariate plot of the maxillary bicanine breadth (Variable 65) against the prepineal skull length (Variable 6).

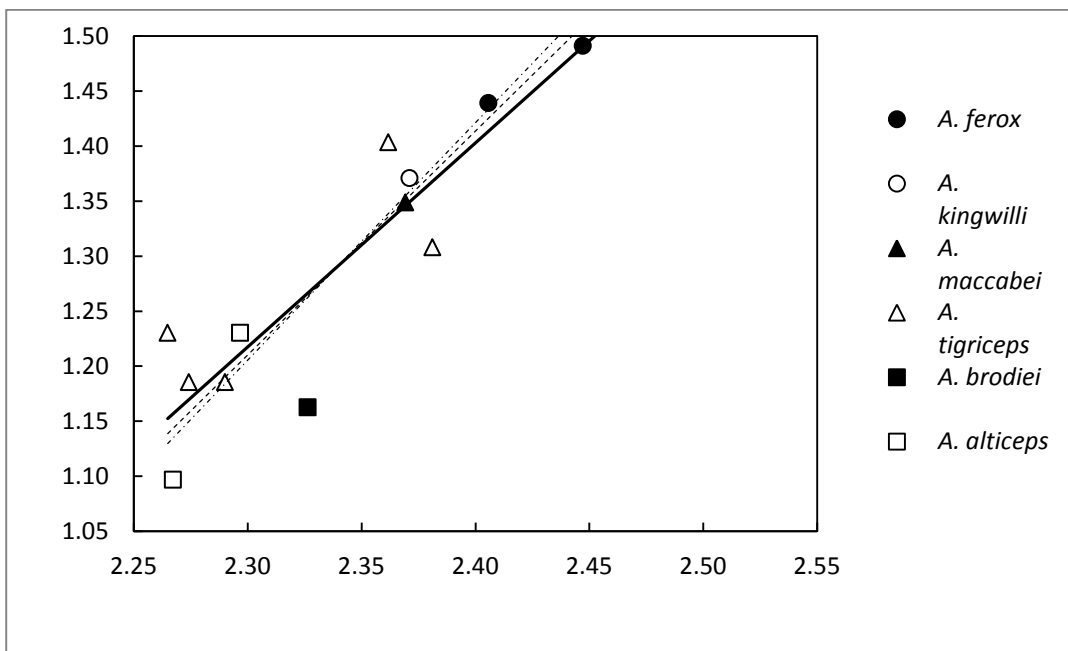


Figure D50 Bivariate plot of the maxillary canine (Variable 67) against the prepineal skull length (Variable 6).